NASA Technical Memorandum 4172

A Field Study of Solid Rocket Exhaust Impacts on the Near-Field Environment

B. J. Anderson and Vernon W. Keller

JANUARY 1990

NASA

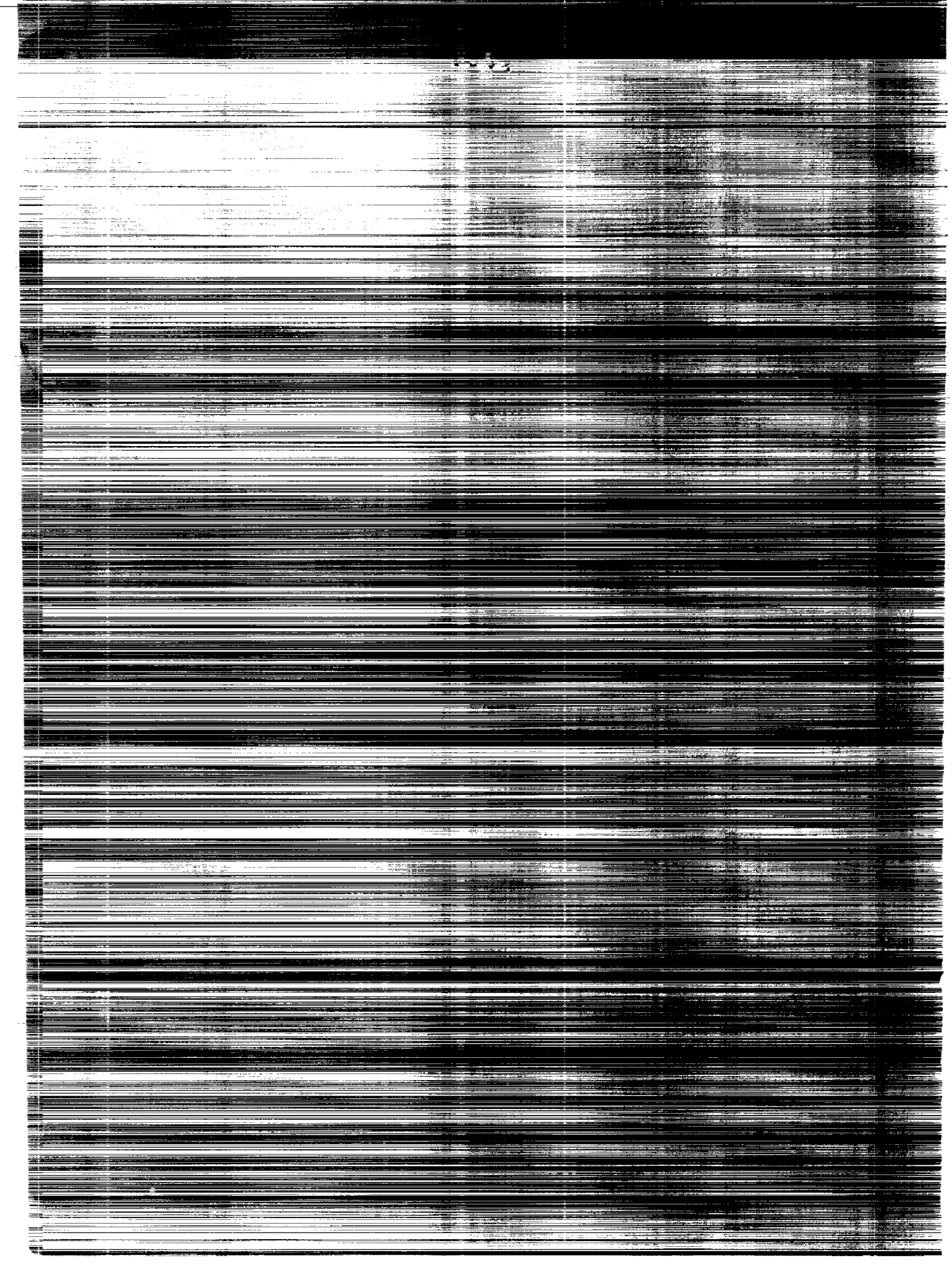

NASA Technical Memorandum 4172

A Field Study of Solid Rocket Exhaust Impacts on the Near-Field Environment

B. J. Anderson and Vernon W. Keller
George C. Marshall Space Flight Center
Marshall Space Flight Center, Alabama

National Aeronautics and
Space Administration
Office of Management
Scientific and Technical
Information Division

1990

TABLE OF CONTENTS

LIST OF ILLUSTRATIONS

LIST OF ILLUSTRATIONS (concluded)

LIST OF TABLES

TECHNICAL MEMORANDUM

A FIELD STUDY OF SOLID ROCKET EXHAUST IMPACTS ON THE NEAR-FIELD ENVIRONMENT

I. INTRODUCTION

The launch facilities for the Space Transportation System (STS), the space shuttle, are unique in the sense that copious quantities of water are sprayed into the base region below the vehicle and into the flame ducts during each launch for the purpose of dampening the acoustic and initial overpressure waves generated by the vehicle. At the Kennedy Space Center (KSC) launch facilities, this amounts to approximately 900,000 liters from when the flow begins (a few seconds prior to main engine ignition) to 10 sec after lift-off. If the shuttle launch facilities at Vandenberg Air Force Base are activated, the flow is expected to be roughly twice as great. It has been shown (1) that this amount of water exceeds the amount that can be vaporized by the exhaust heat. Some of the excess is atomized, mixed with the exhaust, and results in a deposition of hydrochloric acid and solid material (mostly aluminum oxide from the solid rocket motors). The deposition is quite heavy near the launch pad. In trace amounts it has been detected as far as 22 km downwind on some occasions. Its impact has been characterized by a number of careful studies conducted at KSC (2-4). The chemistry and ice nucleation properties of the solid fraction of the deposition are discussed in Refs. (5)-(7).

The properties, location, and behavior of this deposition are of interest primarily because of the potential for impacting launch pad operations and the near-pad environmental quality. The acid content is great enough that it impacts both vegetation (8) and animal life near the launch facilities (9). Likewise, it can be highly corrosive to man-made structures. It has also been found (10) that gaseous hydrogen chloride is released into the atmosphere as the deposition dries. This "revolatilization" process is of potential concern in both the areas of human health and corrosion control.

This report presents results from a series of field studies and analysis which were undertaken to help quantify and understand the near-field effects of this deposition. Primary emphasis was given to measuring and understanding the effects at KSC launches in order to provide a basis for developing reasonable estimates of what to expect from launches involving either new vehicles or new launch facilities. Measurement and analysis techniques suitable to the situation were developed. The work developed out of previous studies of the far-field effects of rocket exhausts (1). It was conducted over a period of more than 4 years and included field studies at two shuttle launches, 41D and 51A. Additional studies of the exhaust cloud properties from these two launches are reported in Refs. (11) and (12).

An important aspect of this work was the use of the Acoustic Model Facility of the Test Laboratory at the Marshall Space Flight Center (MSFC). Here a 6.4 percent scale model of the space shuttle is statically fired to study the acoustic environments and other phenomena produced during a launch. From May 1982 through April 1984, a series of test firings were conducted to examine the initial overpressure (IOP) wave to be expected from Solid Rocket Booster (SRB) ignition of the space shuttle at the Vandenberg Air Force Base launch site (VLS), the acoustic environment of a VLS shuttle launch, and the acoustic environment of the aft cargo carrier in a KSC launch. Selected tests from among these were monitored to study the production and properties of acidic deposition produced during a shuttle launch. This provided an important opportunity to

develop and test measurement techniques and to study deposition formation in the VLS configuration.

II. BACKGROUND INFORMATION

A. Model Description

In the Acoustic Model Facility the shuttle SRBs are modeled by Tomahawk Missile solid rocket motors manufactured by Morton-Thiokol Chemical Corporation. The motor contains 175.57 kg of type TP-H-3095 propellant (20.4 percent aluminum) which burns in approximately 9 sec. Chemically this propellant is very similar to the propellant in the shuttle SRBs. The average mass flux from the motor is thus 19.5 kg s^{-1} which is a factor of about $4.096 \times 10^{-3} = 0.064^2$ smaller than the typical mass flux from the shuttle SRBs. Actually the mass fluxes of both the model and shuttle motors vary with time during the burn cycle. Likewise, propellant temperature and changes in shuttle SRB design also make a difference. The shuttle began using higher performance motors with STS-8.

For the purposes of this study, a value of 5560 kg s^{-1} is used as representative of output from each shuttle SRB. This figure represents the average mass flux in the first 18 to 20 sec following ignition as computed for the preflight analysis of mission STS-13. The output is less later in the burn. Before STS-8 the output was about 5400 kg s^{-1}, a value which is still within the ±5.3 percent variation which may occur because of changes in the temperature of the propellant.

The scaling of the model for acoustic and initial overpressure studies is based on the ratio of mass fluxes from the solid motors. Linear dimensions are scaled by 0.064 so that areas are scaled by 4.096×10^{-3} (0.064 squared); thus the model is commonly known as the "6.4% Model." As illustrated in Figure 1, the launch mount including the flame trenches and launch platform is modeled in plate steel and "Fondu Fyr," a concrete-like refractory material. The orbiter and external tank are also modeled to the same scale. The orbiter model contains three working engines fueled by gaseous hydrogen and liquid oxygen which were originally used to model the Saturn J-2 upper stage engine. The scaling factors for the model are summarized in Table 1.

The most important parameters involved in the formation of acidic deposition in the launch process are the mass of HCl released, the thermal energy released, and the volume of cooling water in the cloud/flame trench system. Note from Table 1 that the exhaust mass flow rate is scaled by the factor $0.064^2 = 0.0041$. Since propellant composition in the model is very similar to the shuttle propellant, the HCl and the thermal energy fluxes scale very closely to the same factor. To estimate the relative total mass of HCl and thermal energy, the interaction time between the shuttle SRM plume and the on-pad water must be known. From launch photographs, the interaction time is estimated to be 7 to 10 sec, compared to the 9 sec that the Tomahawk burns. On the model, IOP/acoustic suppression water flow rate is also scaled by the same 0.064^2 factor. However, for tests in the VLS configuration, the water flow time interval prior to ignition is much shorter in the model, less than 1 sec, compared to the 15-sec full scale. This timing difference is necessary to maintain the properly scaled cross sectional area in the duct. As a result, the total volume of cooling water in the model VLS system is scaled by a factor much smaller than 0.064^2. Water flow into the ducts is illustrated by Figures 2 and 3; scale factors are given in Table 2.

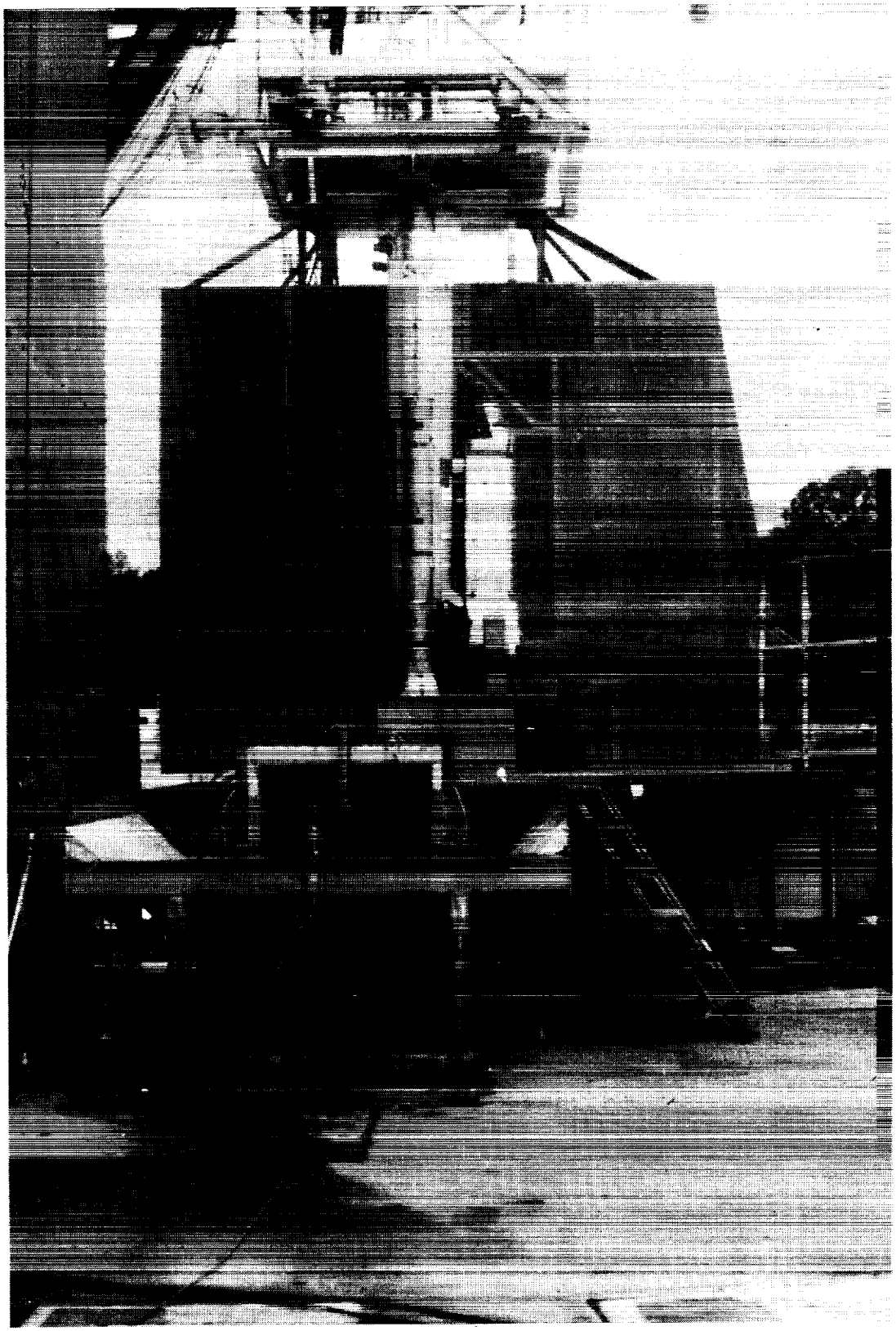

Figure 1. "6.4 percent model" facility configured for Western Test Range testing.

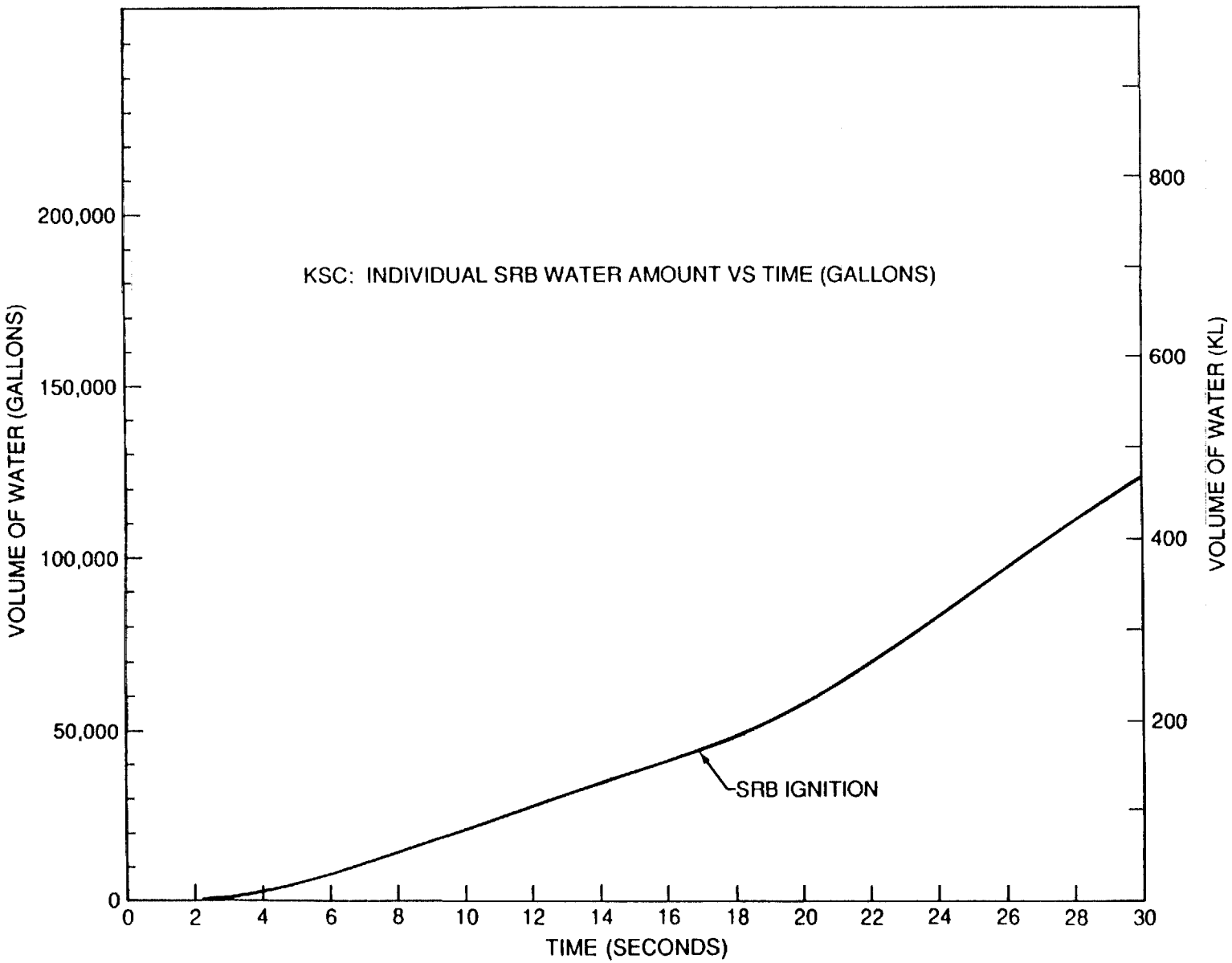

Figure 2. Total cumulative water flow per SRB at Kennedy Space Center which may interact with the solid motor exhaust. (Flows on the SSME side are excluded.)

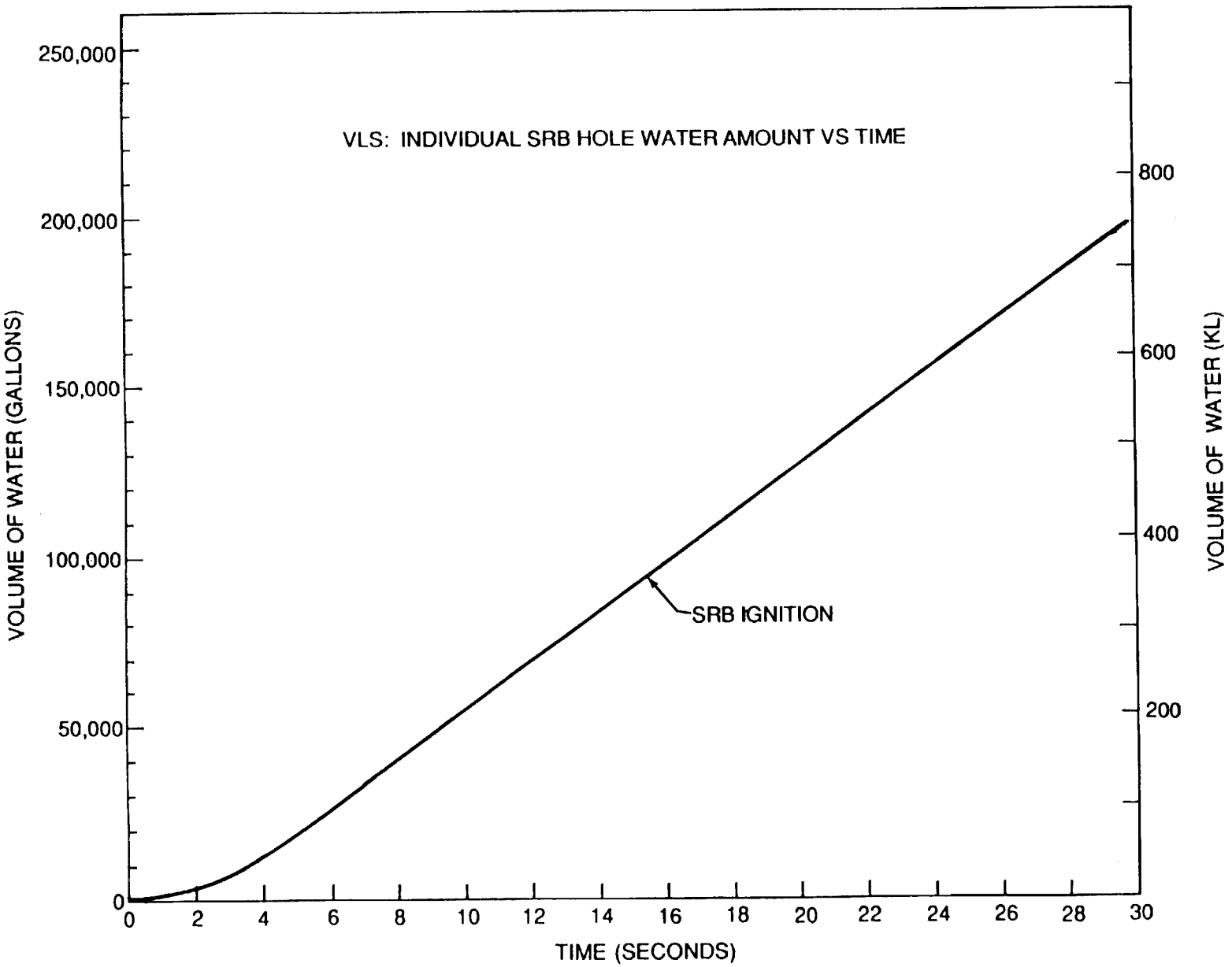

Figure 3. Total cumulative water flow per SRB planned for the Vandenberg launch site which would interact with the solid motor exhaust. (Flows on the SSME side are excluded.)

TABLE 1. COMPARISON OF MODEL AND FULL-SCALE* PARAMETERS

Parameter	Full-Scale	n	Full x 0.064^n	Model
Shuttle SRM (one)				
Sea Level Thrust (Newtons)	13.3×10^6	2	54,700	47,200
Mass Flow Rate (kg s^{-1})	5560	2	22.8	21.2
Exit Area (m^2)	11.3	2	0.0465	0.0406
Expansion Ratio	7.72	0	7.72	7.36
Exit Half Angle (deg)	6	0	6	15
Exit Mach Number	2.95	0	2.95	2.81
Exit Diameter (cm)	380	1	24.3	22.7
Supersonic Core Length (m)	59	1	3.77	3.35
SSME (one)				
Sea Level Thrust (Newtons)	1.68×10^6	2	6870	6790
Mass Flow Rate (kg s^{-1})	472	2	1.93	1.81
Exit Area (m^2)	4.17	2	0.017	0.0062
Expansion Ratio	77	0	77	8.5
Exit Half Angle (deg)	5.4	0	5.4	20
Exit Mach Number	4.234	0	4.234	3.325
Exit Diameter (cm)	230	1	14.7	8.9
Supersonic Core Length (m)	54	1	3.5	1.6

*SSME at 100 percent power, high performance SRM. Data are reduced to three figures since motor performance varies several percent with time and temperature.

B. Background on Acid Deposition Production

The data presented in Table 2 illustrate a critical point relative to formation of deposition from the STS exhaust; an excess of water enters the pad/flame trench system over and above the amount that can be vaporized by the available exhaust heat. The excess, which is of order 200 kl (50,000 gal) per SRB at KSC, 500 kl (130,000 gal) per SRB at Vandenberg, interacts with the exhaust plume. Much of this water is atomized by the mechanical shears and turbulence generated by both the Space Shuttle Main Engine (SSME) and SRB exhaust flows. It is then expelled into the near field or mixed into the exhaust "ground cloud," which lifts and blows away with the wind. In this interaction, it scavenges significant quantities of SRB exhaust products; gaseous hydrogen chloride and aluminum oxide particles. The composition and spatial distribution of this material is of primary interest in this study.

TABLE 2. PARAMETER SCALES FOR HCl EFFECTS

	ETR		WTR		MODEL	RATIO MODEL/ETR		RATIO MODEL/WTR	
	7 sec	10 sec	7 sec	10 sec	100% WTR	7 sec	10 sec	7 sec	10 sec
Suppression Water/SRB[a]	264 kl	340 kl	547 kl	630 kl	1.09 kl	0.0041	0.0032	0.0020	0.0017
Thermal Energy (cal)/SRB[b]	8.94×10^{10}	1.28×10^{11}	8.94×10^{10}	1.28×10^{11}	4.15×10^{8}	0.0046	0.0033	0.0046	0.0033
Maximum Water Vaporized/SRB	152 kl	218 kl	152 kl	218 kl	0.71 kl	0.0046	0.0033	0.0046	0.0033
Excess Liquid Water[c]	112 kl	122 kl	395 kl	412 kl	0.38 kl	0.0034	0.0031	0.0010	0.0009
HCl Released/SRB	7,940 kg	11,340 kg	7,940 kg	11,340 kg	36.9 kg	0.0046	0.0033	0.0046	0.0033
HCl/Excess Water Mass	0.071	0.093	0.020	0.028	0.097	1.37	1.04	4.86	3.47

NOTES: [a]Includes IOP, acoustic suppression, and, for ETR, 44 percent of Rainbird water per SRB.
[b]Includes 198 cal/gm from propellant burning plus 167 cal/gm from afterburning.
[c]Line one minus line three.

The IOP/acoustic suppression water is injected around the launch mount "holes" at the base of the vehicle. In the KSC configuration, water is also injected into the flame trenches and spread out onto the surface of the mobile launch platform. In both configurations, most of the interaction between water and exhaust occurs in the exhaust ducts. The excess water is ejected with the exhaust. At Kennedy, both SRBs are directed into one duct which empties horizontally toward the north. There are no structures to deflect the plume upward, but thermal buoyancy causes lifting after the initial jet decays. The KSC SRB exhaust duct configuration is shown in Figure 4.

At Vandenberg the situation is quite different. First, each SRB is directed into a separate duct, one toward the north and the other south. Second, the ducts are covered and of a more complex design, as illustrated by Figure 5. The covered portion of the north duct runs horizontal for 16 m, then upward at an 8-degree angle for 40 m. For the south duct, the horizontal run is 21 m, and the 8-degree run is 35 m. Both ducts open onto an uncovered apron area which extends upward at 15 degrees to ground level. Beyond the exit of the duct on the north side, the ground level drops gently beginning a few tens of meters beyond the opening. For the duct opening to the south, it drops quickly into the side of a small ravine, then rises fairly abruptly on the far side to a level above the top of the apron. The crest on the far side is less than 300 m from the launch mount; its elevation is such that it lies on the projection of the centerline of the 8-degree portion of the duct.

III. FIELD TEST RESULTS

A. Observations of Model Firings

The spray pattern of the acidic deposition in the immediate vicinity of the launch mount is primarily dictated by the exhaust duct and launch mount design. The projection angle in the vertical for the material ejected from the north duct was measured on the March 25, 1983, model firing. This was a 100 percent of baseline water flow, VLS configuration test with the vehicle at the zero elevation level (resting on the pad). An 8-m vertical pole was placed 31.5 m from the vehicle directly in line with the north duct. Test tubes were taped to the pole every half meter, each tilted toward the exhaust at about a 45-degree angle. Figure 6 illustrates the amount of material deposited in the tubes as a function of the projection angle above the horizontal relative to the lip of the apron. The maximum amount of material was found in the 8- to 10-degree range, indicating that the covered portion of the duct controls the elevation angle more than the 15-degree open apron. The distance of the measurement site to the vehicle, 31.5 m, corresponds to nearly 500-m full scale (applying a simple 0.064 scale factor).

In more than half of the 20 test firings that were studied, the primary objective of the measurement effort was to determine the deposition pattern on the ground. All of these tests were of the VLS configuration with 100 percent of baseline water flow. In some cases, the vehicle was elevated above the pad to simulate lift-off. Deposition measurements were made by setting out an array of collectors in the target area and volumetrically measuring the amount of deposition collected. In the first test, plastic petri dishes and 1-liter beakers were tried as collectors. The petri dishes were blown away by the exhaust and so were not usable. Beakers worked fairly well, but some of the exhaust material remained on the side walls rather than running down into the beaker. Even though the time from rocket firing to analysis was minimized (typically 1 hr) there was still concern that a substantial fraction of the deposition might evaporate before the beakers were gathered and the contents measured. Therefore, plastic cups with sealable

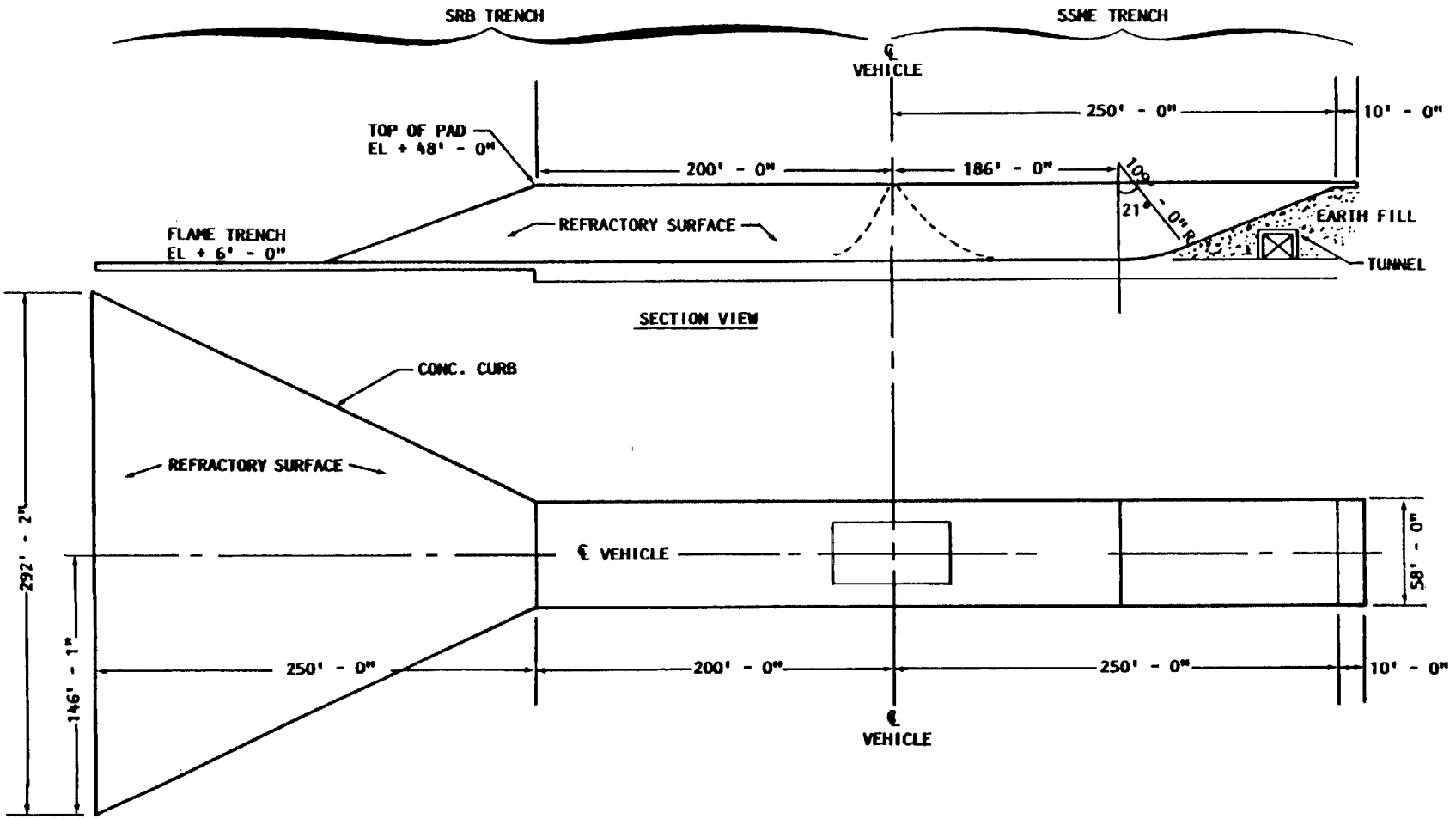

KSC CONFIGURATION
PLAN OF SSME & SRB FLAME TRENCH

Figure 4. Schematic of the Kennedy Space Center SRB exhaust duct.

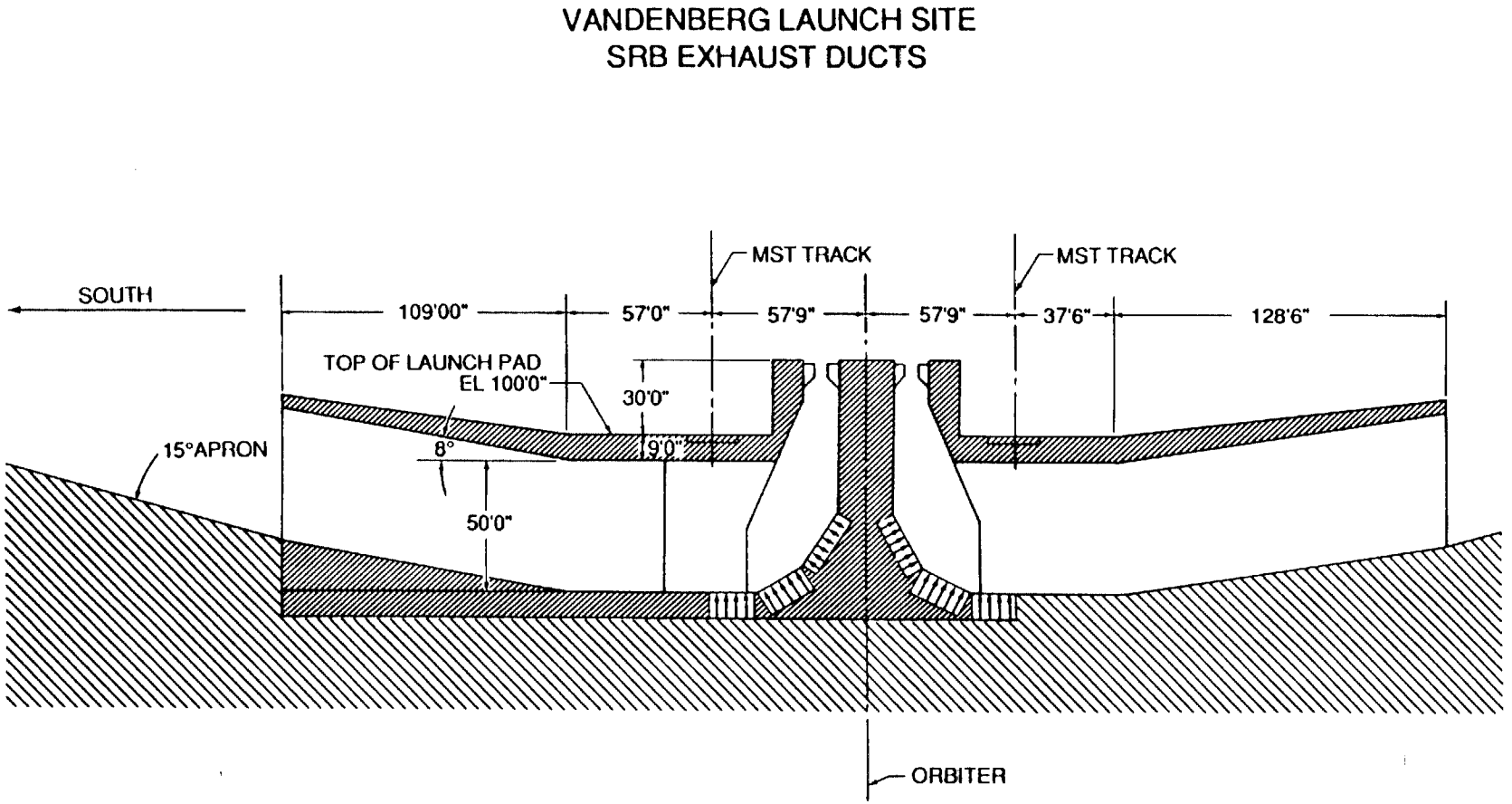

Figure 5. Schematic of the Vandenberg launch site SRB exhaust duct system as viewed from the east, looking west.

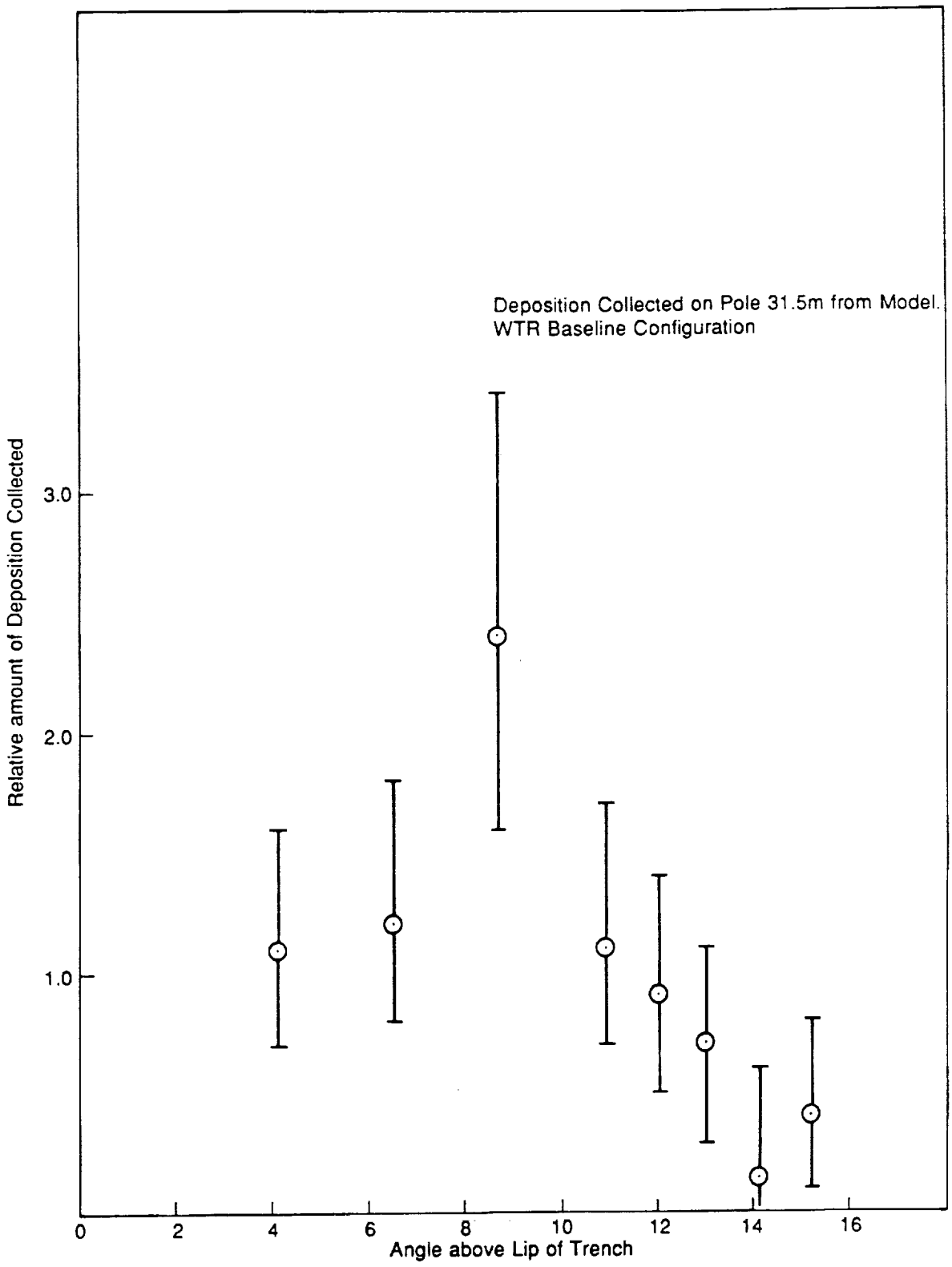

Figure 6. Angular distribution of deposition measured from the horizontal in a Western Test Range (Vandenberg) model configuration.

lids, 8.1-cm diameter by 6.3-cm deep, filled to within about 1 cm of the top with silicone oil, were used. The oil cups were much more labor-intensive and messy, but they provided more reliable results. Comparison with the first tests using beakers shows essentially identical results with both methods. The beakers, however, were used only during February and March when the temperature was 5 to 13 ^{o}C and evaporation was slow. The comparison would probably be less favorable if the beakers were used in summer.

Figures 7 through 10 display four of the measured deposition patterns, two with calm or very light winds and two with moderate winds. The outside contour shown in these figures represents the limit of the area completely wetted by deposition, or about 0.1 mm of liquid depth. This contour is easily located in the area to the left-hand side of the duct centerline because this area is paved out to 80 m from the vehicle and permanently marked with a polar coordinate grid. Immediately after a firing, the full wet/partial wet boundary was marked in chalk. However, 3 to 4 m to the right-hand side of the duct centerline, the pavement ends and the area is grass covered. A broad ditch, 5-m wide by 1.5-m deep, parallels the duct centerline with its center displaced about 12 m to the right. In this area, and beyond 80 m in all directions, the full wet/partial wet boundary must be estimated from the collector cup data with some loss in precision.

With little or no wind and the model vehicle at the zero elevation level (resting on the pad), the fully wetted area extends to about 80 m from pad center. Maximum breadth occurs at a range of about 50 m and is of order 35 m. To interpret this as an expectation for full scale one must apply a scale factor which, for the sake of simplicity, we assume to be 0.064. This simple linear scale factor would be expected to apply for a single phase, constant density gas jet. In actuality we are dealing with a two-phase flow with substantial temperature differences. Thus drag, gravitation, and buoyancy may be expected to play an important role. The 0.064 factor will lead to an over estimate of effects in the far field. Scaling the low wind values given above implies an upper limit range of about 1250 m and a maximum width of about 550 m at 800 m from the pad. With the vehicle raised above the pad the pattern narrowed and lengthened. At the maximum vehicle elevation tested, equivalent to 36.6-m (120 ft) full scale, the fully wet area extended to about 150 m which corresponds to a 2300-m full scale upper bound, measured from the pad center. As a point of comparison, observations at KSC indicate that the fully wet area extends 600 to 700 m north of the pad center. From a single observation made with the model in the KSC configuration, it appears the 0.064 factor over estimates the length of the wet zone by a factor between 1.3 and 2.1. For rough "best estimates" a scale factor of (1.7 x 0.064) = 0.11 is probably suitable.

The data set was also analyzed to obtain an indication of the range from the vehicle where the maximum depth of deposition may be expected. The location of this point varied from test to test. The lowest value observed occurred on the March 9, 1983, test (Fig. 9), which was certainly influenced by the wind. The value of 15 m would scale (x 1/0.11) to about 140 m at Vandenberg. The maximum distance of 40 m was observed on the September 9, 1983, test in a 4 m s^{-1} crosswind (Fig. 8). In this case the plume centerline was blown to the side of the main array of collectors so the true maximum may have been missed. At full scale, 40 m corresponds to about 360 m. The best data set for the vehicle at zero elevation (the March 25, 1983, test, illustrated in Fig. 7) and one other poor set show the maximum at 20 m (180-m full scale). Two tests with the vehicle elevated slightly gave maxima at 30 m (270-m full scale). However, since better than half of the water which becomes deposition is already in the trenches at L = 0 for both the Kennedy and Vandenberg launch sites, the actual full-scale pattern will tend to

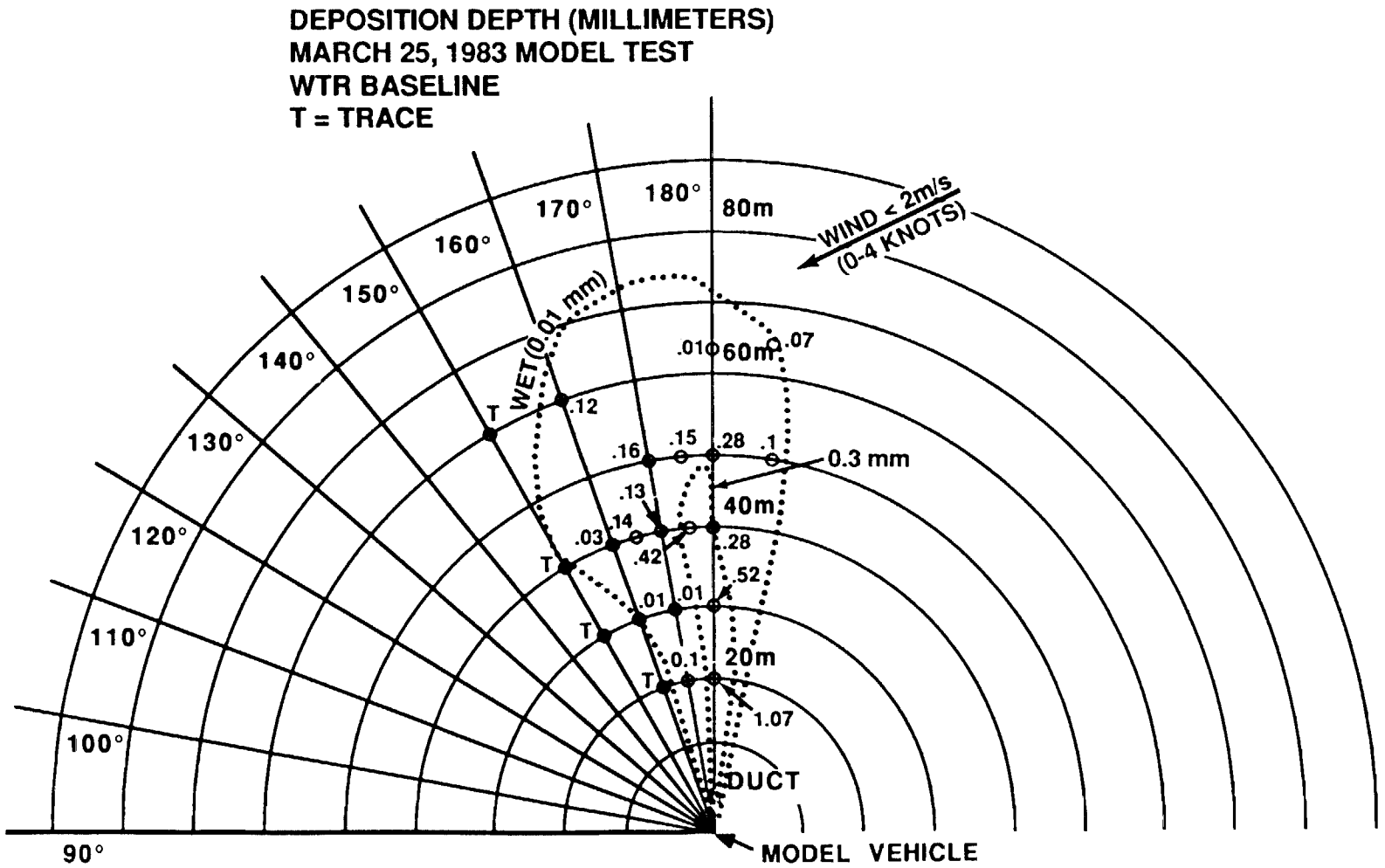

Figure 7. Deposition pattern for the March 25, 1983, VLS configuration model test. Depth figures are for total deposition, liquid plus solid. Distances indicated are for the model system.

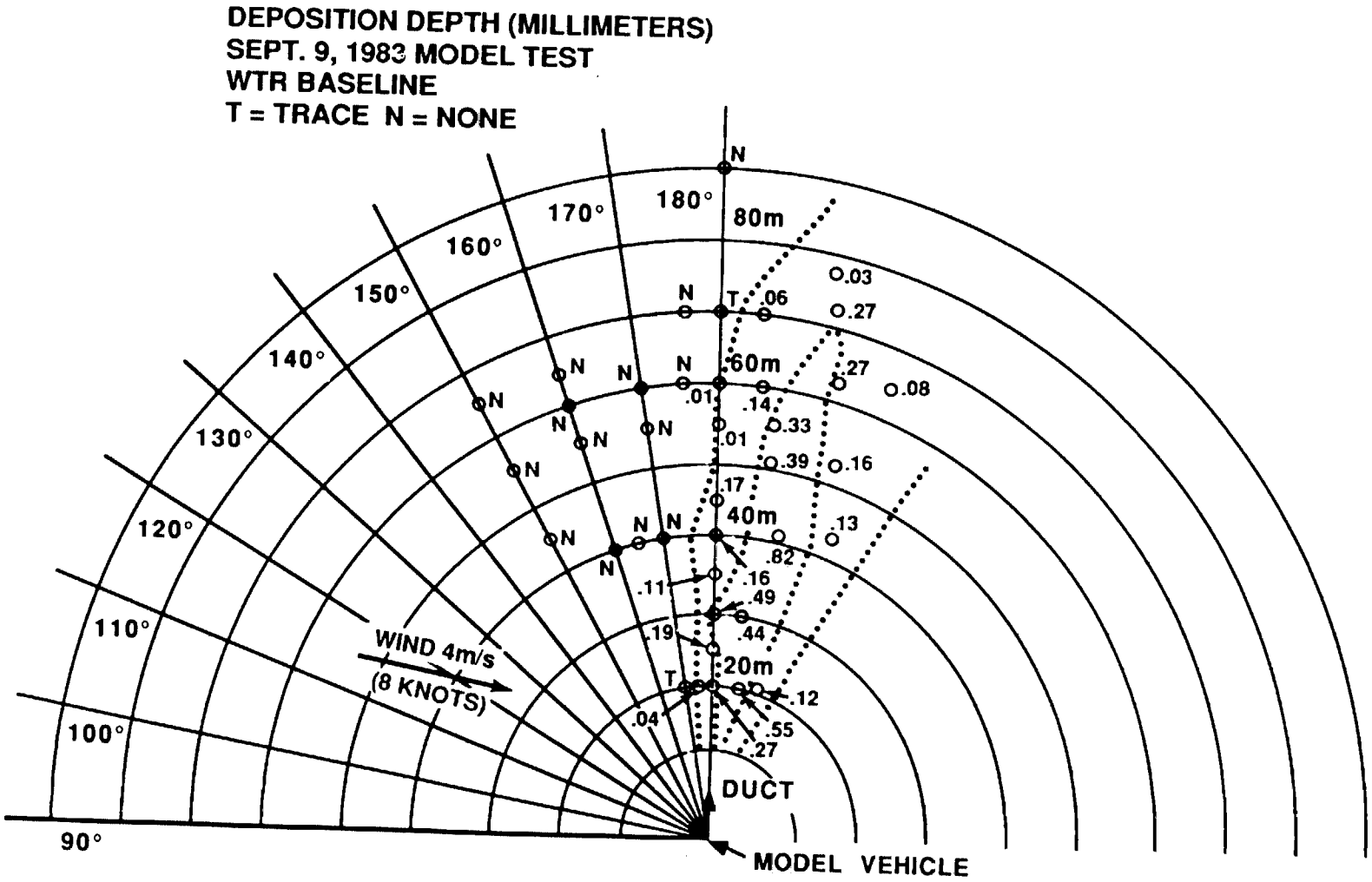

Figure 8. Deposition pattern for the September 9, 1983, VLS configuration model test. Depth figures are for total deposition, liquid plus solid.

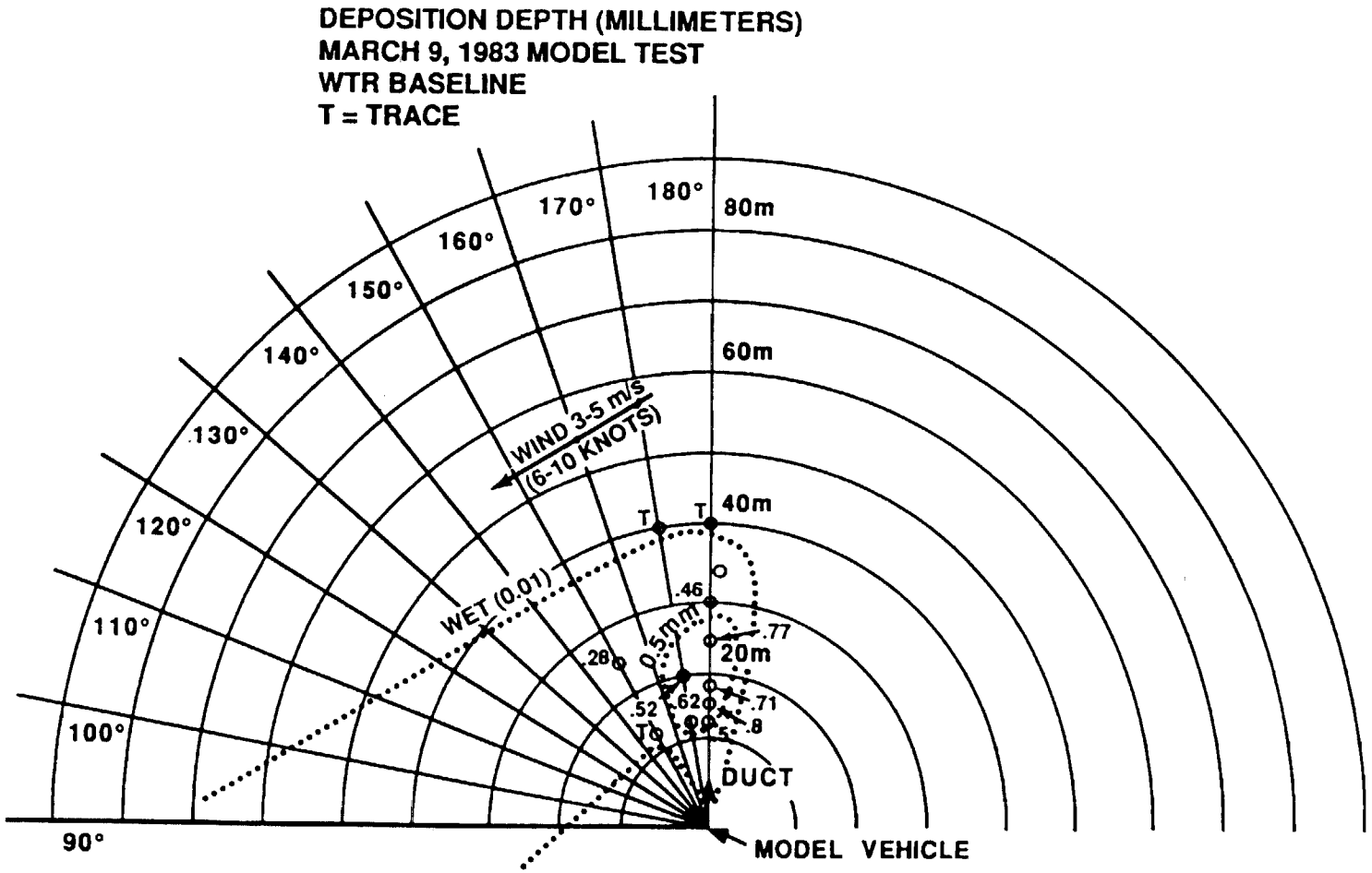

Figure 9. Deposition pattern for the March 9, 1983, VLS configuration model test. Depth figures are for total deposition, liquid plus solid.

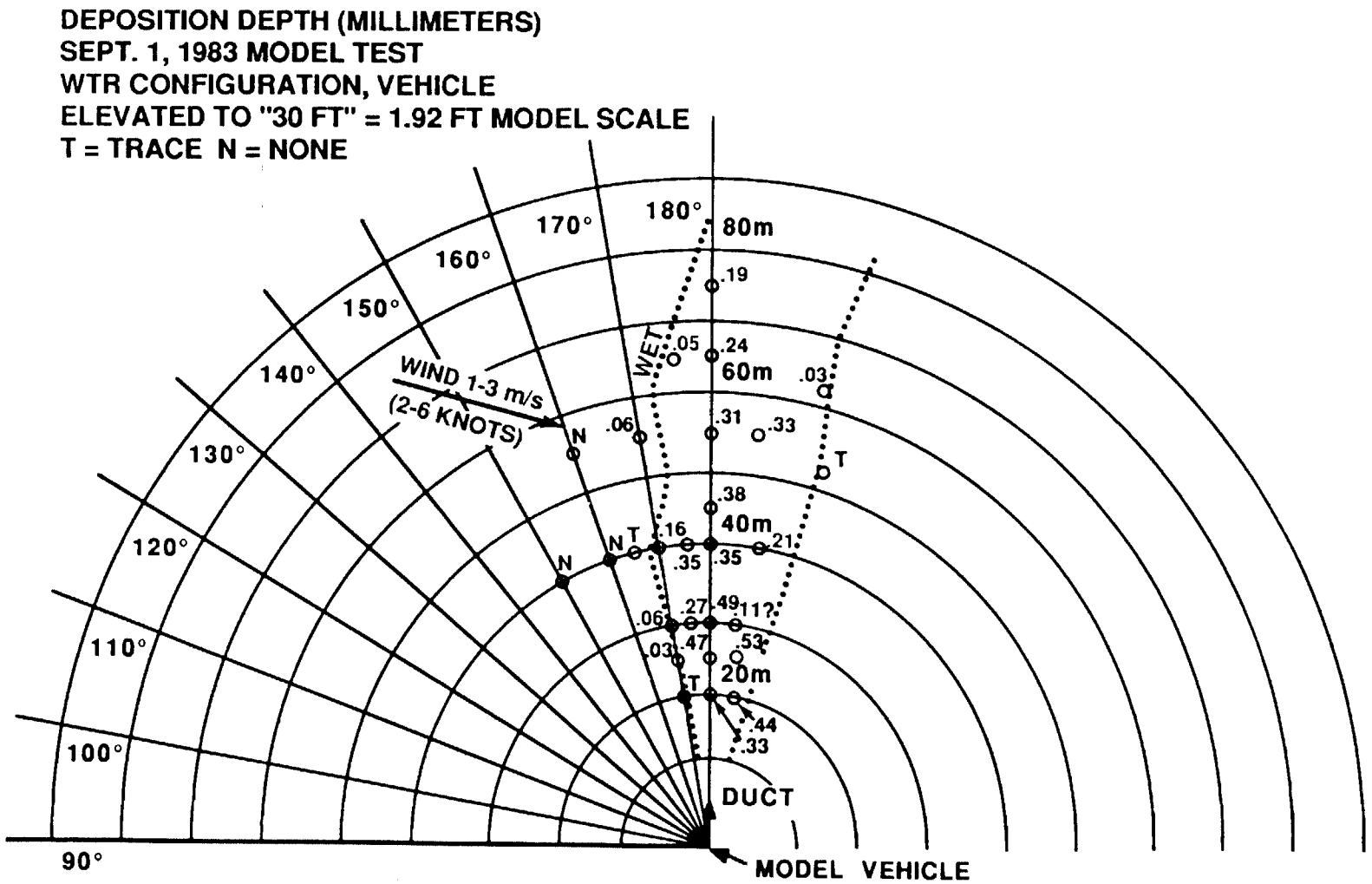

Figure 10. Deposition pattern for the September 1, 1983, VLS configuration model test. For this test, the model was anchored in an elevated position to simulate lift-off conditions.

look like the low vehicle elevation patterns. Thus at Vandenberg the maximum deposition depth may be expected at the 200 to 360 m range for calm or light crosswind launch conditions, assuming a 0.11 scale factor.

The deposition from both the model and actual shuttle launches is a solid/liquid mixture; hydrochloric acid, aluminum oxide granules from the solid rocket motors, bits of sand, seeds and other debris from the near pad area, and various dissolved trace elements. For the September 1 and September 9, 1983, model tests, the solid fraction of the deposition was found to be 11 percent in both tests with standard deviations of 4 and 5 percent, respectively. (The smallest samples were disregarded in obtaining these figures because the measurement is not believed to be reliable when the total amount of material is less than 0.5 ml. In the very small samples the solid fraction tends to appear much larger. Their inclusion in the data would drive the averages to 18 and 13 percent with standard deviations of 16 and 10 percent.) By comparison, samples from actual shuttle launches show a greater solid fraction. A single sample collected under oil during the STS-4 launch was 30 percent solid, 70 percent liquid. During the launch of STS 41D, samples were taken from an array of oil dishes identical to those used for the model tests. The average solid fraction for 12 samples was 27 percent with a standard deviation of 10 percent.

Apparently the solid fraction is determined by the rate of scavenging and the amount of time the drops spend in the cloud. At full scale the drops have much more time to collect solid material. At Vandenberg the physical size of the cloud should be about the same as at KSC, so one would expect about the same solid fraction in the deposition, about 30 percent, unless the aluminum oxide supply is limited relative to the amount of water; the amount of water is greater at VLS.

The data on the acid content of the deposition samples collected from the various model tests can be summarized as follows:

1. Eleven samples collected in beakers, without oil, in four test firings, all on cold days. Temperature at test time ranged from 5 to 13 ^{o}C: mean acidity = 1.26 normal (N), std. deviation = 0.20.

2. Samples collected under silicone oil (Dow Corning 200 Fluid, 500 cs) in "Freezettes," 9-cm diameter cups, from a test on a warm day. Model at "zero level" elevation, resting on the pad. Fifteen samples from September 9, 1983, test; temperature = 28 ^{o}C: mean acidity = 1.69 N, std. deviation = 0.27.

3. Samples collected by same method as 2 above, but from a test with the model elevated to the "30-ft" level. Thirteen samples from August 26, 1983, test; temperature = 32 ^{o}C (see Fig. 11): mean acidity = 1.64 N, std. deviation = 0.39.

4. Samples collected on warm days by the "milk stand" method. The bottom was cut out of a cleaned, polyethylene, gallon-size milk container that was mounted in an inverted position over a sample bottle. The milk container formed a large funnel and the sample jars could be quickly capped after the firing. The results are summarized in Table 3.

This data set contains considerable variability which is traceable to several causes. Some samples taken on or near the 0-degree azimuth show a systematically lower acid concentration than those from the 180-degree azimuth. Certainly this may be

expected because of the additional water from the SSME duct that is exhausted in this direction. It was also observed when examining the deposition drops in the oil cups, that some of the drops were clear liquid (plus solids) and some were definitely a light green color (plus solids). Both clear and green drops were found together in the same cups. It is suspected that the color difference is due to a chemical reaction of the HCl with some substance in the solid fraction of the deposition which is randomly mixed into some drops and not others. The effect is seen in samples collected well away from the influence of the SSME duct exhaust and it is not the effect of dew fall since the oil cups were usually deployed in the late morning or afternoon, a few hours before the firing.

TABLE 3. DEPOSITION NORMALITIES FROM "MILK STAND" COLLECTORS

Test Date	Temp. (^{o}C)	Location	Normality
Aug. 26, 1983	32	180^{o}, 25 m	2.07
		180^{o}, 30 m	1.94
		180^{o}, 40 m	2.63
Sept. 1, 1983	33	0^{o}, 30 m	1.40
		0^{o}, 50 m	1.56
		10^{o}, 30 m	0.75
		180^{o}, 40 m	1.63
Sept. 9, 1983	28	0^{o}, 25 m	1.70
		0^{o}, 35 m	1.83
		0^{o}, 45 m	2.19
		180^{o}, 25 m	2.20
		180^{o}, 35 m	2.40
		180^{o}, 45 m	2.45
Sept. 15, 1983	27	180^{o}, 30 m	1.84
		180^{o}, 40 m	1.97
		180^{o}, 55 m	2.05

Samples collected with the "milk stands" tend to show a higher acid concentration than samples collected under silicone oil. This is probably the result of water evaporation from the funnel surface; note that the "milk stands" were only used in the warm weather tests. To verify the silicone oil method, 20-ml samples of 2.5 N HCl were left in sample bottles for 10 weeks, one tightly capped and the other under 2.3 cm of oil (open part of the time). When titrated, the acid concentrations were equal within the expected accuracy of the titration, indicating that significant amounts of HCl were not absorbed into the silicone oil. Acid concentration of the cold weather samples collected in beakers is lower than the warm weather samples, indicating a significant temperature effect. The beaker samples must have been concentrated somewhat by water evaporation in the 30 to 60 min required to gather and transfer the samples into closed bottles, although at the cold temperatures involved the effect may not have been too great. However, the mean concentration, 1.26 N, is still less than the samples collected under oil on warm days, 1.64 and 1.69, but the difference is about the same magnitude as the

standard deviations in the data sets. Thus the temperature effect cannot be precisely quantified because of the scatter in the data. The temperature effect is even more noticeable when comparison is made with the "milk stand" samples which averaged 2.12 N for samples from the 180-degree azimuth.

Looking at Figure 11 and the data tabulated in Table 3, it is also noted that there is a systematic increase in acid concentration with range from the model within each data set. If the 11 data points from the 4 cold day tests are plotted together, they likewise show an increase in normality with range. In all cases, the scatter in the data set is large compared to this effect; but, considering the complete data set, it appears that the increase is of the order of 0.02 N/m.

B. Shuttle Launch Observations

A small field program designed to verify HCl revolatilization was conducted at KSC in conjunction with two launches in the late summer and fall of 1984. A time-resolved, spatially-averaged measurement of the total HCl concentration was desired to provide a general picture of the post-launch work environment on the pad. Hydrogen chloride can occur as either gas or as aerosol in combination with water, so simultaneous measurements of both forms are required. Both gas and aerosol measurements, and measurements of the amount of deposition near the pad, were made after the first launch studied, STS 41D. For the second launch, STS 51A, only HCl gas concentrations were measured. Deposition measurements for the 41D launch will be discussed first, followed by a description of the gas and aerosol measurements.

The same oil-cup technique developed for the model tests was used to sample the acid deposition on and around the launch pad at KSC. For safety reasons personnel must clear the pad area before fueling of the external tank begins on the night prior to the launch, and they cannot return until the pad is cleared several hours after lift-off. Thus the oil cups were deployed and left uncapped from prior to 8 p.m. the night before and picked up beginning shortly after noon on the day of the launch. Figures 12 and 13 show the deployment array. On Figure 12 the sites are annotated to indicate the appearance of the oil and the depth of the solid material collected; on Figure 13 they are annotated with acid normality (when the sample was large enough to obtain a measurement) and liquid depth. Both clear and greenish deposition drops were noted in the samples. The milky appearance of the oil in some cups was probably due to collection of fine liquid spray from the launch; the milkiness was greatest at locations where one might expect the most intense spray. In some samples the oil remained clear, so the possibility that the milkiness was caused by dew fall can be discounted in this case.

The HCl gas measurement effort was undertaken as a joint project sponsored by NASA and the Air Force Engineering and Services Center, Environmental Sciences Branch, Tyndall Air Force Base, Florida. The work was performed by the Arnold Engineering Development Center (AEDC), Air Force Systems Command. Michael G. Scott and Charles W. Pender, Jr., of Sverdrup Technology, Inc. (operating contractor for the propulsion test facilities at AEDC) were the principal investigators. Lt. Floyd Wiseman, AFESC/RDVS, was the Project Officer for the Engineering Services Center and Capt. Frank Tanji, AEDC/DOTR, was Project Manager for AEDC.

A long path infrared absorption technique using a Fourier transform spectrometer (FTS) was selected for this study because the launch site is on the sea coast and the background chloride concentrations may be high at times. Thus a gas measurement

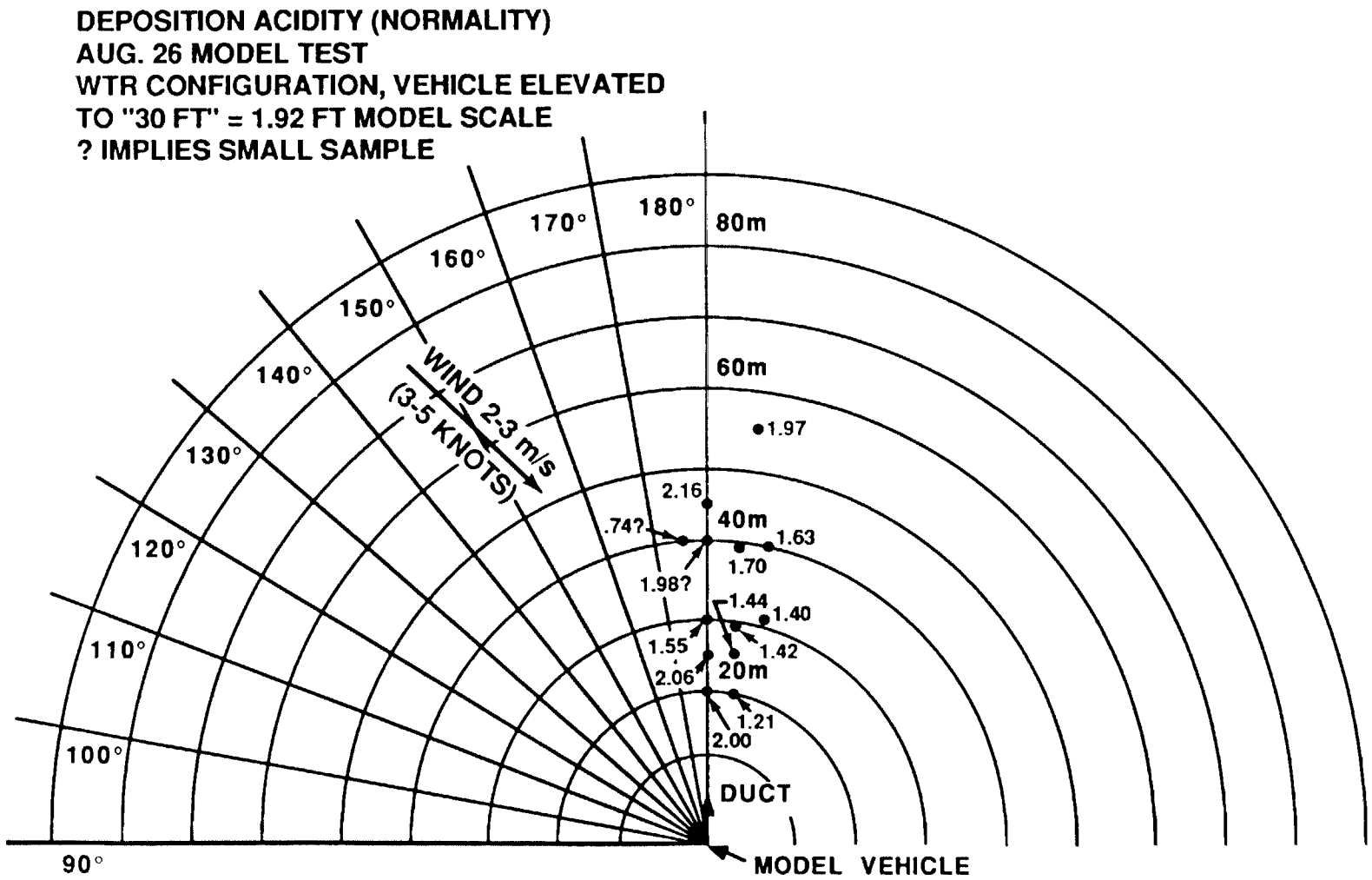

Figure 11. Deposition acidity pattern for the August 26, 1983, VLS configuration model test. For this test, the model was anchored in an elevated position to simulate lift-off conditions.

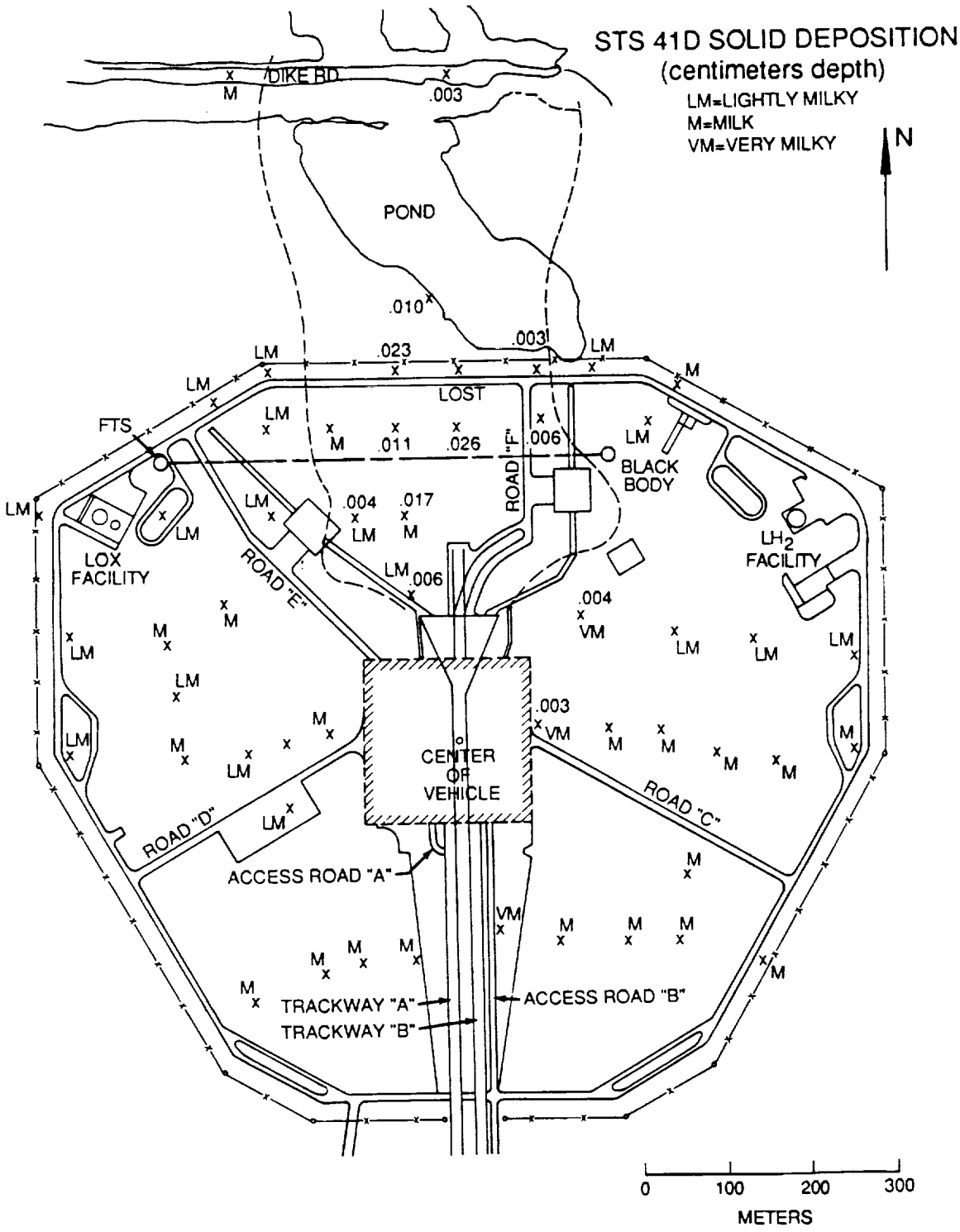

Figure 12. Deposition pattern found after the STS 41D launch. The line of site for the Fourier transform spectrometer gaseous HCl measurement is also indicated (FTS to blackbody).

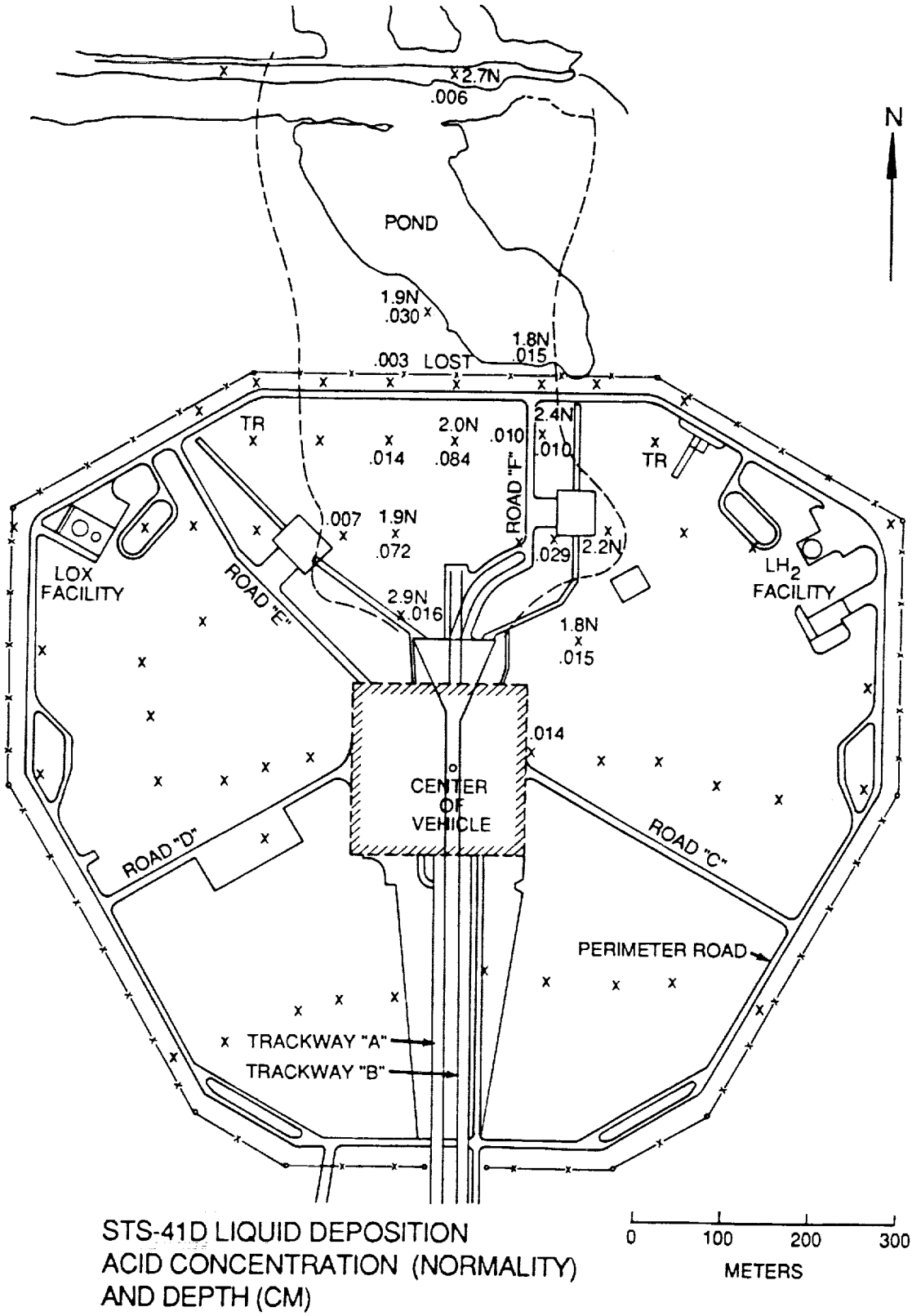

Figure 13. Liquid deposition depth and acidity pattern for the STS 41D launch. Depth is indicated in centimeters.

technique which is highly specific for HCl was required. In this technique, an infrared light source (a high temperature blackbody) is set up at one location and viewed with a telescope-FTS system from several hundred meters away. The spectrometer measures, as a function of wavelength, the absorption of the infrared energy caused by the gases along the path from the blackbody. Since HCl and other gases absorb at specific, known, wavelengths in the infrared, the presence of HCl can be definitely determined and the quantity measured from the ratio of the strength of the absorption lines to the background envelope. Laboratory calibration showed that the detection threshold for the system was about 0.5 ppm by volume.

At KSC the exhaust from both SRBs is ejected from a single horizontal trench which opens to the north onto a flat grass-covered area. The grass extends approximately 400 m from the launch pad to a lagoon and brush-covered area beyond the launch complex perimeter. The bulk of the wet acidic deposition from each launch falls onto this grass-covered area and the lagoon and brush beyond, making this the primary source of HCl revolatilization. Measurements for both the 41D and 51A launches were made directly over the grass-covered area within the perimeter fence. The absorption was measured along a 500-m path oriented east-west, approximately 1.2 m above the surface. The blackbody was east of the HCl source region; the FTS was on the west side. From 55 to 60 percent of the path was directly over the HCl source (Fig. 12).

The FTS used in this study was a Block Model RS197 configured for maximum sensitivity in the spectral region of interest, 3000 to 2700 cm^{-1}. The system used a germanium beam splitter on a potassium bromide substrate and an indium antimonide detector cooled to 77 K. Special precautions in the mounting and housing of the instrument were observed to enable it to withstand the severe acoustic vibration and corrosive HCl gas environments produced by the shuttle launch. At regular intervals, the system would collect 124 interferograms in a 2-min period, average the digitized data, and store the results on magnetic tape. The averaged interferograms were transformed into the spectral domain and the amount of HCl absorption determined at a later time. Sample absorption spectra from the laboratory calibration and the field data are illustrated in Appendix I. The interval between data collection was 20 min for the 41D launch; software improvements allowed this to be reduced to 10 min for 51A. For additional details on the system design, calibration, and operation, the reader is referred to Appendix I.

Hydrogen chloride revolatilization was measured after the 41D and 51A launches as shown in Figure 14. In Table 4, meteorological data and other relevant information concerning these launches are summarized. The HCl gas concentrations plotted as functions of time in this figure are computed assuming the gas is evenly spread throughout the 500-m path between the blackbody radiation source and the FTS receiver. In actuality, the concentration is expected to be somewhat greater over the source and less elsewhere. The precision of the 41D data is ±19 percent, ±15 percent for 51A. The difference is due to changes in the blackbody radiation source made between launches which resulted in a factor of 4 improvement in the signal-to-noise ratio.

For both launches, the HCl concentration reached a peak just over an hour after launch, remained high for an hour or so, then slowly decayed. The measurements were continued for 3 days following each launch. After 41D, no HCl was detectable after the 7-hr period illustrated by Figure 14. This was not the case after 51A. Trace amounts, less than a part per million, were detected between 8 a.m. and 2 p.m. local time on the day following the launch, and again between 10 a.m. and 1 p.m. on the second day after

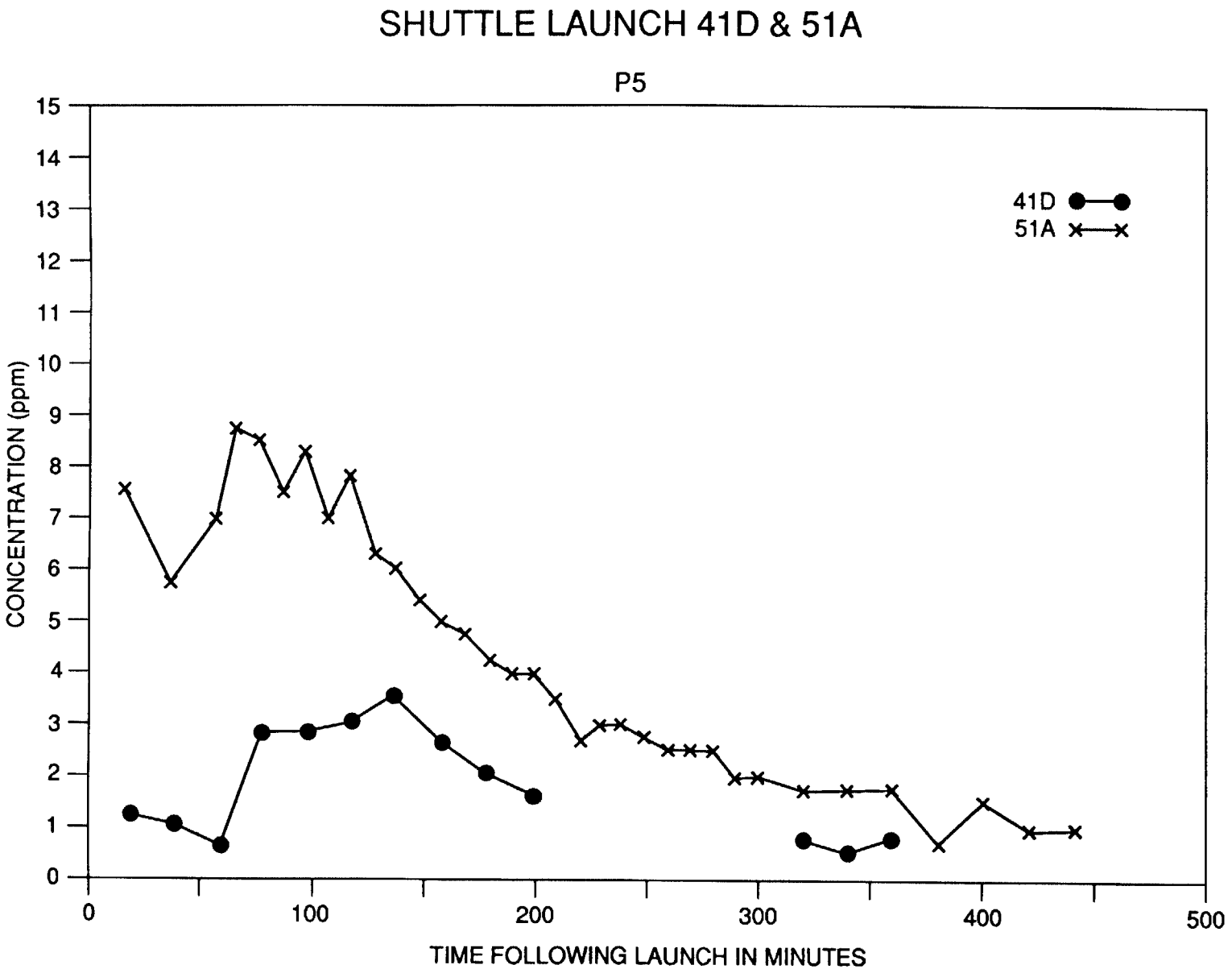

Figure 14. Post-launch HCl gas concentrations measured at the pad with an IR Fourier transform spectrometer: (1) STS 41D; (2) STS 51A.

the launch. The improvement in signal-to-noise ratio may account for the difference, but the initial source strength was also stronger after 51A.

TABLE 4. ENVIRONMENTAL CONDITIONS FOR 41D AND 51A LAUNCHES

Condition	STS 41D	STS 51A
Launch Date	Aug. 30, 1984	Nov. 8, 1984
Launch Time (local)	08:42 EDT	07:15 EST
Temperature (Celsius)	26	20
Relative Humidity (percent)	81	59
Wind Speed at 60 ft. (m s^{-1})	5	7
Wind Direction (degrees)	106	24

NOTE: The ground was dry during the 41D launch except for possible due from the night before. After the 51A launch, the ground was observed to be quite wet with standing water in some locations, apparently from thunderstorms in the area during the night.

Since the measurement method discussed above only detects gaseous HCl, the possibility that HCl vaporizes from the ground and then condenses to an aerosol phase must also be considered. In the aerosol phase, HCl in concentrations of a few parts per million should be readily detected by standard aerosol counting and sizing techniques, assuming there is no undue interference from local anthropogenic sources. For example, 1 ppm HCl by volume is equivalent to about 1.5 mg HCl per cubic meter. On the coast at ground level, sea salt aerosol concentrations of 1 to 15 μg m^{-3} for wind speeds up to 8 m s^{-1} may be expected (13). If the relative humidity is high, the background aerosol mass will increase by deliquescence, but it must exceed 98 percent relative humidity before the background would match the HCl mass concentration. Thus the HCl aerosol should, as a minimum, double the background levels if the concentration is 1 ppm or more in aerosol form.

Aerosol number concentration and size distributions were measured after the 41D launch using a Gardner counter to provide the total Aitken nucleus count (particles between 0.01 and 0.2 μm) and a Climet optical particle counter to give the number and size distribution for particles between 0.3 and 10 μm. The raw pulse output from the Climet was fed to a multichannel analyzer so that the entire size spectrum could be determined for each sample. The spectrum accumulated by the multichannel analyzer was dumped to paper tape at regular intervals. The system was housed in a van so that it could be moved alternately upwind and downwind of the source area.

It was intended that the Climet system would operate automatically, beginning the night before, right through the launch and post-launch period. Unfortunately, an equipment malfunction prevented this from happening so data were obtained only while the instrument was manually attended, beginning 1:49 p.m., after access to the pad was allowed. (The launch occurred at 08:42 EDT.) Eight 70.8-liter air samples, each drawn over a 10-min period, were taken downwind from the source area (at the FTS instrument location) between 1:49 and 3:53 p.m. Then between 4:30 and 5:30 p.m., five samples were taken upwind, at the camera site on the east side of the pad. Finally, four additional samples were collected downwind at the FTS site between 5:40 and 6:40 p.m. With the exception of one sample drawn just after 2 p.m., there was no systematic difference

between the up- and downwind samples; the difference between the average counts was less than the standard deviation. The count in the sample taken just after 2 p.m. was 2.8 times the mean, and the following sample also showed a high count, but traffic in the area was high at the time so the high counts are probably due to road dust.

The question of HCl/H_2O aerosol formation has been treated analytically by Rhein (14) and, more extensively, by P.V.N. Nair et al. (15). Their work indicates that at 20 °C the threshold for HCl aerosol condensation is 10 ppm at 80 percent relative humidity and 1 ppm for relative humidities over 91 percent. Thus examining the gas concentration data for the times of the aerosol measurements, aerosol formation would not be expected under these conditions, in agreement with the aerosol measurements.

IV. HCl REVOLATILIZATION ANALYSIS

The qualitative features of the HCl revolatilization process as illustrated by the 51A and 41D data (Fig. 14) may be explained quite simply. As discussed above, the launch leaves the pad area and the immediate vicinity on the north (SRB exhaust) side of the pad covered with drops or small pools of hydrochloric acid. Initially the acid is fairly dilute, about 2 N or less. For these low concentrations, the equilibrium vapor pressure of HCl is more than five orders of magnitude less than that of water over the solution. Thus the initial acid vapor concentration in the air is relatively low. However, it increases rapidly as the drops, small ones first, lose water by evaporation and increase in acidity. When evaporation has proceeded to the point that less than a quarter of the mass of a drop remains, the concentration reaches a value on the order of 11 N and the acid and water vapor pressures are equal. Thus most of the acid is released in the final stage of evaporation of each drop. Therefore, the ambient HCl vapor concentration rises to a peak as the majority of drops evaporate, small ones first. Then it falls slowly, fueled only by the much slower evaporation of the largest drops, small pools, and acid in the surface soil layer.

To develop a quantitative treatment of this process we note first the great similarity to the problem of evaporation of water or other pure liquid from a pool or field. These problems have been treated extensively in the literature because of their great importance to hydrology, agriculture, and the study of chemical spills. A full treatment is quite complex, since the evaporation rate depends on many variables including wind speed, ambient humidity, solar insolation and cloud cover, atmospheric stability and turbulence, terrain features and surface roughness, vegetation cover, etc. The HCl revolatilization is more complex, however, because it involves the interdependent evaporation of two substances, acid and water.

In this study, an attempt is made only to elucidate the basic nature of the revolatilization process and the measurements already discussed. Development of a detailed revolatilization model is beyond the current scope of the project. Instead, a highly simplified treatment of the key aspects of the problem has been developed which will serve to explain the basic physics. This treatment is expressed as a simple numerical model listed in Appendix II. The essential aspects of the model are as follows:

1. The source area is assumed to be covered initially with a Gaussian distribution of hemispherical drops, all of the same acid concentration. Initial parameters to be specified: mean radius, total liquid volume per square meter, standard deviation of size distribution, and acid content (weight percent).

2. The rate at which pure water would evaporate from the surface is computed using a simple empirical formula defined in the classic work by Penman (16). The evaporation rate is expressed as a function of the following variables: wind speed, ambient humidity, air temperature, and surface temperature. The surface temperature is typically not measured and it is fairly difficult to calculate since it is a function of a number of parameters. Specifying it as an input is one of the major simplifications of this treatment.

3. Beginning with the initial conditions, the evaporation of acid and water is calculated as a function of time. The evaporation from each drop size class is determined by the number of drops and the microphysical parameters, drop radius, acid concentration, surface temperature, and an estimate of the near-field acid and water vapor concentrations from the prior time step. At each time step, the total amount of material evaporated is normalized via the ratio of latent heats to the amount of evaporation (water) given by the Penman equation.

4. As the evaporation process proceeds and the surface begins to dry, the total amount of evaporation given by the Penman equation is adjusted down in proportion to the ratio of wet to dry surface.

The model outputs the HCl source strength per square meter of surface as a function of time. The mixing process into the atmosphere is not modeled. For this reason, and because ground temperatures were not measured following the launches for which data were obtained, a direct comparison between model output and measurements is not possible. However, comparing Figure 15, which displays the model output for cases approximating the 41D and 51A post-launch conditions, to Figure 14, it is clear that at least the basic form of the functional dependence with time is correct. If the HCl from a strip 100 m long by 1 m wide (aligned with the wind) is assumed to mix into a volume of air 2 m high by 1 m wide by U x Dtime long (U = wind speed and Dtime = the time interval), it is found that the model output is the right order of magnitude to explain the observed results. Examination of Table 5 and Figures 16 through 22, which illustrate the dependence of the HCl source on the various parameters, shows that the model results are quite sensitive to these variables. Thus considerable additional work is required to complete validation of this analysis. It is presented here to indicate the types of dependence the HCl revolatilization is expected to show on the various parameters and to serve as a basis for future modeling efforts.

It is anticipated that a complete model of the revolatilization process could be developed quite readily based results is desired, it could be obtained by replacing the empirical Penman equation with a simple model for evaporation from a pool such as the modified Ille and Springer model as discussed by Kunkel (17); coupling the results (the source term) to a Gaussian diffusion model like that discussed in Refs. (18) through (20). Additional work to improve the numerical methods and reduce the computation time required by the current model would be well worthwhile.

V. SUMMARY

Whenever large solid rocket motors which produce hydrogen chloride as an exhaust product are launched or test fired from a facility which causes the exhaust to mix with large volume water sprays (more than can be evaporated by the exhaust heat), an appreciable acid deposition in the near field is going to result. Some details of the production mechanism and, more importantly, the scaling are not yet fully worked out, so

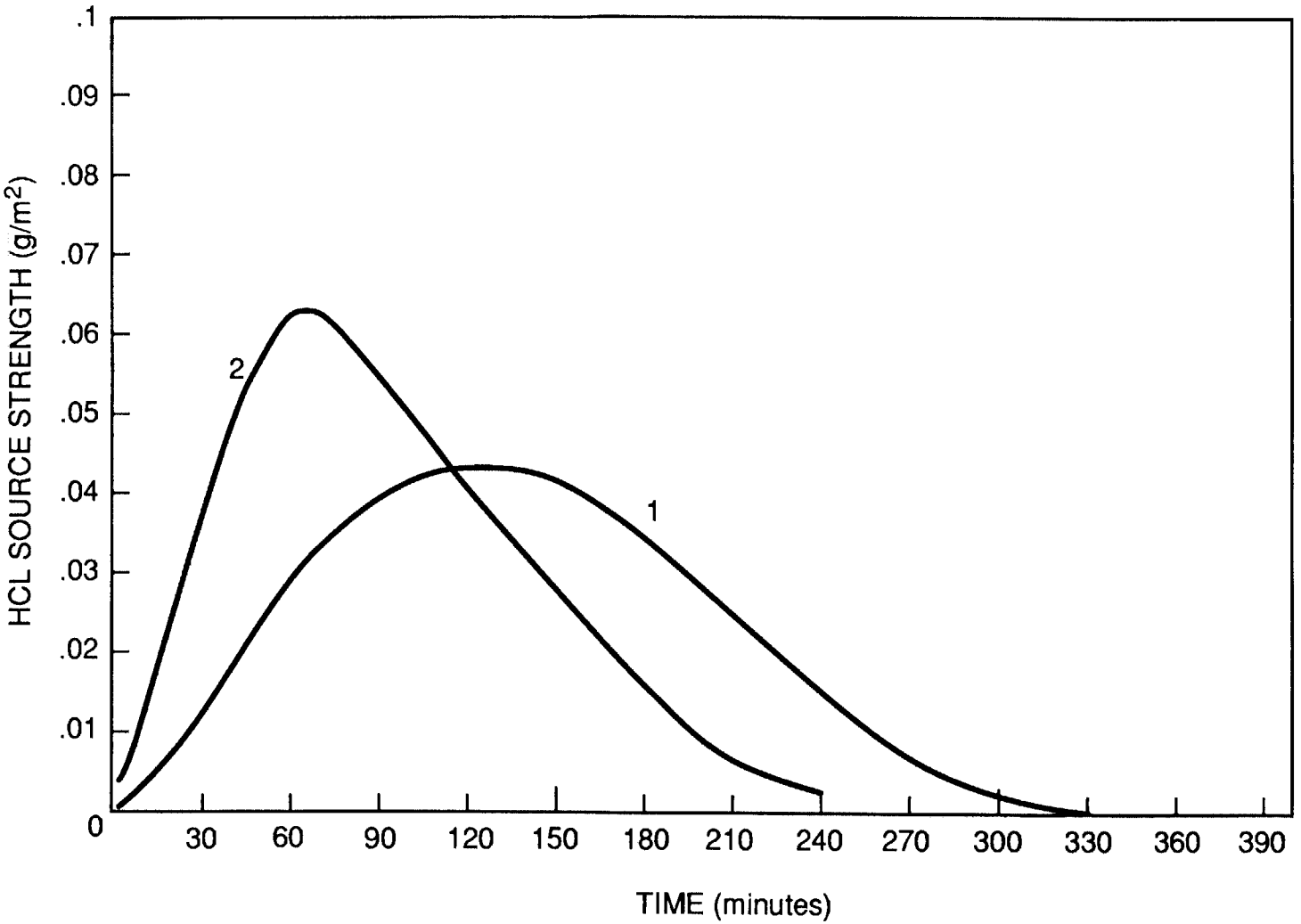

Figure 15. Analytical model HCl source strength: (1) STS 41D conditions; (2) STS 51A conditions.

TABLE 5. CROSS TABLE OF PARAMETER VARIATIONS FOR ANALYSIS MODEL CASE STUDIES

Case Designation	Sigma (cm)	T Delta (C)	U Delta (m/s)	D Delta (C)	Acid Conc. (wt. %)	Init. Vol. (cm^3/m^2)	Mean Drop Rad (cm)	Area Factor
BAS47L (Baseline)	0.08	4	0	0	7	100	0.1	2
U-VAR 1	0.08	4	1	0	7	100	0.1	2
U-VAR 2	0.08	4	5	0	7	100	0.1	2
U-VAR 3	0.08	4	**	0	7	100	0.1	2
D-VAR 1	0.08	4	0	+3	7	100	0.1	2
D-VAR 2	0.08	4	0	-3	7	100	0.1	2
D-VAR 3	0.08	4	0	-6	7	100	0.1	2
T-VAR 1	0.08	6	0	0	7	100	0.1	2
T-VAR 2	0.08	10	0	0	7	100	0.1	2
T-VAR 3	0.08	0	0	0	7	100	0.1	2
A-VAR 1	0.08	4	0	0	7	100	0.1	1
A-VAR 2	0.08	4	0	0	7	100	0.1	3
A-VAR 3	0.08	4	0	0	7	100	0.1	4
R-VAR 1	0.08	4	0	0	7	100	0.05	2
R-VAR 2	0.08	4	0	0	7	100	0.15	2
R-VAR 3	0.08	4	0	0	7	100	0.20	2
V-VAR 1	0.08	4	0	0	7	50	0.1	2
V-VAR 2	0.08	4	0	0	7	150	0.1	2
V-VAR 3	0.08	4	0	0	7	200	0.1	2
SGVAR 1	0.02	4	0	0	7	100	0.1	2
SGVAR 2	0.04	4	0	0	7	100	0.1	2
SGVAR 3	0.06	4	0	0	7	100	0.1	2

**No wind.

NOTE: The baseline case is the best fit to the STS 41D post-launch data. The actual time variations of air temperature, dew point, and wind speed were approximated by linear curve fits.

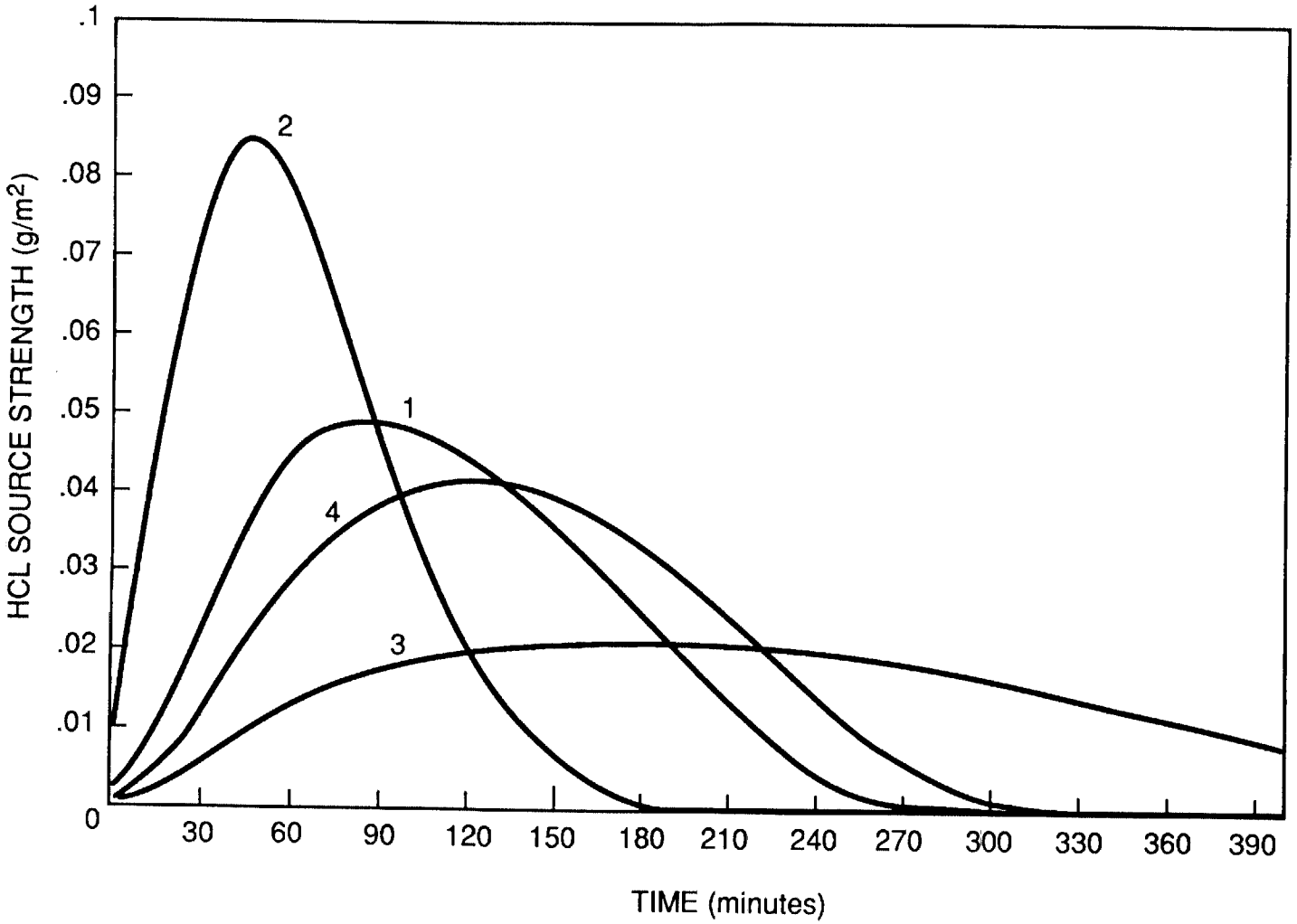

Figure 16. Analytical model HCl source strength results illustrating dependence on wind speed: (1) U-VAR 1, 1 m s^{-1}; (2) U-VAR 2, 5 m s^{-1}; (3) U-VAR 3, 0 m s^{-1}; (4) BAS47L.

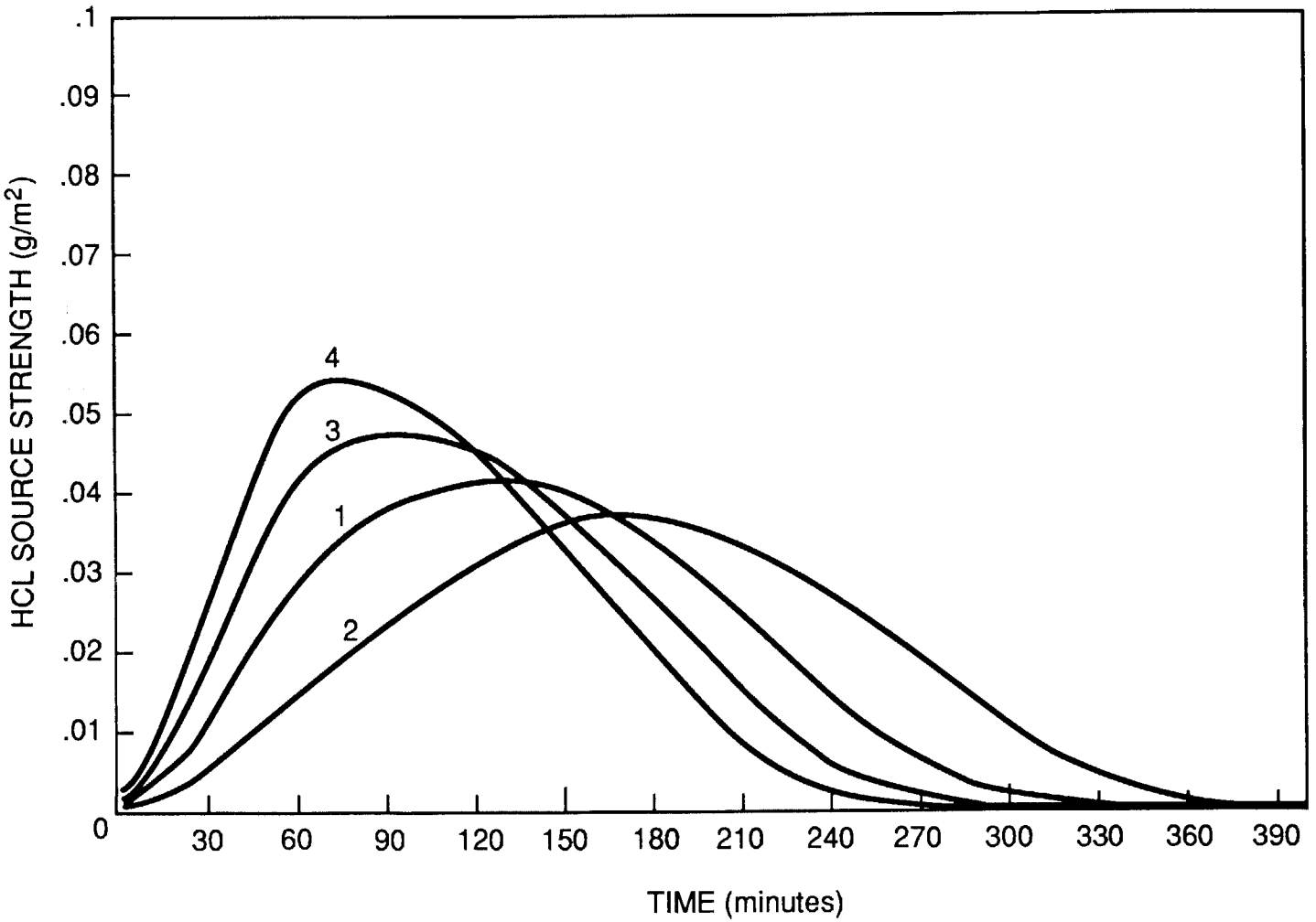

Figure 17. Analytical model HCl source strength results illustrating dependence on dew point temperature: (1) BAS47L; (2) D-VAR 1, +3 °C; (3) D-VAR 2, -3 °C; (4) D-VAR 3, -6 °C.

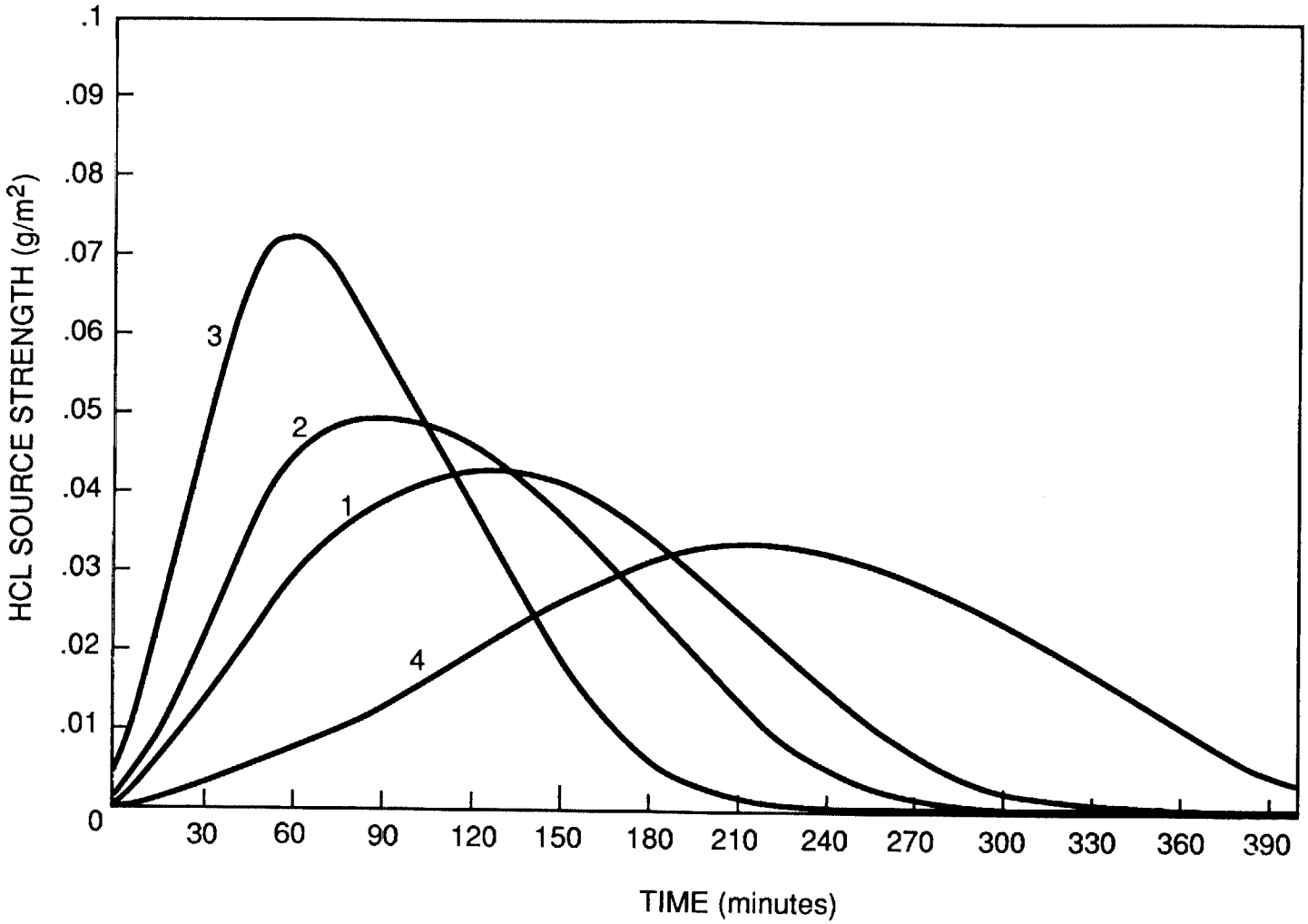

Figure 18. Analytical model HCl source strength results illustrating dependence on surface temperature: (1) BAS47L; (2) T-VAR 1, 6 °C; (3) T-VAR 2, 10 °C; (4) T-VAR 3, 0 °C.

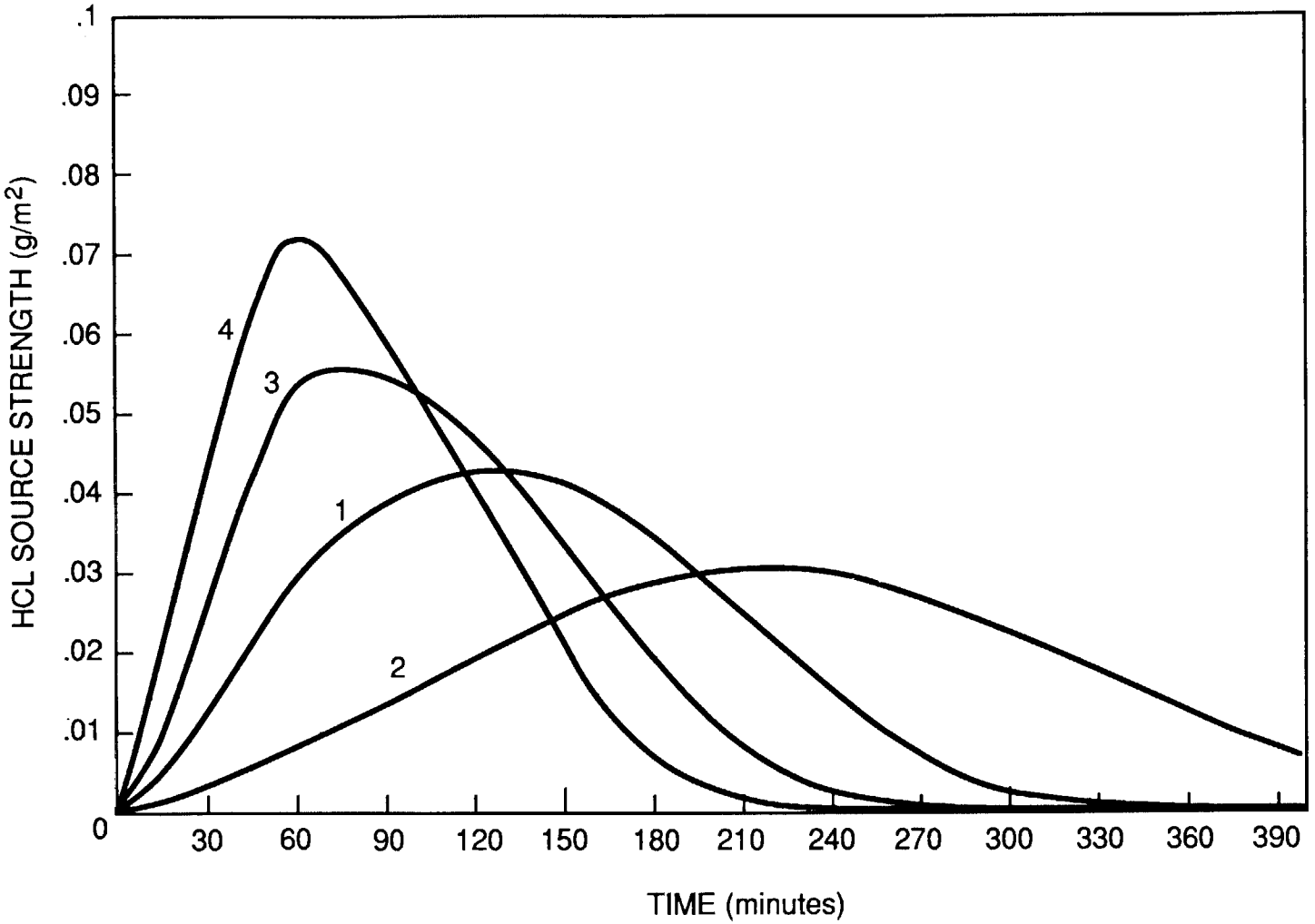

Figure 19. Analytical model HCl source strength results illustrating dependence on area factor for evaporation reduction: (1) BAS47L; (2) A-VAR 1, 1; (3) A-VAR 2, 3; (4) A-VAR 3, 4.

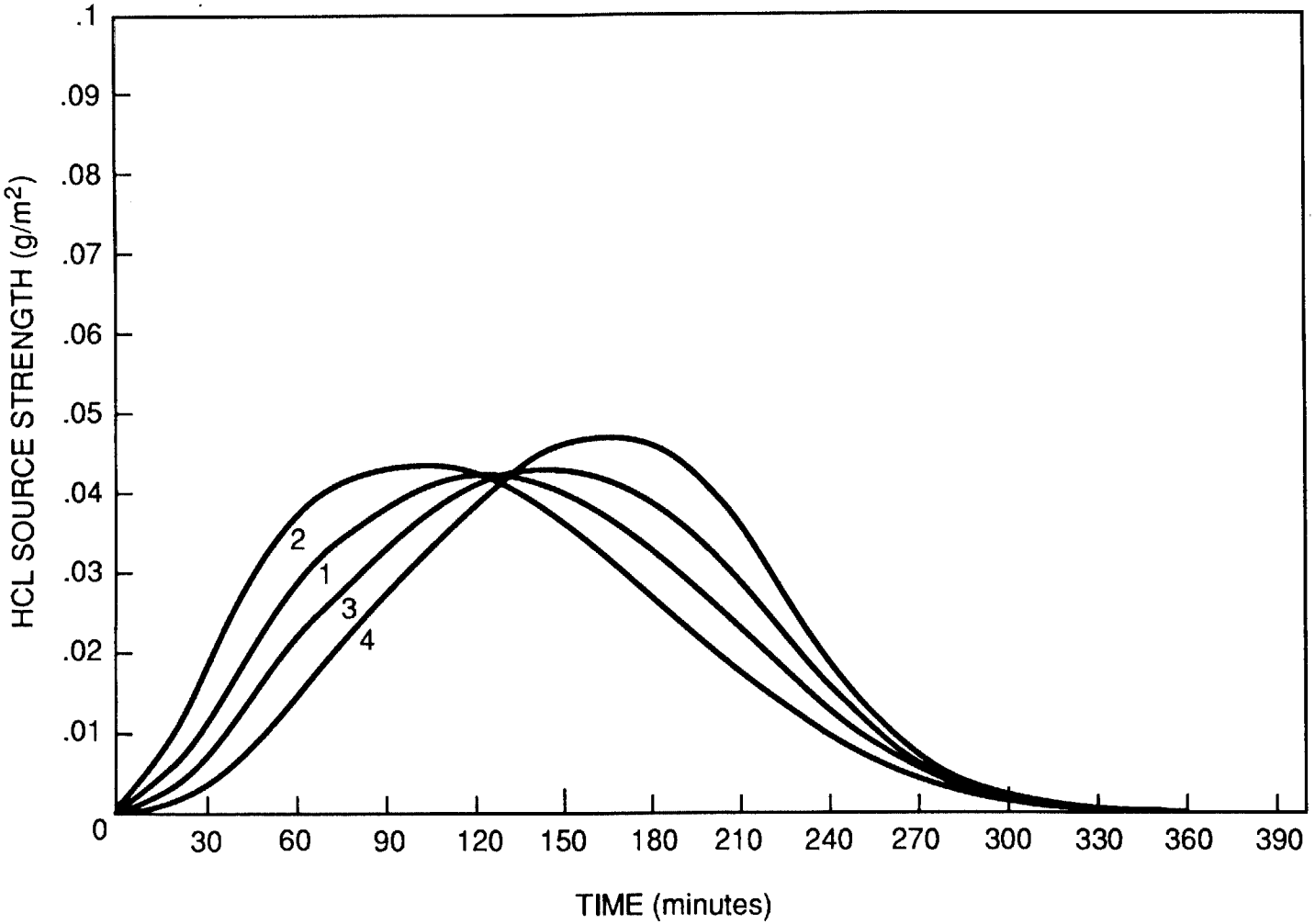

Figure 20. Analytical model HCl source strength results illustrating dependence on drop radius: (1) BAS47L; (2) R-VAR 1, 0.05 cm; (3) R-VAR 2, 0.15 cm; (4) R-VAR 3, 0.20 cm.

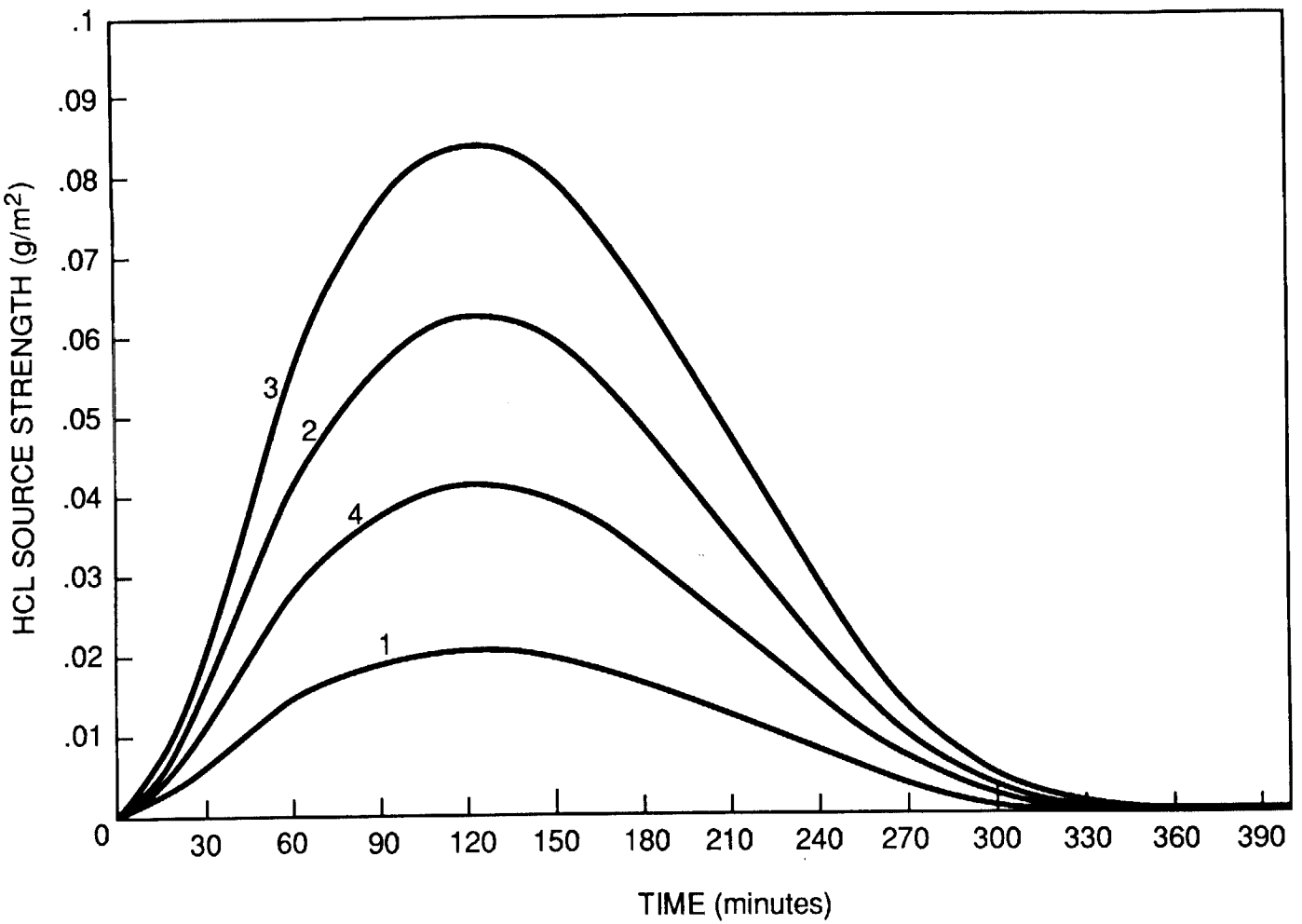

Figure 21. Analytical model HCl source strength results illustrating dependence on initial volume of deposition: (1) V-VAR 1, 100 cm^3 m^{-2}; (2) V-VAR 2, 50 cm^3 m^{-2}; (3) V-VAR 3, 150 cm^3 m^{-2}; (4) BAS47L.

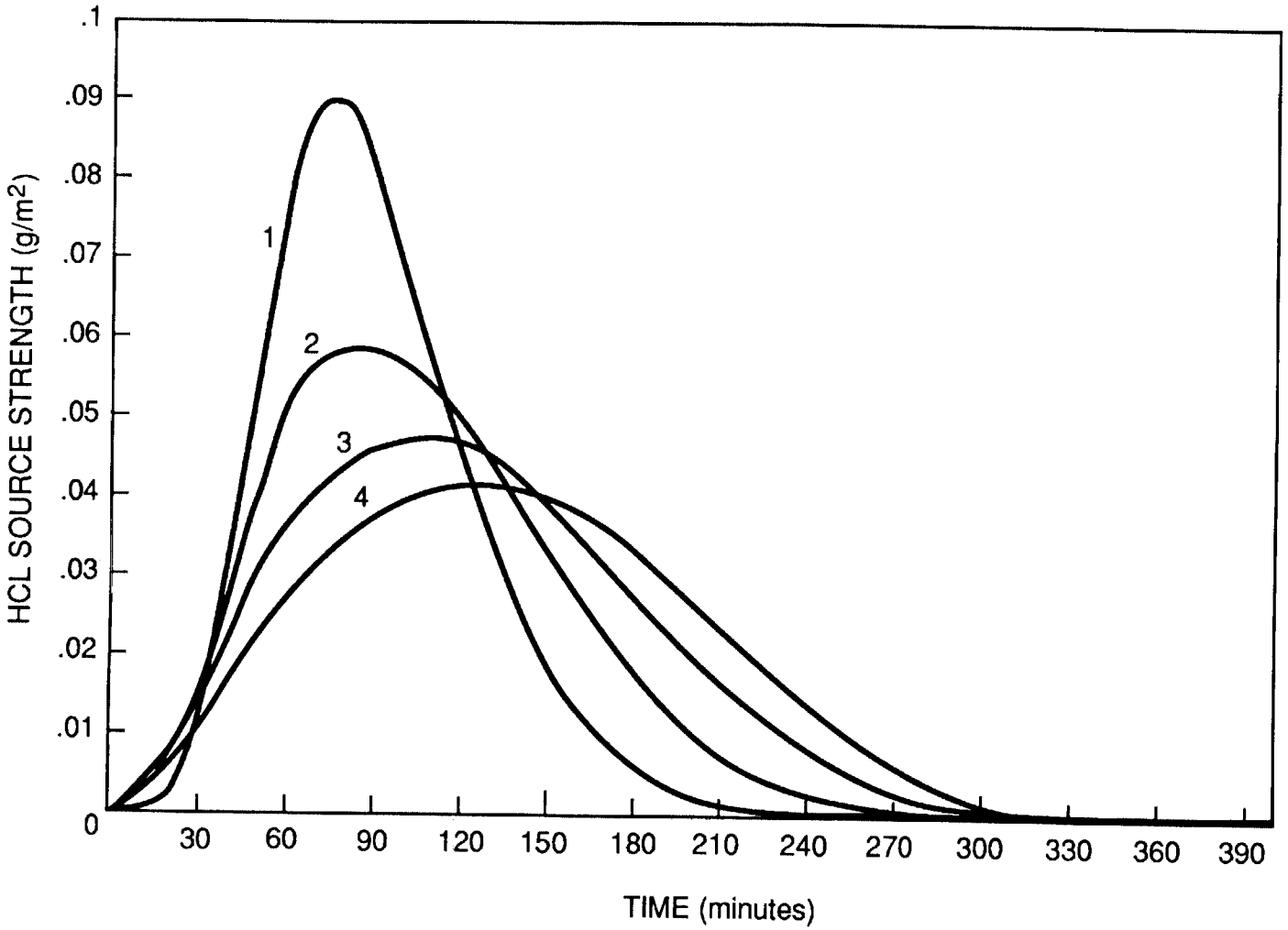

Figure 22. Analytical model HCl source strength results illustrating dependence on the width of the drop size distribution, sigma: (1) SGVAR 1, 0.02 cm; (2) SGVAR 2, 0.04 cm; (3) SGVAR 3, 0.06 cm; (4) BAS47L.

quantitative predictions of the amount and location of the deposition can only be estimated for new systems. However, the important parameters have been identified and the estimates should be adequate for most engineering applications, especially since the wind and other weather effects may be expected to generate considerable variability in the initial deposition pattern and subsequent effects.

The life cycle of the acid deposition, once it occurs, is well established by the field and model scale measurements and the analysis presented here. The initial deposit is moderately acidic, of order 2 N for space shuttle launches at KSC. As the material evaporates, the water vaporizes much more rapidly than the HCl so the acid concentrates until the water and HCl vapor pressures are equal, at about 11 N. If the evaporation potential is high (warm temperatures, low humidity, and moderate to high wind speeds), the evaporation will proceed rapidly enough that corrosion damage from direct contact with the liquid will not be immediately evident except on the most susceptible exterior surfaces. The dominant effect in this case will most often be the aluminum oxide particulate deposition which is scavenged from the exhaust along with the HCl. The acid has the effect of increasing the bonding between the aluminum oxide and structure surfaces, so the surface ends up coated by a powder which is difficult to remove except by direct mechanical scrubbing. At launch or test sites where this coating is expected to be a problem, the addition of chemical additives to the facility water to reduce this bonding should be investigated.

Under meteorological conditions when the evaporation potential is low, experience has shown that the concentrated deposition remains on painted and metal surfaces long enough to cause immediate corrosion damage, spotting on automobile chrome for example, and burn spots on vegetation. The residual aluminum oxide powder is still a problem under these circumstances, although the drying may be slow enough that the timely application of sprinkler systems and washdown hoses may alleviate the situation on the portions of the facilities that can be reached before evaporation is complete.

For Vandenberg SLC-6 and similar facilities where extensive computer and electronic equipment is located in close proximity to the launch pad, the most serious problem associated with acid residue from a firing is not likely to be the liquid deposition itself, but the HCl gas which evolves as the liquid evaporates. Equipment of this type is often very sensitive to corrosion damage from gas concentrations in the 10 to 100 parts per billion level. Exposures of 8 to 10 hours may render a computer system inoperable. The measurements reported here confirm that HCl concentrations above this level may be expected intermittently at the launch site for at least 2 days following a firing. They also verify that the concentration can exceed 5 ppm for brief periods in the first few hours; 5 ppm is the threshold limit value for workers; 1 ppm is the public exposure limit. Dangerous levels in low, enclosed, or partially enclosed structures are also a possibility. Thus the safety aspects of the HCl evaporation must not be ignored, although fairly straightforward precautions should be adequate for most situations.

VI. REFERENCES

(1) Anderson, B. J., and V. W. Keller: Space Shuttle Exhaust Cloud Properties, NASA TP-2258, December 1983, 112 pages.

(2) Knott, W., A. Koller, Jr., and J. Puleo: Environmental Effects of STS-1 through STS-4 Launches: Comprehensive Report, from Space Shuttle Environmental Effects: The First Five Flights (proceedings of the NASA/USAF Space Shuttle Environment Conference, Kennedy Space Center, Florida, December 14-16, 1982), July 1983, 30 pages.

(3) Dreschel, T. W., and C. R. Hall: Near-Field Deposition Patterns of Chlorides and Particulates Resulting from Launches of the Space Transportation System at the John F. Kennedy Space Center, NASA TM-89194, October 1985, 21 pages.

(4) Schmalzer, P. A., C. R. Hinkle, and T. W. Dreschel: Far-Field Deposition from Space Shuttle Launches at John F. Kennedy Space Center, Florida, NASA TM-83104, July 1986, July 1983, 42 pages.

(5) Cofer, W. R., III, G. L. Pellett, D. I. Sebacher, and N. T. Wakelyn: Aluminum Oxychloride Formation on Space Shuttle Exhaust Alumina, from Space Shuttle Environmental Effects: The First Five Flights (proceedings of the NASA/USAF Space Shuttle Environment Conference, Kennedy Space Center, Florida, December 14-16, 1982), pp. 141-147.

(6) Keller, V. W.: Ice Nucleus Activity Measurements of Solid Rocket Motor Exhaust Particles, NASA TM-86555, September 1986, 21 pages.

(7) Cofer, W. R., III, G. Garland Lala, and James P. Wightman: Analysis of Mid-Tropospheric Space Shuttle Exhausted Aluminum Oxide Particles, Atmospheric Environment, Vol. 21, No. 5, 1987, pp. 1187-1196.

(8) Schmalzer, P. A., C. R. Hinkle, and D. Breininger: Effects of Space Shuttle Launches STS-1 through STS-9 on Terrestrial Vegetation of John F. Kennedy Space Center, Florida, NASA TM-83103, September 1985, 39 pages.

(9) Milligan, J. E., and G. B. Hubbard: Near Field Effects of STS Launches, AIAA Shuttle Environment and Operations Meeting, Paper 83-2618, Washington D.C., October 31-November 2, 1983 (see also USAF OEHL, Brooks AF Base, Report 83-096EE003AFA by the same authors).

(10) Christensen, W. E., J. D. Langwell, and E. S. Barnes: Temporal and Spatial Gaseous HCl Concentrations in the Near Field STS Post-Launch Environment, AIAA Shuttle Environment and Operations Meeting, Paper 83-2617, Washington D.C., October 31-November 2, 1983.

(11) Zak, A.: The Determination of Exhaust Cloud Dimensions From Films of Space Shuttle Launches, NASA Contractor Report CR-4103, ST Systems Corporation, Hampton, Virginia, December 1987, 53 pages.

(12) Chen, C., and J. A. Zak: A Cloud Model Simulation of Space Shuttle Exhaust Clouds in Different Atmospheric Conditions, NASA Contractor Report CR-4223, ST Systems Corporation, Hampton, Virginia, March 1989, 136 pages.

(13) Blanchard, D. C.: The Production, Distribution, and Bacterial Enrichment of the Sea-Salt Aerosol, Air-Sea Exchange of Gases and Particles, P. S. Liss and W. G. N. Slinn, eds., 1983, pp. 407-454.

(14) Rhein, R. A.: Hydrochloric Acid Aerosol Formation by the Interaction of Hydrogen Chloride with Humid Air, NASA TM-33658, Jet Propulsion Laboratory, Pasadena California, November 15, 1973, 10 pages.

(15) Nair, P. V. N., P. V. Joshi, U. C. Mishra, and K. G. Vohra: Growth of Aqueous Solution Droplets of HNO_3 and HCl in the Atmosphere, J. of the Atmospheric Sciences, Vol. 40, January 1983, pp. 107-115.

(16) Penman, H. L.: Natural Evaporation from Open Water, Bare Soil and Grass, Proc. Royal Soc., Series A, Vol. 193, 1948, pp. 120-145.

(17) Kunkel, B. A.: A Comparison of Evaporative Source Strength Models for Toxic Chemical Spills, AFGL-TR-83-0307, Air Force Surveys in Geophysics No. 445, November 16, 1983, 511 pages.

(18) McCrary, J. H., and G. E. McCrary: An Area Source Model for XM-825 and XM-819 Munitions, U.S. Army Electronics Research and Development Command, Atmospheric Sciences Laboratory, CR-84-0009-1, January 1984, 15 pages.

(19) Hansen, F. V.: The Longitudinal Dispersion Length for Gaussian Diffusion, U.S. Army Electronics Research and Development Command, Atmospheric Sciences Laboratory, TR-0164, April 1985, 20 pages.

(20) Hansen, P. S.: Mobile Smoke for Apple II+ Microcomputer, U.S. Army Electronics Research and Development Command, Atmospheric Sciences Laboratory, TR-0155, September 1984, 34 pages.

APPENDIX I

AEDC-TR-85-52
ESL-TR-83-54

Space Shuttle HCl Gas Detection

M. G. Scott and C. W. Pender, Jr.
Sverdrup Technology, Inc.

May 1987

Final Report for Period April 15, 1984 – May 15, 1985

ARNOLD ENGINEERING DEVELOPMENT CENTER
ARNOLD AIR FORCE STATION, TENNESSEE
AIR FORCE SYSTEMS COMMAND
UNITED STATES AIR FORCE

PREFACE

The work reported herein was conducted by the Arnold Engineering Development Center (AEDC), Air Force Systems Command (AFSC), at the request of Air Force Engineering Services Center (AFESC/RDVS), Tyndall Air Force Base, Florida, and the Atmospheric Effects Branch, Marshall Space Flight Center, NASA H-73999B. The reported measurements were conducted and results obtained by Sverdrup Technology, Inc., AEDC Group, operating contractor for the propulsion test facilities at the AEDC, AFSC, Arnold Air Force Station, Tennessee, under Project Number DB07EW. The Air Force Project Managers were Captain Frank Tanji and Captain Bradley Biehn, AEDC/DOTR. The data analysis was completed on May 15, 1985, and the manuscript was submitted for publication on July 1, 1985.

CONTENTS

ILLUSTRATIONS

Figure | Page

1.0 INTRODUCTION

Large amounts of gaseous hydrogen chloride (HCl) are one of the combustion by-products generated during the launch of the Space Transportation System (Shuttle) by the Shuttle's solid-propellant rocket boosters (SRB's). Significant quantities of HCl are present in the plume cloud that lingers near the launch structure. The HCl gas remains entrained in the atmosphere near the launch facility, is dispersed by wind, and is deposited on surfaces, such as grass or ground. (See Ref. 1 for deposition mechanisms.) The HCl gas that remains in the vicinity of the launch structure, from either initial release or secondary ground release, is important because it corrodes metals and electronic equipment and because it is a health hazard. The problem is currently restricted to the Kennedy Space Center (KSC) launch area but will also be present at Vandenberg when the Shuttle Western Test Range launch facility is activated. The problem may be exacerbated at Vandenberg because of differences in the launch mount, sound-suppression water systems, and the proximity of the launch facilities.

The objective of this project was to develop and apply a nonobtrusive absorption technique employing a Fourier Transform Spectrometer (FTS) to monitor the concentration of gaseous HCl present near the KSC launch pad for several days after a Shuttle launch. Because of safety considerations and the requirement to collect data immediately after a launch, the measurement technique was automated to permit untended operation. The technique was applied for launches 41D and 51A, Pad 39A (Fig. 1), which occurred on August 30, 1984 and November 8, 1984, respectively, at KSC.

To accomplish the objective, a technique based on the absorption of infrared (IR) radiation by the diatomic HCl molecules was developed. The characteristic HCl lines are attributable to absorption of radiation associated with vibrational and rotational transitions within the HCl molecule. A simple model (Ref. 2) to describe this absorption process is a molecule in which the individual atoms, held together by chemical bonds, are in vibratory motion along these bonds, while the entire molecule is rotating. The HCl is in a state of vibratory motion brought about by the alternate stretching and contracting of the chemical bond as the hydrogen and chlorine atoms move away and toward each other, respectively. This vibratory motion is superimposed on a rotation of the molecule about an axis perpendicular to the chemical bond. When IR radiation of the proper frequency (i.e. energy) impinges on the molecule and is absorbed, the vibration and/or rotation states are changed. These changes must satisfy certain selection rules that give rise to discrete absorption lines. These lines are labeled according to their frequency. The lines with frequencies greater than that of the band center are said to be in the R branch, whereas those with frequencies less than that of the band center are in the P branch (Fig. 2). The individual lines making up the P and R branches are identified as P(1), P(2), etc. as the frequency of the lines moves away from the band center.

2.0 TECHNIQUE

A nonobtrusive IR absorption technique was used for monitoring gaseous HCl concentrations over long paths near the Shuttle launch pad (Fig. 1). The technique involved use of an IR spectrometer located approximately 500 m from an IR source. An IR spectrum was acquired at regular intervals (20 min for 41D, 10 min for 51A) for several days following the Shuttle launches. The spectra were then inspected to find the magnitude of absorption because of the presence of gaseous HCl. The concentration of HCl was then calculated using the absorption coefficient measured in the laboratory. The spectral line used to determine the amount of absorption is in the band centered at 2,886 cm^{-1}. This technique is not dependent on absolute magnitudes of the spectra; therefore, the intensity of the source is not relevant to the measurement, and only relative intensities will be presented in this report.

Naturally occurring HCl contains two isotopes of chlorine. They are ^{35}Cl and ^{37}Cl, in the ratio of 3 to 1, respectively. The IR absorption lines of $H^{35}Cl$ and $H^{37}Cl$ are separate, but very close. A spectrum of these isotopic species is shown in Fig. 2b.

The absorption attributable to HCl gas is well understood and documented. The HCl absorption lines are described by (Ref. 3)

$$I(\lambda) = I_o(\lambda) \exp \left\{ -SP\gamma_o L/[(\lambda - \lambda_o)^2 + \gamma_o^2]\pi \right\}$$

where

I_o (λ) is the intensity of the incident radiation

I (λ) is the intensity of the transmitted radiation

S is the line strength of the absorption line (cm^{-2} atm^{-1})

P is the partial pressure of the absorbing species (atm)

γ_o is the pressure-broadened half-width at half-maximum of the HCl line (cm^{-1})

λ_o is the line center of the absorption line (cm^{-1})

L is path length

Figure 3 shows the P(1) lines calculated using parameters contained in Ref. 4. The figure shows the theoretical absorption assuming 6 ppm HCl over a 500-m path. Because of limited resolution and the apodization function, the Fourier transform spectrometer (FTS) that produced the actual spectra influences the spectra shape. The convolution of the instrument line shape (ILS), using 0.5-cm^{-1} resolution and a triangular apodization function, produces the P(1) line shown in Fig. 3b. As can be seen by comparing Figs. 3a and b, the ILS shortens

and broadens the spectral lines. (Note: The scales of these plots are not the same.) The effect is detrimental in that the resultant spectrum is not an accurate portrayal of the true line shape. However, it is still possible to use the resultant spectra since the effect can be calibrated. The calibration will be discussed later in this report.

A complicating factor was the presence of additional absorption lines in the spectra obtained in the field. The effect of neighboring absorption lines is to give the impression of a greater amount of gaseous HCl. The spectral region of interest included absorption lines attributable to other molecules present in the atmosphere such as H_2O and, Hydrogen Deuterium Oxide (HDO) (Ref. 5). Therefore, the spectra were obtained at 0.5-cm^{-1} resolution to separate the HCl lines from the lines of interference. In Fig. 4a the HCl doublets can be easily discerned when compared to a background spectrum with no HCl present, Fig. 4b. Figure 4a is a portion of a typical spectrum acquired during the 51A launch. This figure shows only the lines within the P branch. The R branch is unusable because of domination by water vapor bands at 2.7 and 3.2 μm. The P(5) line was used to determine the HCl concentrations because it had the least interference.

3.0 APPARATUS

The Shuttle launches took place at KSC Pad 39A. Figure 1 shows the major features of the launch pad and the AEDC equipment location. The test apparatus consisted of an FTS and a collimated light source with associated control and data acquisition instrumentation. The sample path length was 500 m. The distance to the launch structure was approximately 350 m. The equipment was located so that the plume deflected by the flame trench passed through the center of the sample path.

The FTS used was a Block Model RS197 field-rated instrument (Refs. 6 and 7). It was configured to have the maximum sensitivity possible in the spectral region of interest, 3,000 to 2,700 cm^{-1}. This was accomplished by using a germanium beamsplitter on a potassium bromide substrate and an indium antimonide detector cooled to 77 K. The detector dewar had a maximum hold time of 6 hr, so an automatic fill system was developed to replenish the liquid nitrogen (LN_2) from a large auxiliary reservoir. The FTS was rigidly mounted to maintain optical alignment with the source during the large vibrations associated with the Shuttle launch. The instrument was enclosed in a Plexiglas® container that was kept at a slight positive pressure with a gaseous nitrogen (N_2) purge to reduce the possibility of HCl corrosion (Fig. 5b). The IR radiation entered the FTS through a hole in the Plexiglas container that matched the entrance aperture of the FTS. An O-ring seal was made between the FTS and the container. In this way, the FTS was in the same configuration in the field test as

in the calibration. The only difference in the optical paths was that the quartz sample cell was fitted with IR transmisive quartz windows on each end.

The source units used in launches 41D and 51A were different. Modifications were made to the equipment for launch 51A because of insight gained during the 41D launch. The original configuration (See Fig. 6a) used in the 41D launch consisted of a Barnes Model 112017 blackbody with collimator and an Optronics Model 100U, 1,000-w tungsten halogen lamp with a 25.4-cm Cassegrain telescope used as a collimator. The use of multiple sources was required to provide adequate intensity since the FTS was located 500 m distant and also as insurance against optical misalignment from the shock of the booster ignition. In the second configuration (See Fig. 6b), for the 51A launch, three, 30.48-cm spherical mirrors with 1,000-w tungsten halogen lamps at their focal points were used to provide an intensity increase of 400 percent. In each case the sources were securely mounted and covered with a hood that provided protection from inclement weather and SRB plume debris. The sources were mounted so that the optical path between the FTS and sources was approximately 1.2 m above the ground (Fig. 6b).

The digital data acquisition system collected a set of 124 interferograms (the raw data) during each sampling period of approximately 2 min. Each set was averaged and stored on magnetic tape as one data point. A spectrum is obtained by taking the Fourier transform of the interferogram (Ref. 6). For launch 41D, data points were collected every 20 min. This time interval was reduced to 10 min for 51A after improvements were made to the software that reduced the processing time from 17 to 8 min. The data were not converted to the spectral domain until later in order to permit the collection of additional data during the postlaunch period.

4.0 CALIBRATION AND ANALYSIS

The absorption technique involved the comparison of spectral data acquired in the field with similar data acquired in the laboratory. As explained in Section 2.0, calibration data generated in the laboratory were used in lieu of published HCl absorption coefficients to negate the influence of the spectrometer instrument line shape.

In the laboratory (Fig. 5a), a previously evacuated quartz sample cell (2.54 diam by 25.4 cm) was filled with mixtures of HCl and dry N_2 with known concentrations simulating the absorption expected following the launch. The concentration of HCl in the sample cell is stated in terms of partial pressures (x) with units of psia, and the concentration (y) in the field is expressed as parts per million (ppm). The relationship is $x/14.7 = y/1{,}000{,}000$. Specific sample cell concentrations of HCl were achieved using a partial pressure technique in which

the cell was filled in several stages. Each stage consisted of partially evacuating the cell followed by bringing it back up to 14.7 psia with dry N_2. This process was continued until the desired partial pressure of HCl was reached. To simulate the field conditions, the concentrations used in the laboratory were greater by an amount dictated by Beer's law. A simple form of Beer's law,

$$\ln(I/I_o) = -ABC$$

where

I = transmitted radiation
I_o = incident radiation
A = absorptivity (constant at a given wavelength)
B = path length
C = concentration of the absorbing medium

states that the ratio of I/I_o will remain constant if C is varied inversely to B. For example, I/I_o is equivalent for a gas at either 1 psia over a 1-m path or for 10 psia over 0.1 m. Therefore, in the laboratory the concentrations needed to be greater by a factor of 1,968 (the ratio of the range in the field, 500 m, to the cell length, 25.4 cm).

A set of nine spectra corresponding to nine calibration pressures were obtained. The x axis of these curves is in terms of path-averaged concentrations over 500 m. Calibration curves were obtained by plotting $\ln(I_o/I)$ versus x for six P lines. The plots are shown in Figs. 7a through f. The partial pressures of HCl, in psia, used in the test cell were 0.018, 0.036, 0.053, 0.080, 0.120, 0.181, 0.272, 0.544, and 1.633. The conversion relationship to the equivalent field concentration is given by y (ppm) = 34.6 x(psia).

The analysis of the KSC spectra consisted of measuring the difference between the baseline and the peak depth of the six P absorption lines. An important feature of this technique is that atmospheric haze does not invalidate the measurement. Atmospheric scattering attributable to haze does not affect the procedure since both I and I_o (Fig. 2b) are influenced by the same amount, leaving the ratio I/I_o constant. This feature negates the necessity of performing an instrument or source calibration.

The error associated with the resultant measurements of the 41D launch is estimated to be ± 19 percent (root sum of the squares). This error is caused by an error of ± 10 percent because of pressure transducer uncertainty, ± 10-percent gas-handling technique, ± 10 percent

in FTS measurement uncertainty, and ±8 percent in data handling (digitization and processing). The error associated with the resultant measurements of the 51A launch is estimated to be ±15 percent (root sum of the squares). This reduction in error is caused by the use of the alternate source unit with a higher intensity during the second measurement. The FTS measurement uncertainty was reduced to ±3 percent, and the data handling uncertainty was reduced to ±2 percent.

5.0 RESULTS

The application of the IR absorption technique following the 41D launch showed the presence of average concentrations of gaseous HCl as great as 4 ppm (± 19 percent). Figure 4a is a representative spectrum taken postlaunch. The HCl lines are clearly apparent among other atmospheric absorption lines. Figure 8 gives the concentration of gaseous HCl as yielded by examination of five $H^{35}Cl$ absorption lines. The spread in the results is attributed to the presence of absorption lines of other molecules. Note that in Fig. 8 the concentration determined using the P(5) line is less than concentrations determined using the other lines. In the case of most of the HCl absorption lines, their frequencies are nearly the same as other atmospheric constituents, such as HDO and H_2O (Ref. 5). Therefore, the resultant absorption is greater than that caused only by the HCl. Since it is difficult to determine how much of the absorption is caused by the other molecules, the most isolated line, the P(5) line, was used to determine the HCl concentration.

The concentration peaked approximately 100 min postlaunch, remained high for nearly 1 hr, and then began to diminish. There unfortunately exists a gap in the data because of a period in which instrumentation was realigned following the loss of one of the sources during the high vibration experienced during the launch. The instrumentation was operated for three days following the launch, and HCl was detected only in the 6-hr interval following the launch.

Data obtained from the 51A launch are better in two ways. Data were acquired more frequently and with an improvement in the signal-to-noise ratio by nearly a factor of four. During the 51A launch, higher HCl concentrations were measured than were detected during the 41D launch. Figure 9 is a summary of six concentration curves from the P-branch lines. The curves have a significant scatter caused by absorption attributed to other molecules present in the sample path. The most isolated line again is the P(5) line. Figure 10 shows the best estimate of the HCl concentration. The HCl concentration peaked at about 9 ppm ± 15 percent approximately 1 hr postlaunch, fluctuated for about an hour, and then decayed. In the two days following the launch, HCl was detected in minute quantities after sunrise until early afternoon. Long-term, low levels of HCl were visible in the 51A launch either because of

greater revolatilization attributable to atmospheric and ground conditions or better signal-to-noise ratio. Atmospheric conditions during the measurement periods of both launches are available (Refs. 8 and 9).

6.0 SUMMARY

The objectives of the project were completely fulfilled. An unobtrusive absorption technique to monitor concentrations of gaseous hydrogen chloride was developed and then applied on two space shuttle launches at the Kennedy Space Center. The technique developed exploited the intrinsic property of gaseous HCl to absorb IR radiation in specific, narrow, spectral lines. This IR absorption is measured by a Fourier Transform Spectrometer that features accuracy and precision without a calibrated source. The minimum detectable concentration of the instrument is 0.10 ppm with an error of 15 percent (obtained by taking the square root of the sum of the squares of all possible errors or uncertainties in the measurement system including calibration). The application portion of this project enabled refinement of field use of the measurement technique. Increased source radiance and larger source collimating optics improved the signal-to-noise ratio by a factor of four. Improvement in data processing software decreased uncertainty by 4 percent.

Measured quantities of gaseous HCl following launches of both 41D and 51A displayed similar trends. The concentration after each launch first increased, then decreased, then increased to a maximum approximately 100 sec after the launch. The concentration decreased gradually to less than 1 ppm approximately 10 hr after each launch. The peak concentration measured was 4 and 9 ppm for 41D and 51A, respectively. For two days after the 51A launch only, detectable levels were recorded for a period of approximately 6 hr following sunrise. Atmospheric and ground conditions were different for each launch (Refs. 8 and 9). Additional considerations in interpreting the concentration levels are that the data are both path and time averaged, and that the ground scar from the plume makes up approximately 60 percent of the 500-m sample path length. These considerations imply that the concentration along the path is not uniform. Additionally only gaseous HCl will be detected by this technique.

7.0 RECOMMENDATIONS

Improvements to the instrument developed on this project can be made in two areas. The signal can be increased by enlarging the collection optics on the FTS, and the noise can be reduced by increasing the data averaging period. Some improvement in calibration accuracy could be realized by using gas-mixture ratios prepared by the National Bureau of Standards.

The technique developed by this project could use computed tomography with multiple paths to generate a two-dimensional map of HCl concentration levels to determine areas of highest concentration and change over time. This technique would enable determination of safe areas around solid-propellant rocket motor launch complexes where people, wildlife,

or machinery may be adversely impacted. Additional analysis (not within the scope of this project) should be conducted to determine the impact of atmospheric and ground conditions, aerosol entrapment of HCl, and flame trench cooling water runoff and holding pond contributions to gaseous HCl concentration levels.

REFERENCES

1. Anderson, B. J. and Keller, V. W. "Space Shuttle Exhaust Cloud Properties." NASA TP-2258, December 1983.

2. Szymanski, H. A. *Theory and Practice of Infrared Spectroscopy*. Plenum Press, New York, 1964.

3. Thorne, N. P. *Spectraphysics*. Chapman and Hall, London, 1974.

4. Lin, C. L. et al. "Line Parameters of HCl Obtained by Simultaneous Analysis of Spectra." *Optical Spectroscopic Radiation Transfer*. Vol. 20. Pergamon Press Ltd., Great Britain, 1978.

5. Wolf, W. L., editor. *Handbook of Military Infrared Technology*. US Government Printing Office, Washington, D. C., 1965.

6. Bell, E. E. *Introduction to Fourier Transform Spectrometry*. Academic Press, New York, 1972.

7. Martin, A. E. *Infrared Interferometric Spectrometers*. Elsevier Scientific Publishing Company, New York, 1980.

8. Johnson, D. L. et al. "Atmospheric Environment for Space Shuttle (STS-41D) Launch." NASA-TM-86484, October 1984.

9. Johnson, D. L. et al. "Atmospheric Environment for Space Shuttle (STS-51A) Launch." NASA-TM-86497, December 1984.

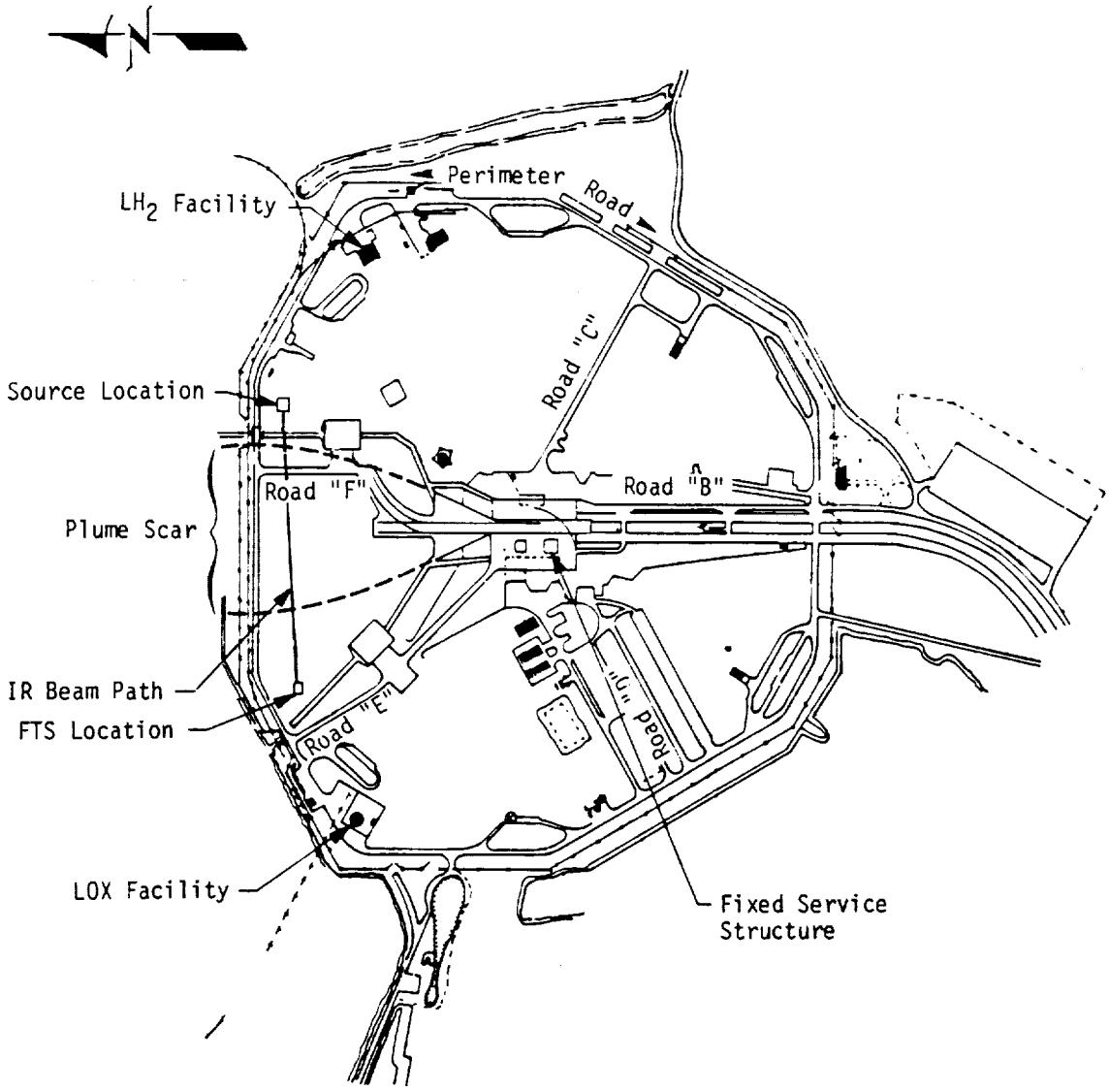

Figure 1. Kennedy Space Center 39A launch pad.

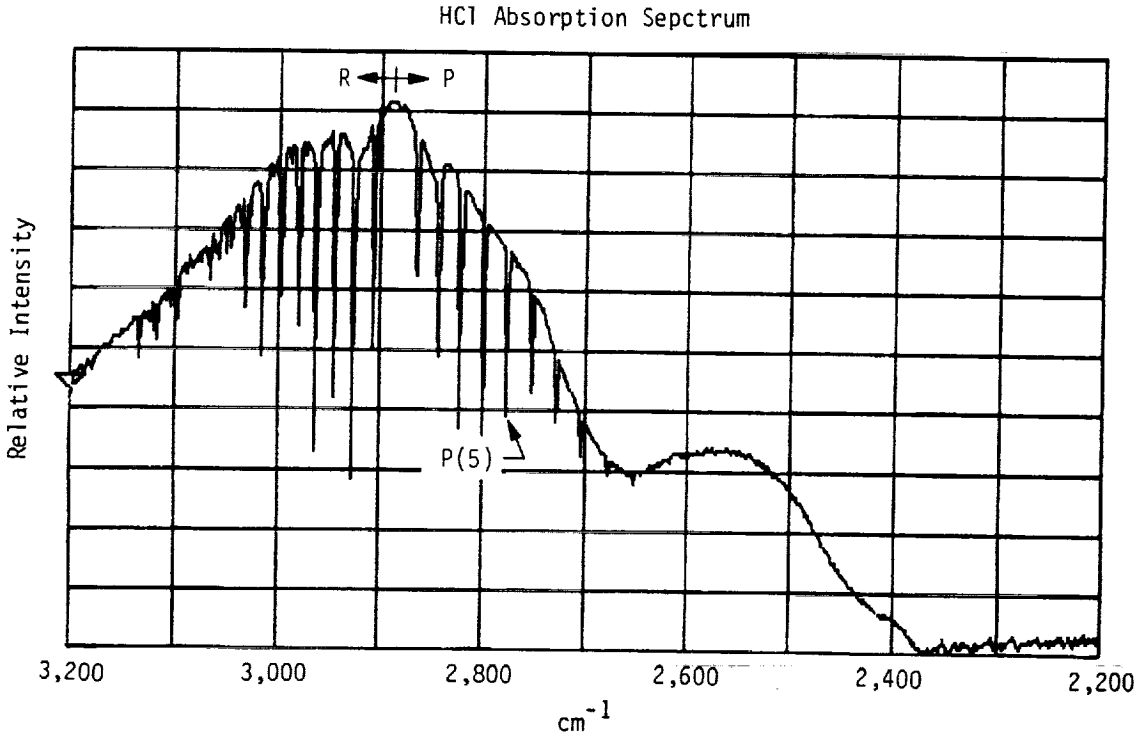

a. Covering 3,200 to 2,200 cm^{-1}

Figure 2. Sample spectrum showing HCl fundamental absorption band.

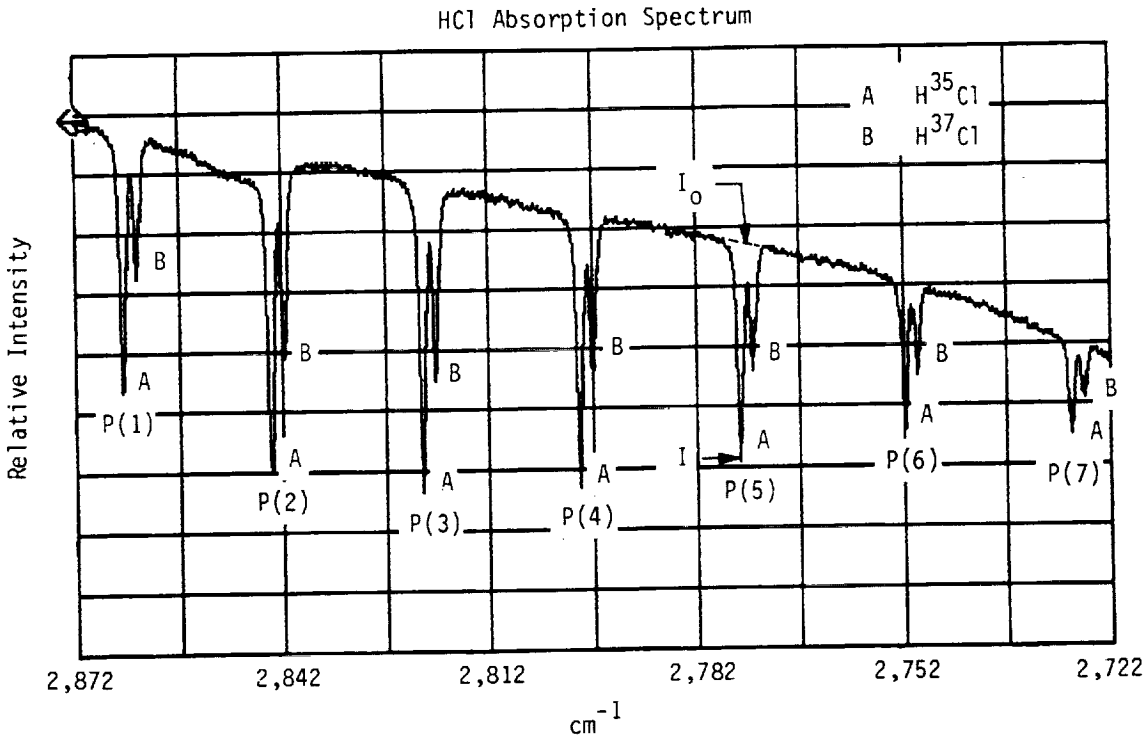

b. Showing only the P branch and how I_o and I are determined
Figure 2. Concluded.

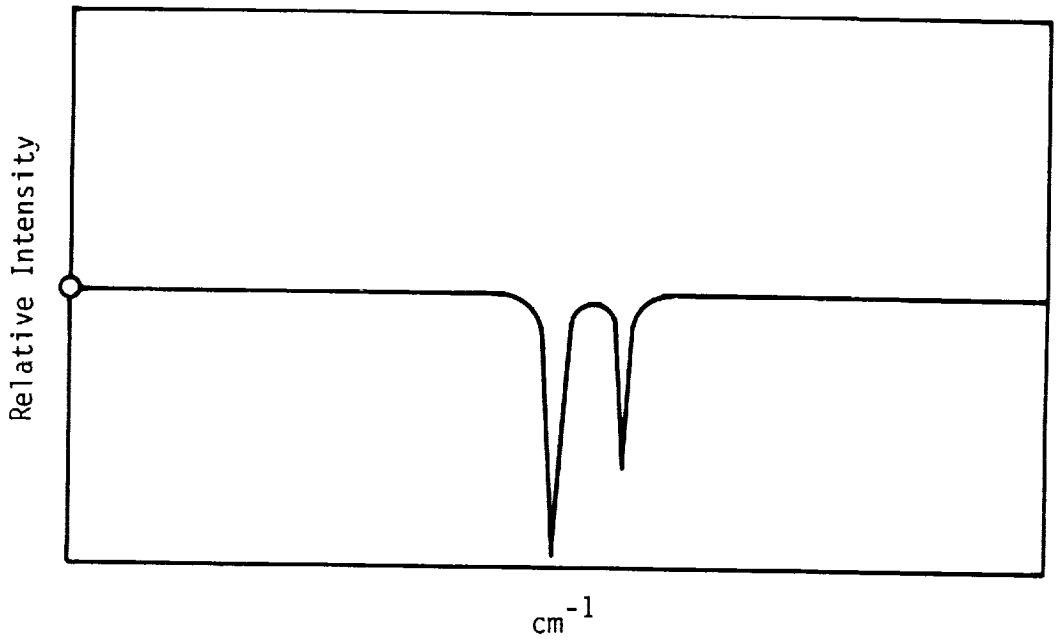

a. Calculated

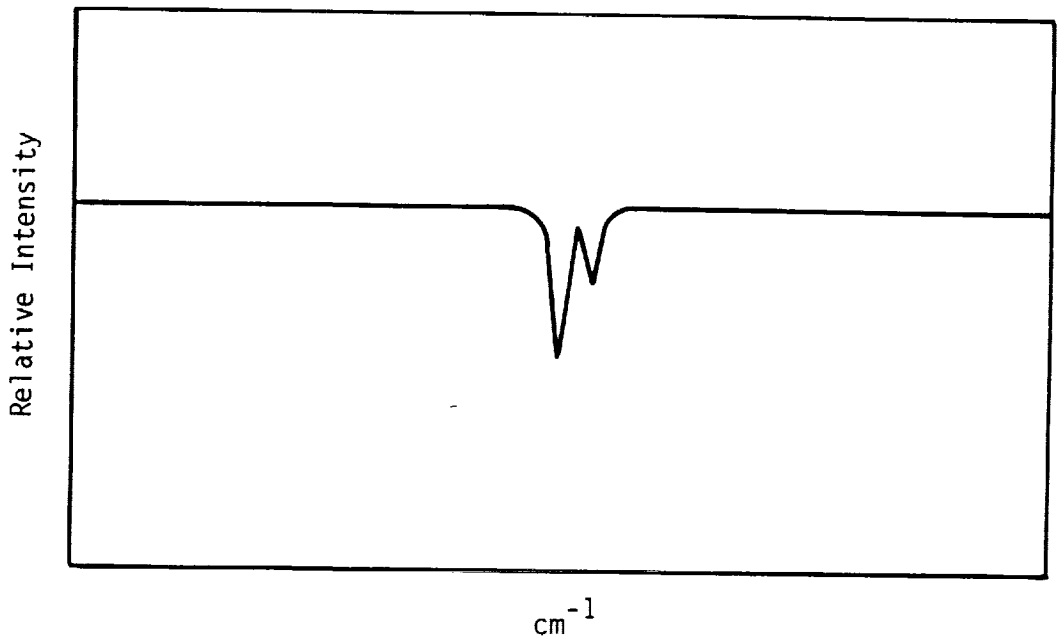

b. Convolved with the ILS

Figure 3. P(1) absorption line.

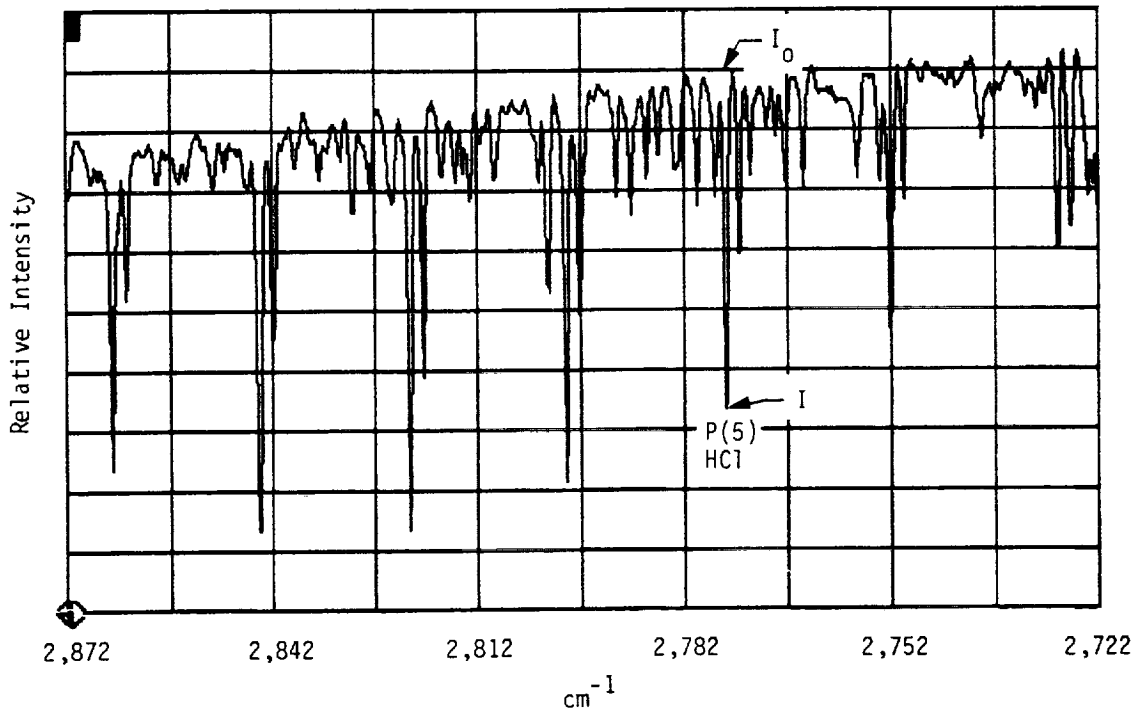

a. Typical spectrum obtained after the 51A launch.
Figure 4. 51A launch spectra.

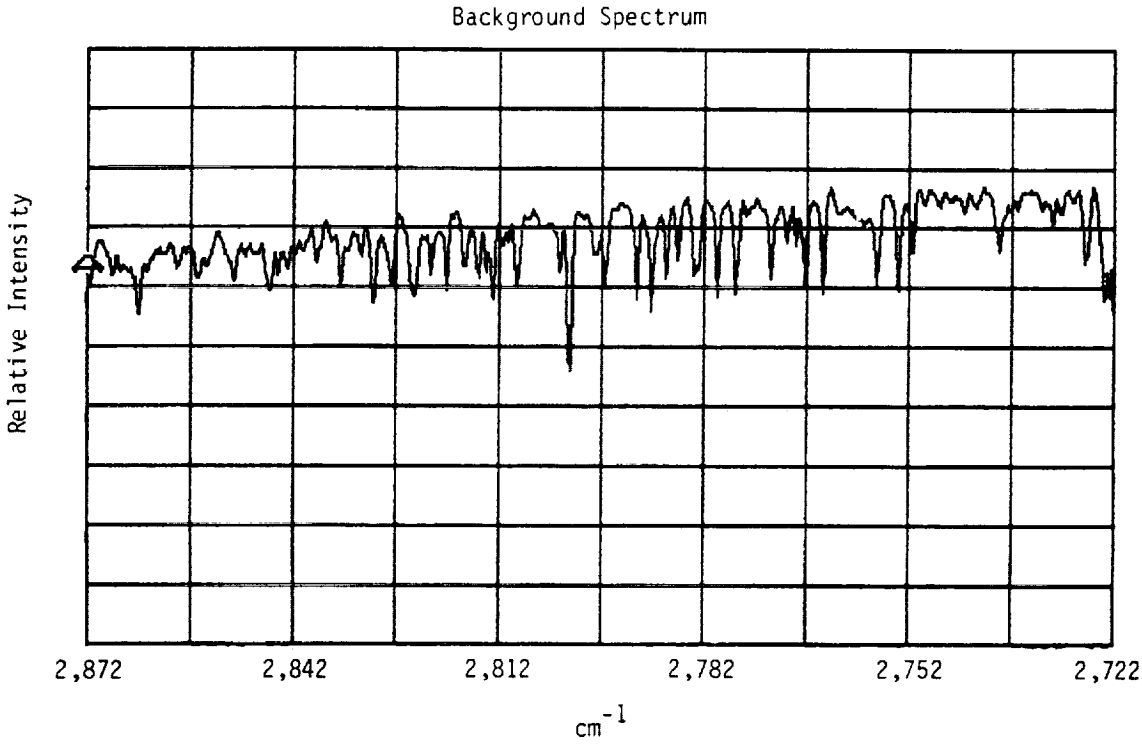

b. Background spectrum obtained before the 51A launch
Figure 4. Concluded.

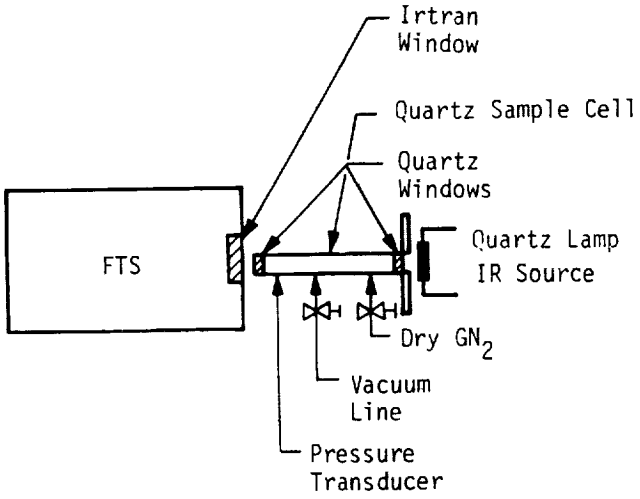

a. Calibration setup

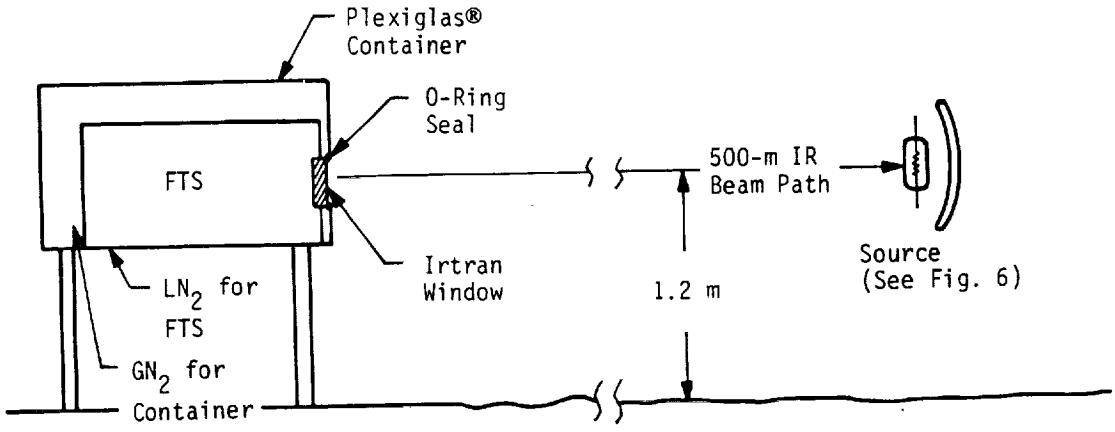

b. Test setup

Figure 5. FTS schematic.

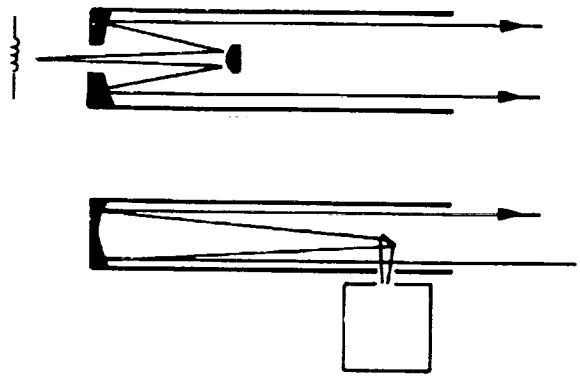

a. 41D

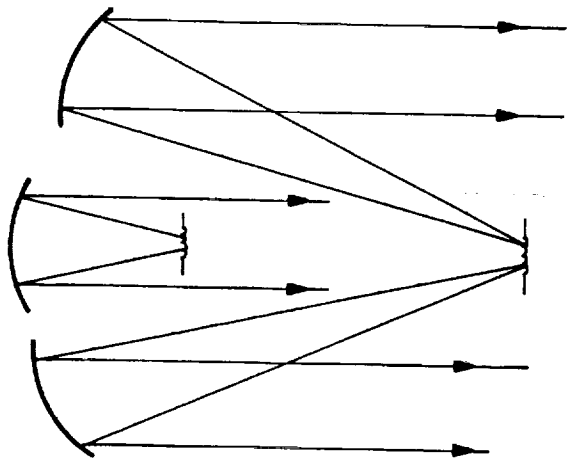

b. 51A

Figure 6. Source configuration.

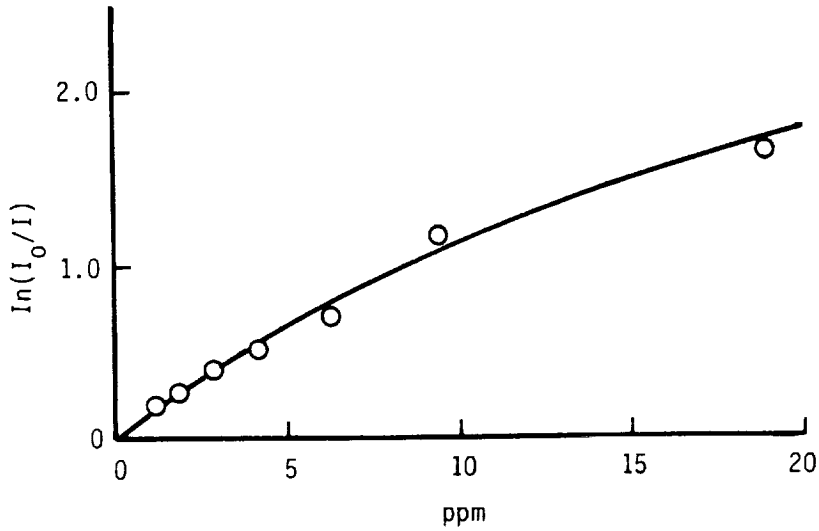

a. P(1) line

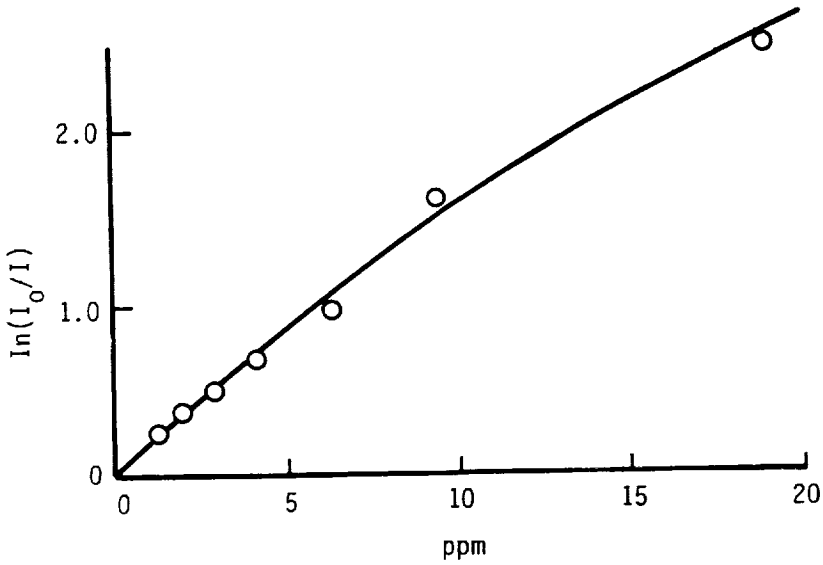

b. P(2) line

Figure 7. Calibration curves for HCl cells.

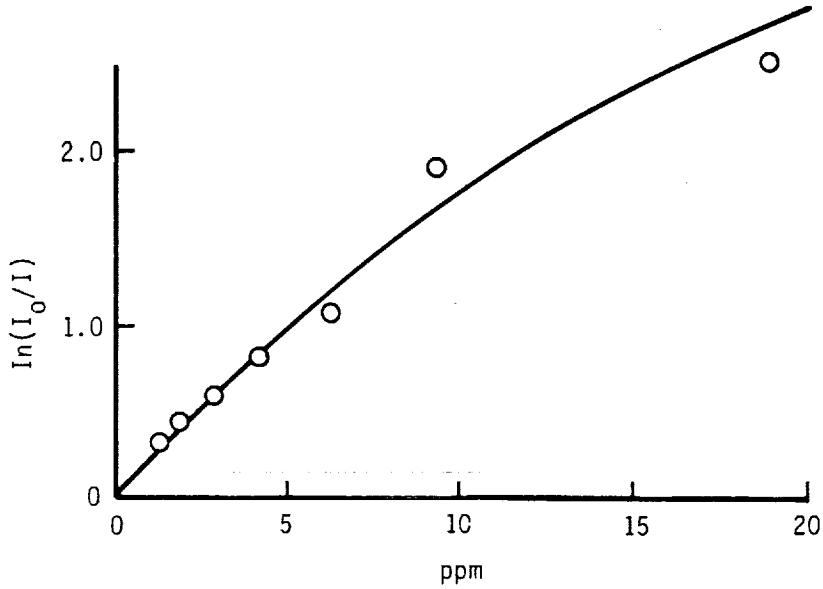

c. P(3) line

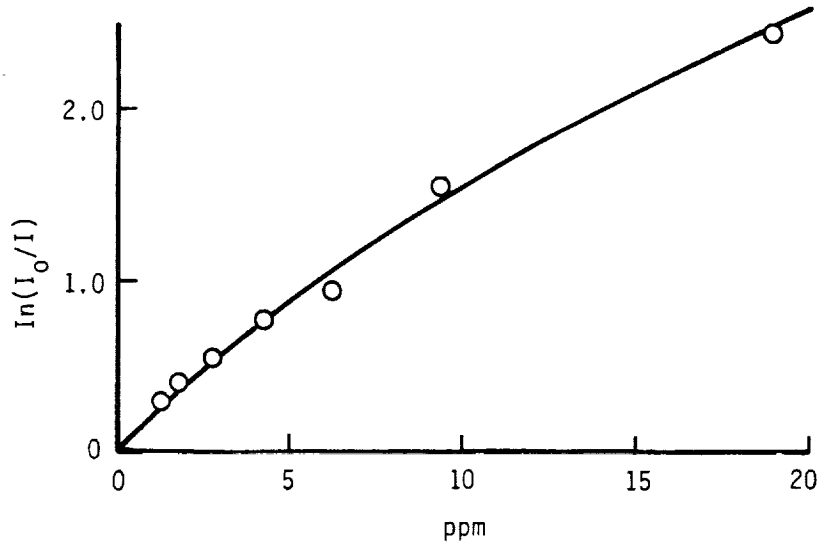

d. P(4) line

Figure 7. Continued.

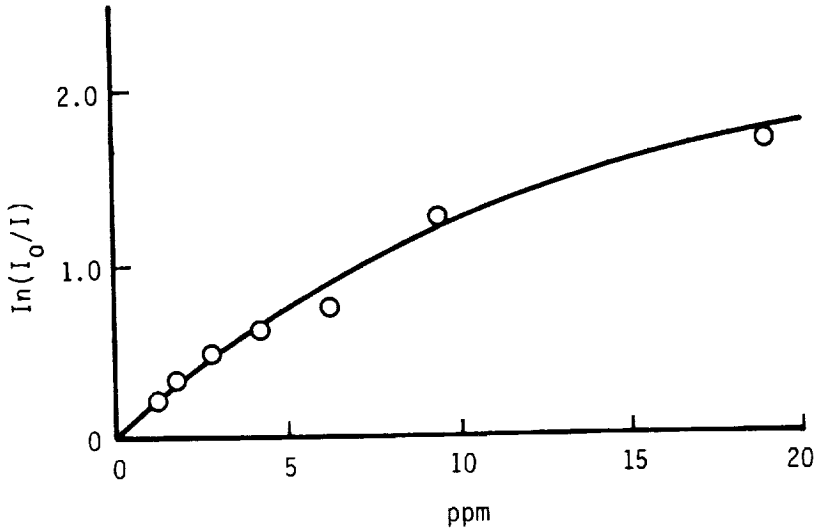

e. P(5) line

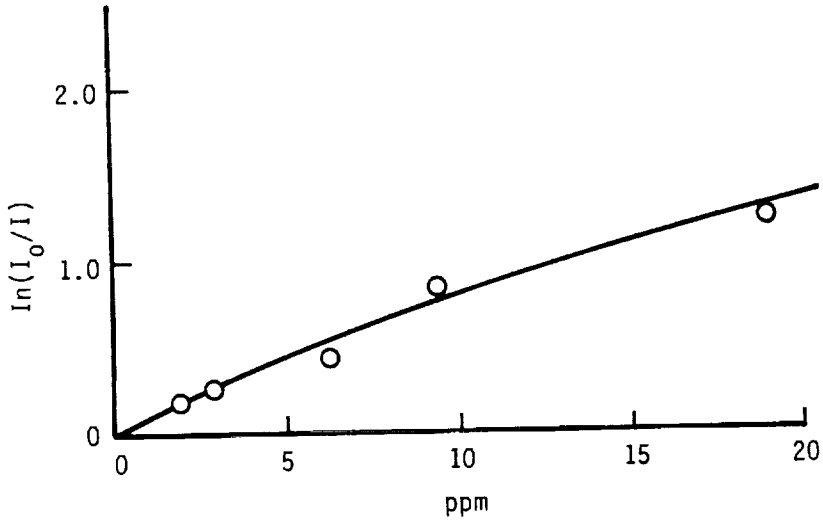

f. P(6) line

Figure 7. Concluded.

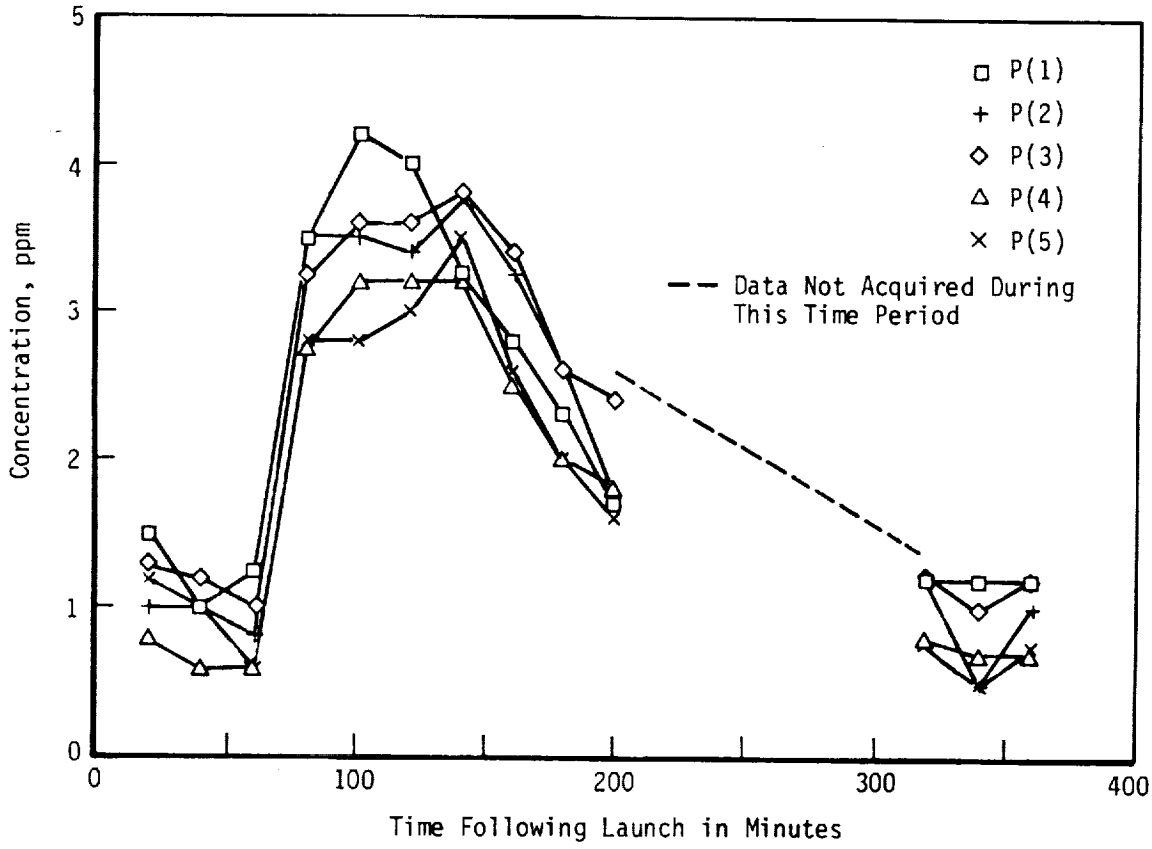

Figure 8. Summary of 41D HCl concentrations measured using several P-branch absorption lines.

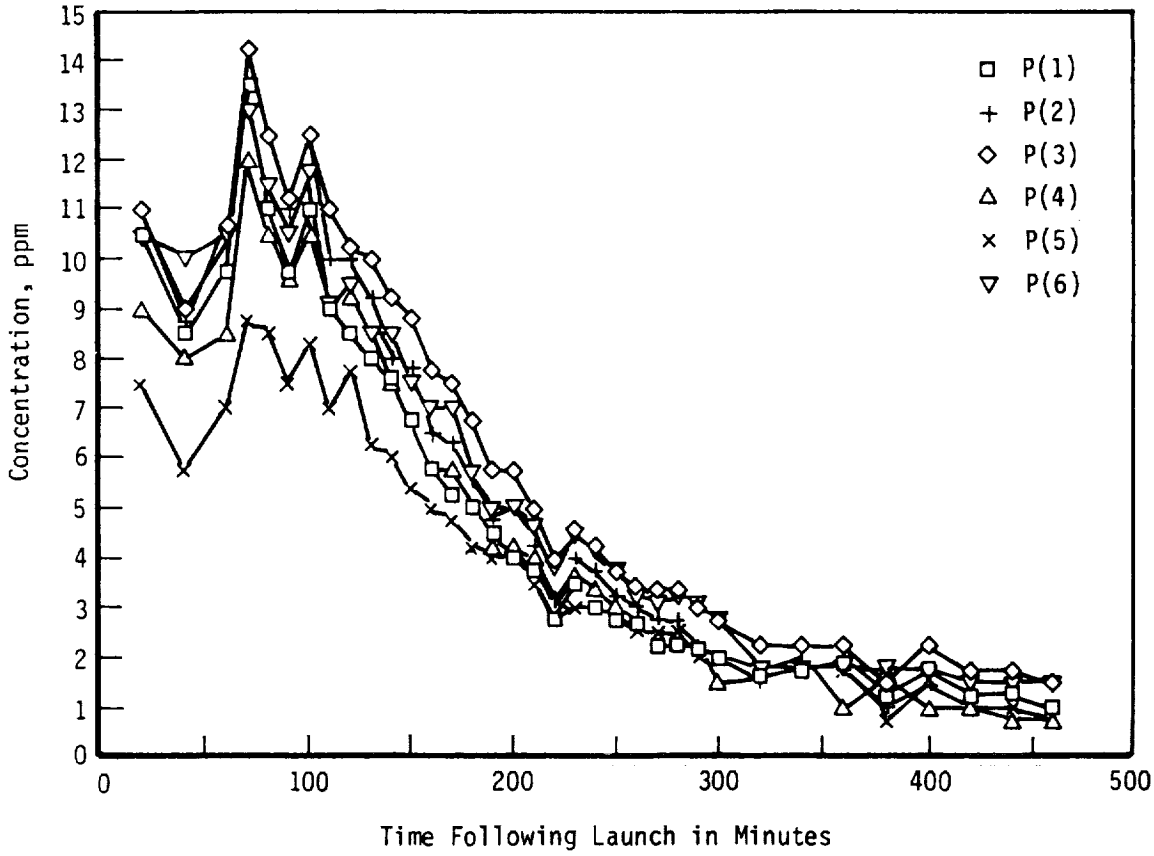

Figure 9. Summary of 51A HCl concentrations measured using several P-branch absorption lines.

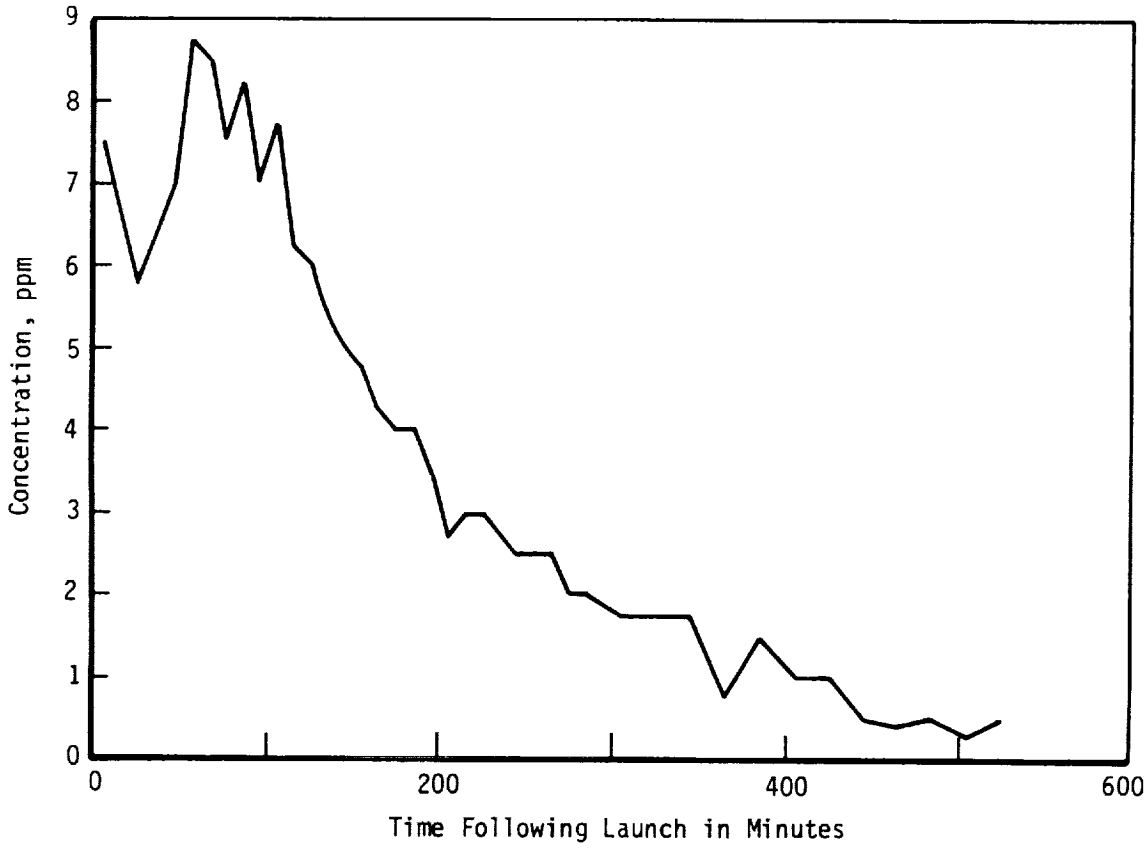

Figure 10. 51A HCl concentration using P(5) line for 10 hr following launch.

UNCLASSIFIED

SECURITY CLASSIFICATION OF THIS PAGE

REPORT DOCUMENTATION PAGE

1a. REPORT SECURITY CLASSIFICATION UNCLASSIFIED	1b. RESTRICTIVE MARKINGS
2a. SECURITY CLASSIFICATION AUTHORITY	3. DISTRIBUTION/AVAILABILITY OF REPORT Approved for public release; distribution is unlimited.
2b. DECLASSIFICATION/DOWNGRADING SCHEDULE	
4. PERFORMING ORGANIZATION REPORT NUMBER(S) AEDC-TR-85-52	5. MONITORING ORGANIZATION REPORT NUMBER(S)
6a. NAME OF PERFORMING ORGANIZATION Arnold Engineering Development Center 6b. OFFICE SYMBOL (If applicable) DOT	7a. NAME OF MONITORING ORGANIZATION
6c. ADDRESS (City, State and ZIP Code) Air Force Systems Command Arnold Air Force Station, TN 37389-5000	7b. ADDRESS (City, State and ZIP Code)
8a. NAME OF FUNDING/SPONSORING ORGANIZATION Air Force Engineering Services Center 8b. OFFICE SYMBOL (If applicable) RDVS	9. PROCUREMENT INSTRUMENT IDENTIFICATION NUMBER
8c. ADDRESS (City, State and ZIP Code) Tyndall Air Force Base, Florida 32403	10. SOURCE OF FUNDING NOS. PROGRAM ELEMENT NO.: 921A67 PROJECT NO.: TASK NO.: WORK UNIT NO.:
11. TITLE (Include Security Classification) Space Shuttle HCl Gas Detection	
12. PERSONAL AUTHOR(S) Scott, M. G. and Pender, C. W., Jr., Sverdrup Technology, Inc., AEDC Group	
13a. TYPE OF REPORT Final 13b. TIME COVERED FROM 4/15/84 TO 5/15/85	14. DATE OF REPORT (Yr., Mo., Day) May 1987 15. PAGE COUNT 30
16. SUPPLEMENTARY NOTATION Available in Defense Technical Information Center (DTIC).	

17. COSATI CODES		
FIELD	GROUP	SUB. GR.
21	02	
01	03	

18. SUBJECT TERMS (Continue on reverse if necessary and identify by block number)
HCl concentrations; Fourier transform spectrometer; Space Shuttle data acquisition; combustion byproducts; solid-propellant rocket boosters

19. ABSTRACT (Continue on reverse if necessary and identify by block number)

Hydrogen chloride (HCl) gas is one of the byproducts produced by the Space Shuttle solid-propellant rocket boosters. This report describes a nonobtrusive absorption technique to measure concentrations of gaseous HCl for four days following Shuttle launches 41D and 51A at Kennedy Space Center (KSC). The peak concentrations measured near ground level about 400 m from the launch structure were found to be less than 10 ppm averaged over a 500-m path after both launches.

20. DISTRIBUTION/AVAILABILITY OF ABSTRACT UNCLASSIFIED/UNLIMITED ☐ SAME AS RPT. ☒ OTIC USERS ☐	21. ABSTRACT SECURITY CLASSIFICATION UNCLASSIFIED
22a. NAME OF RESPONSIBLE INDIVIDUAL W. O. Cole	22b. TELEPHONE NUMBER (Include Area Code) (615)454-7813 22c. OFFICE SYMBOL DOS

DD FORM 1473, 83 APR EDITION OF 1 JAN 73 IS OBSOLETE.

UNCLASSIFIED

SECURITY CLASSIFICATION OF THIS PAGE

APPENDIX II

Analysis Program for Estimation of HCl
Revolatilization Source Strength

```
10    REM  HCL REVOLITILIZATION PROGRAM: VERSION "HCL41L"
20    REM  INCORPORATES REDUCTION OF EVAPO IN PROPORTION TO SUMAREA.
21    REM  INPUT MODIFIED TO MATCH 41D LAUNCH, POST LAUNCH CONDITIONS.
22    REM  USING LINEAR CURVE FIT FOR Ts, Tdew, AND U.
30    REM  WRITTEN BY JEFFREY ANDERSON, OCTOER 16, 1986
40    OPTION BASE 1
50    INTEGER Loop
60    DIM N(40),A(40),C(40),V(40),Mga(40),M(40),Mtg(600),Mw(40),Pow(40)
70    DIM Case$[60]
80    INPUT "IS INITIALIZED DATA TAPE IN DRIVE :T14? (Y/N)",A$
90    IF A$="Y" THEN 110
100   GOTO 80
110   REM N(1) = number of drops of radius A(I)
120   REM A(I) = DROP RADIUS IN CM, DROP IS ASSUMED HEMISPHERICAL
130   REM  C(I) = HCL CONCENTRATION IN WEIGHT PERCENT
140   REM V(I) = VOLUME OF DROP IN CUBIC CM
150   REM  Mga(I) = MASS OF HCL GAS EVAPORATED FROM Ith DROP (GRAMS)
160   REM  M(I) = MOLARITY OF DROP
170   REM  Mtg(T) = TOTAL HCL (grams) EVAP IN THE TIME STEP
180   REM  Mw(I) = MASS OF WATER EVAPORATED FROM ALL RADIUS I DROPS
190   REM
200   REM
210   REM        DEFINE CONSTANTS AND INITIAL CONDITIONS
220   REM _____________________________________________________
230   Diffw=.25    !DIFFUSION COEF OF WATER VAPOR, CM^2 /S
```

```
240   Diffa=.18   !DIFF COEF FOR HCL, CM^2 /S, EST FROM ATER VALUE AND
       DEPENDANCE ON MOLECULAR WT.
250   Mhc1=36.47
260   Mh2o=18.01528  !MOLECULAR WEIGHTS
270   LINPUT "ENTER CASE IDENTIFIER (60 CHRS MAX)",Case$
280   INPUT "ENTER SURFACE TEMPERATURE DELTA IN CELSIUS = ",Tdelata
290   INPUT "ENTER DEW POINT DELTA IN CELSIUS = ",Ddelta
300   INPUT "ENTER WIND DELTA SPEED AT 2 METERS ELEVATION, (m/s) = ",Udelta
301   Ts=26.33
302   Tdew=22.59
303   U=.52
304   REM INITIALIZE WITH 41D SPECIFIC DATA
310   INPUT "ENTER INITIAL ACID CONCENTRATION, WT. PERCENT = ",C
320   INPUT "ENTER CALCULATION END TIME (minutes) = ",Tf
330   INPUT "ENTER CALCULATION TIME STEP (minutes) = ",Dtime
340   INPUT "ENTER INTERVAL FOR EXTRA DATA PRINTOUT (minutes) = ",Dtout
350   INPUT "ENTER INITIAL LIQUID VOL PER SQ METER = 100 CM^3? ",V
360   INPUT "ENTER MEAN RADIUS OF INITIAL DROPS = 0.1cm? ",Amean
370   INPUT "ENTER AREA FACTOR FOR EVAPO REDUCTION (4?)",Ra
380   INPUT "ENTER NAME FOR OUTPUT DATA FILE",Dfile$
381   REM FOR Rpt=1 TO 5
383   REM pt=1 THEN Dfile$="A51uu1"
384   REM  IF Rpt=2 THEN U=2
385   REM  IF Rpt=2 THEN Dfile$="A51uu2"
386   REM  IF Rpt=3 THEN U=4
390   Einf=0
400   A=0
410   Cumlgas=0
```

```
420   Cumlw=0
430   Sumarea=1
440   Sigma=.08
450   Da=.0075   ! INITIAL BIN SIZE FOR RADII IN cm
460   Tsum=0     !
470   GOSUB Prival
480   REM
490   REM
500   REM   CALCULATE INITIAL SIZE SPECTRUM
510   REM ----------------------------------------
520   REM
530   FOR I=1 TO 40
540     A(I)=I*Da
550     Pow(I)=-((A(I)-Amean)^2/(2*Sigma^2))
560     Tsum=Tsum+A(I)^3*EXP(Pow(I))
570   NEXT I
580   Numo=V/(2.0944*Tsum)     !2/3 PI = 2.0944
590   Tv=0
600   FOR I=1 TO 40
610     C(I)=C
620     N(I)=Numo*EXP(Pow(I))
630     V(I)=2.0944*N(I)*A(I)^3
640     Tv=Tv+V(I)
641     PRINTER IS 0
650     PRINT USING 651;I,A(I),N(I),Tv
651     IMAGE DDD,"  A(I)=",D.DDDD,"   N(I)=",DDDDDD.DDD,"   TOTAL V=",D.DDE
652     PRINTER IS 16
```

```
660   NEXT I
670   REM
680   REM
681   REM  BEGIN TIME DEPENDANT CALCULATION OF HCL EVAPORATION
682   FOR T=1 TO Tf STEP Dtime
683   Ts=26.33+.0105*T+Tdelta
685   Tdew=22.59-.0019*T+Ddelta
686   U=.5204+.0121*T+Udelta
711   REM END OF 41D LAUNCH SPECIFIC DATA
712   REM
713   REM ------------------------------------------------------
714   REM
718   REM   CALCULATE VAPOR PRESSURE AND EVAPORATION FOR PURE WATER
720   REM  FLEAGLE AND BUSINGER, P 48
730   Pwr=9.4051-2353/(Ts+273.16)
740   Esat=.750062*10^Pwr    ! mm of Hg.
750   Pwr=9.4051-2353/(Tdew+273.16)
760   Edew=.750062*10^Pwr
770   REM PENMAN'S BEST FIT EQUATION ADAPTED TO CURRENT UNITS
780   REM PENMAN, 1947, PROC. ROY. SOC. A, VOL 193
790   Lapse=4.05*60.0*(1+.526*U)/1000
800   Evapo=Lapse*(Esat-Edew)  ! (g/(m^2 min)  see BOOK 8, P9
810   REM
820   REM
830   REM
850   REM ------------------------------------------------------
860   REM
```

```
880     Tsum=0
890     Mtg(T)=0
891     IF T<30 THEN 900
892     IF Mtg(T-1)>.0001 THEN 900
893     Mtg(T)=0
894     GOTO 1460
900     Tw=0
910     Test=0
920     FOR J=1 TO 40
930       Tsum=Tsum+N(J)*A(J)
940     NEXT J
941     IF Tsum=0 THEN 1470
950     Kp=Evapo*Sumarea/Tsum
960   FOR I=1 TO 40
970     IF A(I)=0 THEN GOTO 1330
980     GOSUB Mol
990     Lw=2343     !J/g AT 66 deg C
1000    Al=25.624955
1010    Bl=.014923
1020    Cl=1.079343
1030    La=2343-Al*M(I)+Bl*EXP(Cl*M(I))
1040    IF M(I)>8.06 THEN La=2226
1050    REM  THESE ARE LATENT HEATS OF VAPORIZATION FOUND BY
1060    REM  SIMPLE CURVE FIT TO DATA OF A. C. PLEWES AT 66 DEG C.
1070    REM  ONLY THE RATIO OF LATENT HEATS ENTERS SO ONLY ONE
1080    REM  TEMPERATURE NEED BE CONSIDERED.
1090    Khcl=Lw/La*Kp*Dtime
```

```
1100    Ratio=Diffw*Mh2o*(Ew-Eldew)/(Diffa*Mhcl*(Ea-Elinf))
1110    REM  Ratio IS THE WATER TO ACID EVAPORATION RATIO FOR DROP I.
1120    Delma=Khcl*A(I)/(1+Ratio)  !    MASS OF ACID LOST FROM Ith DROP.
1130    Delmw=Khcl*A(I)/(1+1/Ratio)    !MASS OF WATER LOST FROM Ith DROP.
1140    Mass=2.0944*A(I)^3*(1+.0049*C(I))  ! INITIAL DROP MASS (GRAMS)
1150    Massa=Mass*C(I)/100
1160    Massw=Mass*(1-C(I)/100)
1170    Newmass-Mass-Delma-Delmw
1180    IF (100*Delma>Massa) OR (100*Delmw>Massw) THEN GOTO 1610
1190    IF Newmass<=0 THEN GOTO 1240
1200    C(I)=(Massa-Delma)*100/Newmass
1210    A(I)=(Newmass/(2.0944*(1+.0049*C(I))))^(1/3)
1220    REM NEW CONCENTRATIN AND RADIUS
1230    GOTO 1260
1240    A(I)=0
1250    Newmass=0
1260    V(I)=Newmass/(1+.0049*C(I))
1270    Mw(I)=N(I)*Delmw
1280    Mga(I)=N(I)*Delma   ! HCL EVAP: g/sq.meter in Dtime
1290    Test=Test+Mw(I)*Lw+Mga(I)*La
1300    REM
1310    Mtg(T)=Mtg(T)+Mga(I)   ! SUM FOR TOTAL HCL IN TIME INTERVAL
1320    Tw=Tw+Mw(I)            ! SUM FOR TOTAL HCL IN TIME INTERVAL
1330  NEXT I
1340  Cumlgas=Cumlgas+Mtg(T)
1350  Cumlw=Cumlw+Tw
1360  GOSUB Env
```

```
1370  PRINTER IS 0
1380  REM   PRINT USING 1390;T,Mtg(T),Tw,Test,Cumlgas,Cumlw
1390  IMAGE DDD.DD,3(2X,MD.DDDE),2(2X,DDDD.DDD)
1400  IF T MOD 10 THEN GOTO 1420
1410  PRINT "  T        MASS HCL    MASS WATER    TEST       CUM HCL    CUM WATER"
1415  PRINT USING 1390;T,Mtg(T),Tw,Test,Cumlgas,Cumlw
1420  IF T MOD Dtout THEN GOTO 1440
1430  GOSUB Pout
1440  PRINTER IS 16
1450  REM
1460  REM                END OF PRIMARY (TIME) LOOP
1470  NEXT T
1480  REM
1490  CREATE Dfile$&":T14",14              ! CREATE FILE
1500  ASSIGN Dfile$&":T14" TO #1           ! OPEN FILE
1510  PRINT #1;Case$
1520  PRINT #1;Tf,Dtime,Ts,Tdew,U,C,V,Amean,Ra
1530  FOR I=1 TO Tf STEP Dtime
1540  PRINT #1;Mtg(I)
1550  NEXT I
1560  ASSIGN * TO #1                       ! CLOSE FILE
1570  REM
1571  REM  NEXT Rpt
1580  REM
1590  GOTO 2820  !   GO TO END OF PROGRAM---------------->>>>>>>>
1600  REM
1610  REM  BEGIN FINE RESOLUTION CALCULATION LOOP
```

```
1620  REM
1620  Na=Delma/Massa
1640  Nw=Delmw/Massw
1650  IF Nw>Na THEN Na=Nw
1660  IF Na>1.5 THEN Na=1.5
1670  Loop=2+134.0*Na-36.0*Na*Na
1680  If Na<0 THEN Loop=121
1690  Mw(I)=0
1700  Mga(I)=0
1710  Tivl-Loop
1720  FOR L=Loop TO 0 STEP -1
1730    REM                          TOP OF SUB LOOP
1740    IF A(I)=0 THEN GOTO 1300
1750    GOSUB Mol
1760    Lw-2343     ! J/g AT 66 deg C
1770    Al=25.624955
1780    Bl=.014923
1790    Cl=1.079343
1800    La=2343-Al*M(I)+Bl*EXP(Cl*M(I)))
1810    IF M(I)>8.06 THEN La=2226
1820    REM  THESE ARE LATENT HEATS OF VAPORIZATION FOUND BY
1830    REM  SIMPLE CURVE FIT TO DATA OF A. C. PLEWES AT 66 DEG C.
1840    REM  ONLY THE RATIO OF LATENT HEATS ENTERS SO ONLY ONE
1850    REM  TEMPERATURE NEED BE CONSIDRED.
1860    Khcl-Lw/La*Kp*Dtime/Tivl
1870    Ratio=Diffw*Mh2o*(Ew-Eldew)/(Diffa*Mhcl*(Ea-Elinf))
1880    Delma-Khcl*A(I)/(1+Ratio)  !    MASS OF ACID LOST FROM Ith DROP.
```

```
1890    Delmw=Khcl*A(I)/(1+1/Ratio)     !MASS OF WATER LOST FROM Ith DROP.
1900    Mass=2.0944*A(I)^3*(1+0049*C(I))    ! INITIAL DROP MASS (GRAMS)
1910    Massa=Mass*C(I)/100
1920    Massw=Mass*(1-C(I)/100
1930    Newmass=Mass-Delma-Delmw
1940    IF Newmass<=0 THEN GOTO 2010
1950    C(I)=(Massa-Delma)*100/Newmass
1960    IF C(I)<=0 THEN GOTO 2010
1970    IF C(I)>50 THEN GOTO 2010
1980    A(I)=(Newmass/(2.0944*(1+.0049*C(I))))^(1/3)
1990    REM NEW CONCENTRATION AND RADIUS
2000    GOTO 2030
2010    A(I)=0
2020    Newmass=0
2030    V(I)=Newmass/(1+.0049*C(I))
2040    Mwloop=N(I)*Delmw
2050    Mgaloop=N(I)*Delma    ! HCL EVAP: g/sq.meter in Dtime
2060    Mw(I)=Mga(I)+Mwloop
2070    Mga(I)=Mga(I)+Mgaloop
2080    Test=Test+Mwloop*Lw+Mgaloop*La
2090    PRINT USING 2100;T;I;L;A(I);Mga(I)
2100    IMAGE "T=",DDDD.D,"  I=",DD,"   L=",DDD,"     A=",D.DDD,"
        MGA=",MD.DD
2110  NEXT L
2120  REM                          END OF SUB LOOP
2130  GOTO 1300
2140  REM
```

```
2150  REM
2160 Mol:REM  BEGIN SUBROUTINE TO CALCULATE MOLARITY AND VAPOR PRESSURE
2161  IF C(I)>40 THEN C(I)=40
2162  IF C(I)<0 THEN C(I)=.000001
2170  M(I)=1000*C(I)/(Mhcl*(100-C(I)))
2180  Aw=53.56-8.1475*M(I)+1.4352*M(I)^2-.058161*M(I)^3-1.317E-5*EXP(M(I))
2190  Bw=-4.8693+1.2115*M(I)-.21394*M(I)^2+8.6707E-3*M(I)^3+1.9812E-
      6*EXP(M(I))
2200  Cw=-6753.4+363.79*M(I)-66.826*M(I)^2+2.6591*M(I)^3+5.6202E-
      4*EXP(M(I))
2210  Aa=30.542-1.3279*M(I)+.03242*M(I)^2+1.6501*LOG(M(I))
2220  Ba=-14694+987.61*M(I)-24.308*M(I)^2+55.001*LOG(M(I))
2230  Ca=9.1016E5-1.58:E5*M(I)+2045.9*M(I)^2+6331.4*LOG(M(I))+
      23439*M(I)*LOG(M(I))
2240  REM  ABOVE COEF. FROM DINGLE, NASA CR 2928, JAN 1978.
2250  REM  WATER AND ACID VAPOR PRESSURES ARE OBTAINED AS FOLLOWS:
2260  Tsk=Ts+273.16
2270  Ew=EXP(Aw+Bw*LOG(Tsk)+Cw/Tsk)    ! mm OF Hg
2280  Ea=EXP(Aa+Ba/Tsk+Ca/Tsk^2)       ! mm OF Hg
2290  REM
2300  RETURN   !            ENG OF SUBROUTINE Mol
2310  REM
2320 Env: REM    SUBROUTINE TO CALCULATE VAPOR PRESSURES NEAR SURFACE
2330    Sum=0
2340    Sumarea=0
2350    Nt=0
2360    FOR I=1 TO 40
2370      Sum=Sum+N(I)*A(I)
2380      Sumarea=Sumarea+N(I)*Ra*PI*A(I)*A(I)/10000
```

```
2390      Nt=Nt+N(I)
2400    NEXT I
2410    Abar=Sum/Nt
2420    Xbar=(10000/Nt)^(1/3)
2430    IF Sumarea>1 THEN Sumarea=1
2440    Ewtemp=Tw/(Lapse*Dtime)+Edew
2450    Eatemp=Mtg(T)/(Lapse*Dtime)+Einf
2460    Eldew=Ewtemp*Abar/Xbar
2470    Elinf=Eatemp*Abar/Xbar
2480    PRINTER IS 16
2490    IF T MOD 10 THEN GOTO 2510
2500    PRINT "T      ";"Ewtemp    ";"Ew         ";"Eatemp
        ";"Ea       ";"Abar    ";"Xbar"
2510    PRINT USING 2520;T,Ewtemp,Ew,Eatemp,Ea,Abar,Xbar
2520    IMAGE DDD,2X,4(MD.DE,2X),D.DDDD,2X,D.DDDD
2530    PRINTER IS 0
2540    REM
2550    RETURN    !  END OF SUBROUTINE Env
2560    REM
2570 Prival: REM  PRINT INITIAL VALUES
2580      PRINTER IS 0
2590      PRINT "DATA FILENAME =";Dfile$,LIN(2)
2600      PRINT Case$
2610      PRINT "SURFACE TEMP (C)    =";Ts
2620      PRINT "DEW POINT TEMP (C) =";Tdew
2630      PRINT "WIND SPEED (m/s)    =";U
2640      PRINT "INITIAL ACID CONCENTRATION (wt.percent) =";C
```

```
2650       PRINT "T final =";Tf;"     TIME STEP (min) =";Dtime
2660       PRINT "INITIAL VOLUME PER SQ METER (cc) =";V
2670       PRINT "INITIAL DROP RADIUS (cm) =";Amean
2680       PRINT "AREA FACTOR FOR EVAPO REDUCTION =";Ra,LIN(2)
2690 PRINT "  T        MASS HCL    MASS WATER    TEST      CUM HCL    CUM
     WATER"
2700       PRINTER IS 16
2710  RETURN
2720  REM
2730 Pout: Rem    PERIOD PRINT OUT SUBROUTINE
2740       PRINT " I  RADIUS  VOLUME      NUMBER      MOLALITY  WT PER"
2750       PRINT "       cm      cc/drop    per sq m          "
2760       FOR I=1 TO 40
2770       PRINT USING 2780;I,A(I),V(I),N(I),M(I),C(I)
2780       IMAGE DD,2X,D.DDDD,2X,D.DDDE,2X,DDDDDD.DDD,2X,DD.DDD,2X,DDD.DD
2790       NEXT I
2800       PRINT LIN(2)
2810       RETURN
2820  END
```

NASA
National Aeronautics and Space Administration

Report Documentation Page

1. Report No.	2. Government Accession No.	3. Recipient's Catalog No.
NASA TM-4172		

4. Title and Subtitle	5. Report Date
A Field Study of Solid Rocket Exhaust Impacts on the Near-Field Environment	January 1990
	6. Performing Organization Code: ES44

7. Author(s)	8. Performing Organization Report No.
B. J. Anderson and Vernon W. Keller*	
	10. Work Unit No.: M-626

9. Performing Organization Name and Address	11. Contract or Grant No.
George C. Marshall Space Flight Center Marshall Space Flight Center, AL 35812	
	13. Type of Report and Period Covered: Technical Memorandum

12. Sponsoring Agency Name and Address	14. Sponsoring Agency Code
National Aeronautics and Space Administration Washington, DC 20546	

15. Supplementary Notes

Prepared by Earth Science and Applications Division,** Space Science Laboratory, Science and Engineering Directorate

*Currently in Payload & Orbital Systems Office, Program Development

**Formerly within the Structures and Dynamics Laboratory

16. Abstract

Large solid rocket motors release large quantities of hydrogen chloride and aluminum oxide exhaust during launch or testing. This report summarizes measurements and analysis of the interaction of this material with the deluge water spray and other environmental factors in the near field (within 1 km of the launch or test site). Measurements of mixed solid and liquid deposition (typically 2 normal HCl) following space shuttle launches and 6.4 percent scale model tests are described. Hydrogen chloride gas concentrations measured in the hours after the launch of STS 41D and STS 51A are reported. Concentrations of 9 ppm, which are above the 5 ppm exposure limits for workers, were detected an hour after STS 51A. A simplified model which explains the primary features of the gas concentration profiles is included.

17. Key Words (Suggested by Author(s))	18. Distribution Statement
Hydrogen Chloride, Rocket Exhaust, Toxic Vapors, Corrosion, Solid Rocket Booster, Space Shuttle, Environmental Effects	Unclassified—Unlimited Subject Category: 45

19. Security Classif. (of this report)	20. Security Classif. (of this page)	21. No. of pages	22. Price
Unclassified	Unclassified	92	A05

NASA FORM 1626 OCT 86

For sale by the National Technical Information Service, Springfield, VA 22161-2171

NASA-Langley, 1990